12-1-2011

Mechanisms of Brain Edema Formation in Mouse Models of Intracerebral Hemorrhage

Qingyi Ma
Loma Linda University

LOMA LINDA UNIVERSITY
School of Medicine
in conjunction with the
Faculty of Graduate Studies

Mechanisms of Brain Edema Formation in Mouse Models of Intracerebral Hemorrhage

by

Qingyi Ma

A Dissertation submitted in partial satisfaction of
the requirements for the degree of
Doctor of Philosophy in Physiology

December 2011

Each person whose signature appears below certifies that this dissertation in his/her opinion is adequate, in scope and quality, as a dissertation for the degree Doctor of Philosophy.

_____, Chairperson
Jiping Tang, Professor of Physiology and Pharmacology

_____
Jerome Badaut, Assistant Professor of Physiology and Pharmacology

_____
Andre Obenaus, Associated Professor of Biochemistry

_____
John H. Zhang, Professor of Neurosurgery, of Anesthesiology, of Physiology and Pharmacology

ACKNOWLEDGEMENTS

I would like to express my deepest gratitude to my mentor and advisor, Dr Jiping Tang. She is a teacher and a friend, for her continues support and encouragement throughout the time of my doctoral training. I am pleased to thank my advisor, Dr. John H, Zhang, for his motivation, enthusiasm and stimulating suggestions. He opened my eyes to science and kept inspiring me for research. Thanks for your invaluable support and guidance.

I would also like to thank my other committee members, Dr. Jerome Badaut, and Dr. Andre Obenaus for their advice and comments. To all my labmates in Zhang neuroscience laboratory, thank you all for helping me through the years as a graduate student and at the same time providing me with a friendly atmosphere to work.

Especially, I would like to give my special thanks to my family and friends. Their support and encouragement enable me to complete my work.

CONTENTS

FIGURES

Figures Page

Supplemental Figures

ABBREVIATIONS

AMD	age-related macular degeneration
AOC3	amine oxidase, copper containing 3 (vascular adhesion protein 1)
ATF-2	activating transcription factor-2
AVMs	arteriovenus malformation
BBB	blood-brain barrier
bICH	arterial blood-induced intracerebral hemorrhage model
cICH	collagenase-induced intracerebral hemorrhage model
CNS	central nervous system
CSF	cerebrospinal fluid
15d-PGJ2	15-Deoxy-Delta(12,14)-prostaglandin J2
ERK1/2	extracellular signal-regulated kinases 1/2
JNK1/2	c-Jun NH2-terminal kinase 1/2
HEC	human hybrid endothelial cell line
HIF-1 α	hypoxia-inducible factor-1 alpha
H_2O_2	hydrogen peroxide
Iba-1	ionized calcium binding adaptor molecule-1
ICAM-1	intercellular adhesion molecule-1
ICH	intracerebral hemorrhage
LAK	lymphokine-activated killer cells
LJP1586	Z-3-fluoro-2-(4-methoxybenzyl) allylamine hydrochloride
IACUC	Institutional Animal Care and Use Committee
IL-1β	interleukin 1 beta
IL-1ra	interleukin 1 receptor antagonist

MAPK	mitogen-activated protein kinase
MCP-1	monocyte chemotactic protein-1
MDCK	Madin-Darby canine kidney cells
MIF	macrophage/microglial inhibitory factor
MMP-2	matrix metalloproteinases-2
MMP-9	matrix metalloproteinases-9
MPO	myeloperoxidase
NFκB	nuclear factor kappa-light-chain-enhancer of activated B cells
NHE	nuclease hypersensitive element
NMDA	N-Methyl-D-aspartic acid
NRK	normal rat kidney fibroblast cells
PAR	protease-activated receptor
PBS	phosphate buffer saline
PDGF	platelet-derived growth factor
PDGFR-α	platelet-derived growth factor receptor alpha
PIK	phosphatidylinositol 3-Kinase, PI3K
PPAR gamma	peroxisome proliferator-activated receptor gamma
rCBF	regional cerebral blood flow
SCZ	semicarbizade
siRNA	small interfering RNA
SSAO	semicarbazide-sensitive amine oxidase
sVAP-1	soluble vascular adhesion protein-1
TIL	tumor-infiltrating lymphocytes
TNF-α	tumor necrosis factor-alpha
tPA	tissue plasminogen activator

TRAP	thrombin receptor agonist/ activating peptide
VAP-1	vascular adhesion protein-1
VCAM-1	vascular cell adhesion molecule-1
VEGF	vascular endothelial growth factor

ABSTRACT OF THE DISSERTATION

Mechanisms of Brain Edema Formation in Mouse Models of Intracerebral Hemorrhage

by

Qingyi Ma

Doctor of Philosophy, Graduate Program in Physiology
Loma Linda University, December 2011
Dr. Jiping Tang, Chairperson

Perihematomal edema causes major neurologic deterioration following intracerebral hemorrhage (ICH), mainly resulting from the disruption of the blood-brain barrier (BBB) by multiple mediators, including inflammatory mediators and thrombin. The objective of our study was to investigate the mechanisms by which inflammation and thrombin respectively lead to the formation of brain edema following ICH. Our long-term goal is to develop new therapeutic strategies against ICH-induced brain edema by targeting: (1) VAP-1 mediated inflammatory response and (2) PDGFR-α orchestrated BBB impairment. Vascular adhesion protein-1 (VAP-1) was previously shown to promote leukocyte adhesion and transmigration. Additionally, PDGFR-α was also found to play a role in orchestrating BBB impairment.

ICH injury was induced by collagenase-injection (cICH) or autologous arterial blood-injection (bICH) in mice. Two VAP-1 inhibitors, LJP1586 and semicarbazide (SCZ) were administered one hour after cICH. For mechanistic studies, VAP-1 siRNA and human recombinant VAP-1 protein were administered intracerebroventricularly. The data showed that VAP-1 inhibition reduced brain edema and neurobehavioral deficits at 24 and 72 hours after ICH induction. These two compounds were also found to decrease other adhesion molecules and cytokines expression, neutrophils infiltration and

microglia/macrophage activation. The effect of VAP-1 siRNA was consistent with that of pharmacological inhibitions, whereas human recombinant VAP-1 protein abolished the protective effect of VAP-1 inhibition. The anti-inflammatory effects of VAP-1 were also corroborated using blood-induced ICH. We then proceeded to elucidate the role of PDGFR-α inhibitor-induced neuroprotection in ICH.

In our ICH model, we found that PDGFR-α and its endogenous agonist PDGF-AA, were upregulated in response to bICH-induced brain injury. The results showed that suppression of PDGFR-α preserved BBB integrity following bICH while activation of PDGFR-α led to BBB impairment. A p38 inhibitor reversed the effect PDGFR-α activation in naïve animals. PDGFR-α activation was suppressed by thrombin inhibition and exogenous PDGF-AA administration increased PDGFR-α activation, regardless of thrombin inhibition. In our thrombin injection model, animals receiving the treatment of a PDGF-AA neutralizing antibody or Gleevec, a PDGFR-α antagonist, showed minimized thrombin-induced BBB impairment. We concluded that anti-inflammation by targeting VAP-1 or BBB preservation by targeting PDGFR-α may serve as new treatments against brain edema following ICH.

CHAPTER ONE

INTRODUCTION

Spontaneous intracerebral hemorrhage (sICH) is the result of small vessel bleeding into brain parenchyma and the subsequent formation and expansion of hematoma. It is responsible for about 15-20% of cerebrovascular diseases and represents the deadliest and least treatable subtypes of all stoke (Ribo and Grotta 2006). Even if the patient survives the initial attack, the growing hematoma triggers a series of life threatening events leading to the accumulation of brain edema, progression of neurobehavioral deficits, and possibly death (Strbian *et al* 2008).

Multiple pathologies can lead to sICH. Chronic hypotension and cerebral amyloid angiopathy were regarded as primary causes, and accounts for approximately 70-80% of all sICH cases (Fewel *et al* 2003). The secondary causes include vascular malformation, aneurysms, neoplasm and coagulopathy. Vascular malformations, including both arteriovenus malformations (AVMs) and cavernous malformation were one of the most common causes of ICH. AVMs, an abnormal connection between veins and arteries, were associated with an estimated mean annual hemorrhage risk of 4% (Fewel *et al* 2003).

ICH induces both primary brain injury and secondary brain injury. Primary injury is mainly caused by the physical disruption of blood vessels and the mass effect following hematoma formation, which is still untreatable. Hematoma expansion and brain edema formation were considered the major contributors to midline shift and leads to the deterioration consciousness (Mayer *et al* 1994). Rebleeding occurred within the first 24 hours and may contribute to hematoma enlargement (Brott *et al* 1997; Kazui *et al* 1996). Recombinant activated factor VII has been used to minimize early hematoma growth in

order to prevent hematoma expansion and brain injury (Mayer 2003). Secondary brain injury and brain edema occurs within 24 hours after the onset of ICH, which represented potential therapeutic targets. After ICH, inflammatory cells: neutrophils, macrophages and activated microglia can be found in and around the hematoma. Their products such as: cytotoxic enzymes, free oxygen radicals and nitric oxide all contributed to neuronal injury and cell death (Yang *et al* 1994). Thrombin was responsible for the BBB disruption and early brain edema formation (Lee *et al* 1997). Both apoptosis and necrosis have been found in animal model (Matsushita *et al* 2000) and human subjects (Qureshi *et al* 2003). Blood toxicity also contributed to brain edema development and tissue injury following ICH (Xi *et al* 1998).

Blood-Brain Barrier Disruption and Brain Edema

Brain edema resulted in an increase in intracranial pressure, herniation (Ropper 1986) immediately formed around hematoma and is associated with poor neurological outcomes after ICH (Xi *et al* 2006). There are two types edema involved in ICH, vasogenic edema and cytotoxic edema. Both result from BBB disruption, sodium pump failure, and neuronal death (Fewel *et al* 2003). The primary form is vasogenic edema, a consequence that occurs mainly from disruption of the BBB and partly determined the devastating nature of ICH. The profile of brain edema has been examined in blood injection ICH animal model. Brain edema prominently increased at 24 hours, peaked at 72 hours and kept a high level until 7 days (Xi *et al* 2002). Brain edema formation has been widely studied and categorized into three phases (Xi *et al* 2006). In the first few hours following ICH, the brain edema results from the hydrostatic pressure and clot

retraction which lead to the movement of serum from the clot into the surrounding tissue; within two days the coagulation cascade, especially thrombin, contributes to brain edema formation. The third phase involved red blood cell lysis and hemoglobin toxicity (Xi *et al* 2002).

BBB is a physical and physiological barrier which controls the transportation of compounds between blood and brain. It is a complex system made of a layer of endothelium cells which line the blood vasculature throughout the brain. Tight junctions hold adjacent endothelium cells together and restrict diffusion of small molecules through paracellular route (gaps between endothelium cells) (Ballabh *et al* 2004; Neuwelt 2004). Astrocytes, also an important component of BBB, surround the endothelium layer and promote the BBB maturation and maintenance (Rieckmann and Engelhardt 2003).

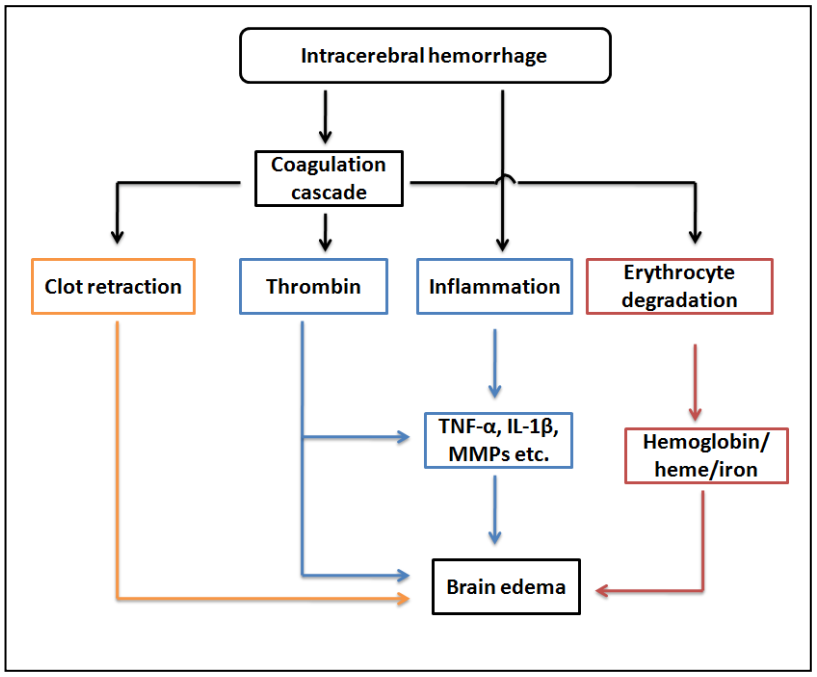

Figure 1: Phases of brain edema formation after ICH. Yellow showed the first early phase (first few hours); Blue showed second phase (first 2 days); Red showed third phase. Adapted from (Xi *et al* 2006).

BBB disruption is the hallmark of ICH-induced brain damage following ICH and contributes to vasogenic edema formation. BBB is not opened immediately but remains impermeable to large molecules for the first several hours following ICH (Wagner *et al* 1996). In a murine blood injection model of ICH, Yang and colleagues found that BBB permeability around the hematoma increased between 12 to 48 hours but not at 4 hours (Yang *et al* 1994). In collagenase injection ICH murine model, BBB damage occurs after 30 minutes due to the degradative effect of collagenase to the endothelial basement membrane, which keeps opening from 5 hours to 7 days (Rosenberg *et al* 1993). Although the underlying mechanisms of brain edema formation following ICH remains to be elucidated, mounting evidences has suggested that multiple factors such as: thrombin, inflammatory mediators, hemoglobin degradation productions and matrix metalloproteinases (MMPs) promote brain edema formation following ICH (Keep *et al* 2008; Yang *et al* 1994). Breaking the balance between hydrostatic and oncotic pressure gradients across systemic capillaries may also contribute to brain edema formation (Xi *et al* 2002). Under normal condition, the tight junction between endothelial cells controls the fluid diffusion and active secretion across capillaries (Betz *et al* 1989). However, BBB dysfunction occurred under pathophysiological conditions, such as ICH, the presence of plasma proteins in the brain tissue breaks down the oncotic pressure gradient that normally acts to retain water in the circulating blood. Hydrostatic pressure may then become the main driving force controlling fluid transportation into brain tissue and promote the brain edema formation (Gazendam *et al* 1979).

Based on these evidences, we expect that focusing our study on brain edema, especially vasogenic brain edema will lead to development of new therapeutic strategies for ICH-induced brain injury.

Inflammatory Response in Brain Injury

It is well known that the leukocytes will infiltrate into brain parenchemal during inflammation. Whether the leukocytes enter into the non-inflamed central nervous system (CNS) for immunosurveillance is still unclear. Previous studies reported that activated lymphocytes cross BBB into the brain parenchymal in the absence of inflammation while resting lymphocytes fail to enter the CNS (Engelhardt and Ransohoff 2005; Hickey 1991; Wekerle *et al* 1986). The mechanisms of lymphocyte entry into CNS under normal condition may be distinct from that during inflammation. Carrithers and colleagues explored the molecular events of the lymphocytes entry. Their results indicated that early migration of lymphocyte is independent of the integrin VLA-4 and endothelial VCAM, but does require increased surface expression of endothelial P-selectin (Carrithers *et al* 2000). However, study from Piccio and colleagues didn`t provide identical result. In a novel intravital microscopy model, they fail to observe the adhesive interaction of lymphocytes and nonactivated endothelium in non-inflamed cerebral microcirculation while the pretreatment with LPS or TNF-α stimulate the adhesion cascade, suggesting that the inflammatory response can be primed by systemic stimuli (Piccio *et al* 2002).

An inflammatory response is a common reaction of the brain tissue to various forms of insult. It also plays an important role in brain injury induced by ICH. This process is marked by inflammatory cells infiltration/activation and pro-inflammatory

cytokine released in and around the injury site. The inflammatory response following ICH comprises of both cellular and molecular components (Wang and Dore 2007). When hemorrhage occurred, blood-borne leukocytes, including neutrophils and macrophages enter into the brain tissue accompanied by resident microglia activation. They are the cellular components of the inflammatory response. The molecular components are the products released by these inflammatory cells, including cytokines, chemokines and other inflammatory factors.

Neutrophils are the major type of leukocytes which mediate secondary brain injury following ICH. In a collagenase-injection mouse model, Wang and colleague found that neutrophils infiltrated into and around the hematoma about 4 hours after injury and peaked at 3 days (Wang and Tsirka 2005a). Other studies conducted in an autologous blood-injection model showed that neutrophils appeared within 1 day and disappeared at 3 to 7 days (Gong *et al* 2000; Xue and Del Bigio 2000a; Xue and Del Bigio 2000b). Microglia is a type of macrophage in the CNS and accounts for about 5-20% of the total glial population (Lawson *et al* 1992). Under normal condition it exists at resting stage. When it is activated by an inflammatory response following brain injury, a series of morphological changes takes place, such as enlargement in size with stout processes, activation of phagocytic function and an upregulation of some specific genes (Wang and Tsirka 2005c). In a collagenase-injection model, studies showed that microglia activation was earlier than neutrophils infiltration. It occurred in the perihematomal region around 1-2 hours, markedly increased at 1 day, peaked at 7 days, and then declined to the base levels at 3 weeks (Wang *et al* 2003; Wang and Tsirka 2005b). A similar time course was observed in an autologous blood model, microglia activation appeared 1-4 hours, peaked

3-7 days and lasted as long as 4 weeks (Gong *et al* 2000; Hickenbottom *et al* 1999; Xue and Del Bigio 2000a).

The role of the inflammatory response has been widely investigated in ICH. Mounting evidences indicated that the accumulation of systemic immune cells, specifically blood-derived leukocytes, are the primary orchestrators of brain injury following ICH (Wang and Dore 2007). The infiltrations of these systemic immune cells result in an enhanced disruption of the BBB, causing an increase in brain edema, and subsequent deterioration in neurobehavioral function. Immune cells lead to brain injury through pro-inflammatory cytokines. Many brain cell types including glial cells, neuron and endothelial can produce pro-inflammatory cytokines, but infiltrated leukocytes and activated microglia/macrophages are the major sources of cytokines after brain injury (Emsley and Tyrrell 2002). Lu and colleagues performed DNA microarray analysis of gene expression following ICH. Their results showed that a large number of pro-inflammatory genes were upregulated, including transcription factors, cytokines, chemokines, extracellular proteases and adhesion molecules (Lu *et al* 2006). TNF-α and IL-1β are two major pro-inflammatory cytokines that have been widely reported in various animal models of brain injury. In ICH model previous studies showed that TNF-α appeared as early as 1 day after ICH (Gong *et al* 2000) and downregulation of TNF-α provided neuroprotective effects in an ICH animal model (Mayne *et al* 2001a; Mayne *et al* 2001b). In both collagenase and autologous blood injection models, TNF-α was markedly increased following ICH injury (Mayne *et al* 2001b; Xi *et al* 2001). In addition, IL-1β levels were upregulated in an autologous blood-injection ICH model in both porcine and rat (Aronowski and Hall 2005; Wagner *et al* 2006). TNF-α and IL-1β may be

responsible for brain edema formation after ICH. Evidences showed that the direct injections of TNF-α and IL-1β into brain resulted in the opening of the BBB and subsequent vasogenic edema formation. (Gordon *et al* 1990; Holmin and Mathiesen 2000; Megyeri *et al* 1992). Hua and colleagues also found that TNF-α contributed to brain edema formation after ICH (Hua *et al* 2006). Thus, TNF-α and IL-1β might be potential therapeutic targets for the treatment of ICH induced brain injury.

Thrombin in Brain Injury

Thrombin, a serine protease generated by the cleavage of prothrombin, and is the final-stage protease in the coagulation cascade. However, thrombin`s cellular effects are pluripotent and not limited to coagulation activation alone. Previous studies showed that thrombin and prothrombin also express in brain cells, including neuronal cells (Dihanich *et al* 1991) and astrocytes (Deschepper *et al* 1991), but its pathophysiological role in human brain is still unclear. It may be involved in microtubule-associated protein tau proteolysis and that failure to metabolize tau may lead to its aggregation in neurodegenerative diseases (Arai *et al* 2006). In vitro studies also indicated that thrombin can cleave amyloid precursor protein (Igarashi *et al* 1992) and apolipoprotein E (Marques *et al* 1996).

Thrombin is not detectable in circulating blood under normal condition, but markedly increases in coagulated blood (Lee *et al* 1997). The dual role of thrombin in ICH has been well described in previous studies. On one hand, thrombin itself can directly damage BBB and cause brain edema formation in ICH, but on the other hand, thrombin is an essential element for the coagulation cascade to stop bleeding. Previous

studies showed that thrombin at high concentrations kills cultured neurons and glia cells. However, at low concentrations thrombin was neuroprotective both *in vitro* and *in vivo* after ischemia (Striggow *et al* 2000). The thrombin receptor activation or an intracellular Ca^{2+} signal (single or repetitive spikes of $[Ca^{2+}]_i$) may contribute to this protective effect. The dose dependent manner of thrombin on ICH induced brain edema has also been determined. Thrombin preconditioning is conducted in an ICH animal model (Hua *et al* 2003; Xi *et al* 1999). They found that low dose thrombin preconditioning reduces brain edema caused by infusion of high dose thrombin, lysed red blood cells or iron. The precise mechanism of thrombin-induced brain tolerance in hemorrhagic stroke is still unclear. However, the upregulation of HIF-1α signals, activation of thrombin receptors, increase of iron handling proteins, and heat shock proteins in the brain may be associated with the induced tolerance.

Generally thrombin is produced in the brain immediately and is responsible for BBB disruption after ICH. Xi and colleagues found that blood clot formation is a mandatory step for rapid (at 1 hour) and prolonged (24 hours) edema in both white and gray matter after ICH (Xi *et al* 1998) and thrombin might be involved in this process. Contributing to BBB disruption and edema formation provides a plausible explanation for the role of thrombin. Mounting evidence showed that thrombin infusion into brain produces the same amount of BBB disruption as seen from blood injection suggesting that thrombin could directly disrupted BBB (Yang *et al* 1994). Furthermore, thrombin can activate PAR receptors and induce downstream protein production, such as vascular endothelial growth factor (VEGF) which results in the increase of endothelial cells permeability (Sarker *et al* 1999; Wang *et al* 1996). Thrombin may also cause brain edema

by enhancing excitotoxicity, activating gelatinases and stimulating cytokine release. Intracerebral infusion of thrombin significantly increased TNF-α level in the brain whereas less brain edema was found in TNF-α knockout mice compared to wild-type mice after ICH (Hua *et al* 2006). Thrombin can also activate matrix metalloproteinases-2 (MMP-2) in endothelial cells (Nguyen *et al* 1999), which causes break-down of extracellular matrix, resulting in BBB disruption. Src kinases may also mediate thrombin induced acute BBB injury, and the administration of Src inhibitor, PP2 attenuated BBB permeability and edema formation at 24 hours after thrombin injection (Liu *et al* 2010).

Proposed Novel Therapeutic Targets for Brain Edema

VAP-1

In 1992, VAP-1 was first discovered as a 90 Kilodalton endothelial cell molecule in synovial vessels from arthritis patients by using a monoclonal antibody 1B2 (Salmi and Jalkanen 1992). It markedly reduced the binding of lymphocyte to high endothelial venules in frozen section adhesion assays and in flow chamber assays. One year later, the localization of VAP-1 expression was determined by the same group. They found that in addition to abundant expression in lymphatic organs, VAP-1 also widely expressed in endothelial cells in several non-lymphatic tissues, including skin, brain, kidney, liver and hearts (Salmi *et al* 1993).

What is VAP-1 in nature? VAP-1 belongs to semicarbazide-sensitive monoamine oxidases (SSAO) family. This characteristic was identified by cDNA cloning which encoded a type II transmembrane protein with high identity to the copper-containing amine oxidase family. Further experiment confirmed that VAP-1 possessed amine

oxidase activity (Smith *et al* 1998), which can catalyze deamination of primary amine and release biological products, including aldehydes, hydrogen peroxide and ammonium. Coinciding with the discovery the enzymatic nature of VAP-1, its adhesion molecule function was observed by Smith and colleagues. In their experiment, they conducted a VAP-1 cDNA transfection in the endothelial cell and found that VAP-1 led to lymphocytes binding that can be partially inhibited with anti-VAP-1 mAbs (Smith *et al* 1998). Taken together, these findings suggested that the VAP-1 is a novel type of adhesion molecule with SSAO enzymatic activity.

Mounting evidences suggest that VAP-1 is an inflammation-inducible endothelial glycoprotein. Studies with human samples by confocal microscope showed that VAP-1 exists both on the luminal surface and in the intracellular granules in human endothelial vessels (HEVs). In samples from patients with inflammatory bowel diseases or chronic dermatoses, VAP-1 level was also found to be upregulated at sites of inflammation (Salmi *et al* 1993). Furthermore, the mechanism controlling VAP-1 functions has been explored. In normal endothelial cells, VAP-1 is stored in intracellular granules within the cytoplasm. Under inflammatory condition, VAP-1 is induced and translocated to the endothelial surface (Salmi and Jalkanen 2001). The translocation of VAP-1 to the cell surface was observed directly after inflammation in experimental canine and pig inflammatory models. VAP-1 increased on the endothelial cell surface 60 minutes after the induction inflammation, peaked at 8 hour and lasted until 48 hours (Jaakkola *et al* 2000). Similar to P-selectin, VAP-1 translocates from the intracellular onto the luminal surface of vasculature at the site of inflammation. However, the underlying mechanism and mediators inducing VAP-1 expression and translocation remains unclear. Thirteen

inflammatory factors including TNF-α and thrombin were used to define the mediators leading to the induction of VAP-1 in human endothelial cells. Unfortunately, none of them increased cell surface expression of VAP-1 (Salmi *et al* 1993). It is very rare that only single mediator is involved in inflammation *in vivo*, therefore, this study suggested that the VAP-1 might be induced by a combination of multiple mediators.

Role of VAP-1 in Inflammatory Response

In Vitro Studies

Yoong and colleagues studied the role of VAP-1 in T cell infiltration in human hepatocellular carcinoma. They found that VAP-1 and ICAM-1 mediated tethering and firm adhesion steps respectively, and VAP-1 antibody inhibited T cell binding to endothelium in an *in vitro* tissue binding assay (Yoong *et al* 1998). Another study showed that VAP-1 was involved in the binding of tumor-infiltrating lymphocytes (TIL), lymphokine-activated killer (LAK) cells, and NK cells to the vasculature. VAP-1 antibody treatment can diminish the number of adhesive cells by 60% (Irjala *et al* 2001). It has been shown that amine oxidase activity is necessary for VAP-1 functions. Lalor et al reported that VAP-1 antibody reduced lymphocyte binding to TNF-α treated HSE cells by 50% while enzymatic inhibition of VAP-1 diminished both adhesion and transmigration of lymphocytes to a level similar to that seen with VAP-1 antibody (Lalor *et al* 2002). This finding suggested that the enzymatic activity of VAP-1 is responsible for both transmigration and adhesion mediated by VAP-1. Study from Koskinen and colleagues further confirmed this finding (Koskinen *et al* 2004). They found a diminished leukocyte rolling and transmigration through human endothelial cells after the

administration of enzyme inhibitors *in vitro*, and also, the capacity of VAP-1 to transmigrate was abolished by point mutation of the enzyme activity.

In Vivo Studies

Functions of VAP-1 in inflammatory response have been studied in human and animal models. In peritoneal inflammatory models in rabbits, VAP-1 mediated the firm adhesion and recruitment steps and functioned as a molecular brake during granulocyte rolling (Tohka *et al* 2001). The authors also observed that the velocity of ganulocytes rolling was increased after VAP-1 suppression. As a result, a 44% of firm bound leukocytes reduction and an approximately 70% of granulocyte extravsasion diminishment were observed after anti-VAP-1 antibodies treatment. Similar results were also obtained in other animals models via blockage of VAP-1 adhesion function. In a rat liver allograft rejection model, Martelius found that lymphocyte infiltration was decreased after suppression of VAP-1 function with a new anti-rat VAP-1 mAb 174-5 (Martelius *et al* 2004). In peritonitis and air pouch inflammation models, VAP-1 antibody inhibited the migration of granulocytes and monocytes (Merinen *et al* 2005).

Since VAP-1 has both adhesion molecule function and enzymatic function which are essential for mediating leukocyte infiltration in vitro (Lalor *et al* 2002), a number of inhibitors targeting VAP-1 enzymatic function have been developed and used to suppress the leukocyte adhesion cascade. In inflamed air-pouch model in rat, Koskinen and colleagues found that a novel SSAO inhibitor BTT-2027 prevented the extravasation of polymorphonuclear(PMN) leukocytes, which was the first report to possibly regulate inflammatory reaction *in vivo* (Koskinen *et al* 2004). Their findings were further

confirmed in VAP-1 knockout mice (Stolen *et al* 2005). In this study, VAP-1 deficit mice resulted in the reduction of lymphocyte homing into lymphoid organs and attenuated inflammatory response in peritonitis. In other animals models, such as an acute rat liver allograft rejection model, semicarbazide, a SSAO inhibitor, markedly diminished lymphocyte infiltration in the grafts (Martelius *et al* 2008).

VAP-1 Signaling Functions

The signaling functions of the catalytic activity of VAP-1 have been studied. The potent biological products of VAP-1, aldehyde, H_2O_2 and NH_3 may induce other adhesion molecules or proinflammatory cytokines expression. They are cytotoxic at high concentration and potentially trigger VAP-1 downstream signals (Salmi and Jalkanen 2001; Yu and Zuo 1997). Reactive oxygen species, H_2O_2 is involved in the regulation of genes expression in vascular endothelial cells (Bogdan *et al* 2000). Mounting evidence showed that the H_2O_2 formation is associated with leukocyte infiltration by the induction of P-selectin expression and leukocyte rolling (Johnston *et al* 1996). In human endothelial cells, both P- and E-selectin are induced on the transcriptional and translational levels by VAP-1 enzymatic activity. In VAP-1 transgenic mouse, P-selectin induction is VAP-1 enzyme activity-dependent (Jalkanen *et al* 2007). In an age-related mouse macular degeneration (AMD) model, VAP-1 suppression diminished the expression of pro-inflammatory cytokines, such as TNF-α, MCP-1, and adhesion molecule, such as ICAM-1 (Noda *et al* 2008). Lalor and colleagues directly provided specific substrates of VAP-1 in the liver endothelial cells and led to the activation of endothelial cells. They also found that the VAP-1 mediated activation was dependent on

NFkB, PIK and MAP kinase pathway. They also found upregulation of E-selectin, ICAM-1 and VCAM-1 as well as chemokine CXCL8, and coupled an intensified inflammatory response (Lalor *et al* 2007).

VAP-1 in Stroke

Limited studies explored the role of VAP-1 in a stroke-induced inflammatory response. Since an inflammatory response contributes to brain injury and immune cells infiltration has also been observed after stroke, it is possible that VAP-1 is involved in immune cell infiltration after stroke. In myocardial samples of ischemic heart in humans, VAP-1 expression was markedly upregulated on endothelial cells and VAP-1 neutralizing antibody reduced the number of adherent granulocytes by 60% (Jaakkola *et al* 2000). In a transient forebrain ischemia rat model, a small molecule VAP-1 inhibitor was administered either at the onset or 6 hours of reperfusion. VAP-1 inhibitor treatment limited neutrophils adhesion and prevented infiltration even when treated 6 hours after reperfusion, and subsequently provided neuroprotection (Xu *et al* 2006).

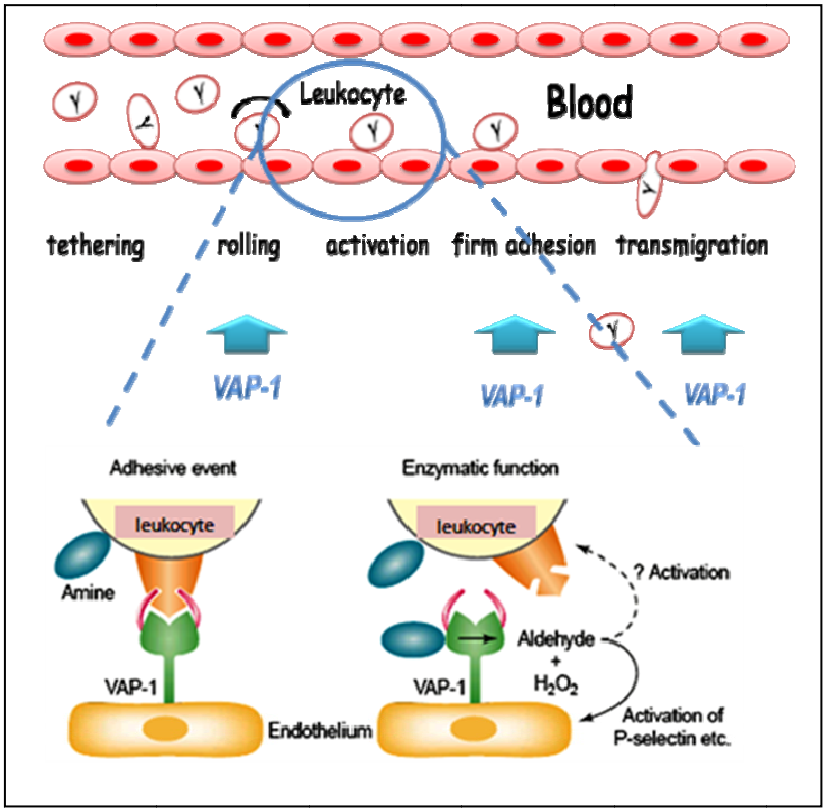

Figure 2: Schematic for the functions of VAP-1 mediating leukocyte transmigration. VAP-1 mediates rolling, activation, firm adhesion and transmigration steps in leukocyte adhesion cascade through its adhesion function and enzymatic function. VAP-1 enzyme can convert primary amines presented on the leukocyte surface to aldehyde and H_2O_2, and stimulate other adhesion molecules expression. Adapted from (Salmi and Jalkanen 2001)

Soluble VAP-1 (sVAP-1) may also play an important role after stroke. Airas and colleagues found that sVAP-1 was markedly increased in the serum of acute stroke patients less than 6 hours after ischemia and may promote vasculopathy (Airas *et al* 2008). Hernandez-Guillamon and colleagues reported that the baseline VAP-1/SSAO activity predicts the intracranial bleeding after tissue plasminogen activator (tPA) treatment (Hernandez-Guillamon *et al* 2010). They found elevated plasma VAP-1 activity in patients who subsequently suffered a hemorrhage and had deleterious neurological outcome. Additionally, in a rat model, they found that the VAP-1 inhibitor prevented the side effect associated with delayed tPA treatment. The authors also elucidated the potential mechanisms: In vitro, tPA promotes neutrophil degranulation and MMP-9 release which mediate the BBB injury. VAP-1 is an adhesion molecule and mediates leukocyte infiltration. Therefore, the inhibition of VAP-1 may protect against tPA induced vascular damage by inhibition of leukocyte infiltration. More currently, the same group found that the plasma VAP-1/SSAO activity is increased in hemorrhagic stroke patients and may predict neurological outcome after ICH (Hernandez-Guillamon *et al* 2011). All these clinical reports suggested that VAP-1 is a potential therapeutic target for ICH induced brain injury.

PDGF/PDGFRs

Platelet derived growth factors (PDGFs), a growth promoting protein in human platelets, has been studied for more than three decades (Alvarez *et al* 2006). PDGF was identified as a serum growth factor in smooth muscle cells (Ross *et al* 1974) and fibroblasts (Kohler and Lipton 1974) in 1974. A number of other cell types also produce

PDGFs, including vascular endothelial cells, astrocytes and neurons (Fager 1995; Heldin and Westermark 1999).

PDGF family has four members, PDGF-A, B, C and D. PDGF was purified from human platelet (Antoniades *et al* 1979) originally identified as a disulfide-linked dimer of two different polypeptide chains, A and B (Johnsson *et al* 1982). Currently other PDGF members, including PDGF-CC and DD were identified as protease-activated ligands (Bergsten *et al* 2001; LaRochelle *et al* 2001; Li *et al* 2000). All of them are assembled into disulphide-linked dimers in the endoplasmic reticulum as inactive precursor molecules, PDGF-AA, AB, BB, CC and DD. Subsequent proteolysis is essential for their activation (Fredriksson *et al* 2004). Both A and B polypeptides are synthesized as a precursor and is processed intracellularly before they are released. The mature PDGF-A and B polypeptide chains have approximately 100 amine acid and share 60 % sequences homology (Heldin and Westermark 1999; Heldin *et al* 2002). PDGF-C and D have an N-terminal CUB domain which does not exist in the PDGF-A and B precursors and keeps the full-length proteins latent by blocking receptor binding. After secretion the CUB domain is cleaved extracellularly by proteolysis in the hinge regions (Fredriksson *et al* 2004). The PDGF ligands have high similarity to vascular endothelial growth factor (VEGF) family which is composed of 8 cysteine residues that are conserved between 2 chains (Joukov *et al* 1997).

Platelet derived growth factor receptors, a subfamily of tyrosine kinase receptors, consist of two members, PDGFR-α and PDGFR-β, and are expressed throughout various cell-types in the brain, including astrocytes, neurons (Heldin and Westermark 1999), and capillary endothelial cells (Marx *et al* 1994). These receptors are transmembrane proteins

that contain 5 immunoglobulin-like extracellular domains for ligands binding and intracellular tyrosine kinase domain. The dimeric structure of PDGF allows it to bind two receptors simultaneously. Ligand binding promotes PDGF receptors homodimerization or heterodimerization and phosphorylation of each other in trans on specific tyrosine residues and initiates downstream signaling cascades (Alvarez *et al* 2006). The different PDGF chains recognize different receptors. PDGF-A chain only bound to receptor α whereas B chain recognizes both receptor α and β. Thus, PDGF-AA only stimulates PDGFR-αα homodimers, PDGF-BB stimulates formation of PDGFR-αα, PDGFR-αβ and PDGFR-ββ formation, and PDGF-AB stimulates formation of PDGFR-αα, and PDGFR-αβ. Two novel PDGFs, PDGF-C and D bound to receptor α and receptor β respectively and therefore, they can induce the dimerization of PDGFR-αα or PDGFR-ββ. As a growth factor, PDGFR signaling pathway plays an essential role during development and it is also associated with a number of pathological disease conditions (Andrae *et al* 2008; Hellberg *et al* 2010).

PDGFs in Physiological Conditions and Diseases

All the PDGFs and their receptors are expressed during the embryo development and have important functions in this process. Knock-out of PDGFs or the receptors is lethal embryonically/perinatally (Hoch and Soriano 2003). Previous study showed that the downregulation of PDGF-B and receptor β resulted in kidney dysfunction and increased heart size (Lindahl *et al* 1997). PDGF-A knock-out caused defective development of lung alveoli (Bostrom *et al* 1996). It was suggested that the main role of PDGF during embryonal development is the formation of the kidneys, blood vessels,

lungs, connective tissue and CNS (Alvarez *et al* 2006). Other studies indicated that PDGFs may orchestrate wound healing process, including cellular migration and proliferation, extracellular tissue production and angiogenesis etc. After being wounded, cells in the injured tissue, including endothelial cells, smooth muscle cells and activated fibroblasts are stimulated by thrombin to secret PDGFs around the site of the wound (Heldin and Westermark 1999). PDGFs stimulate the formation of granulation tissue by the production of fibronectin and hyaluronic acid, components of extracellular matrix (Blatti *et al* 1988; Heldin 1992). PDGFs may play another role in wound healing process, possibly strengthen vessel wall (Risau *et al* 1992).

PDGFs were found to be associated with multiple diseases, especially in tumorgenesis. PDGFs are essential in autocrine stimulation of tumor cells as well as in paracrine signaling between tumor cells and surrounding stroma (Li and Eriksson 2003). It has been reported that PDGF-C and D were expressed in many tumors and tumor cell lines, such as globlastoma and medullobalstoma. Up-regulation of PDGFR-α was also detected in most malignant grades gliomas, the more malignant the higher expression (Andrae et al 2008).

During the study of PDGFs in the CNS development process, the neuroprotective effect of PDGFR-β signaling was found in that PDGF administration to the CNS prevented against NMDA-induced injury (Egawa-Tsuzuki *et al* 2004). Another study showed that PDGF signaling, possibly through PDGFR-α, has also been implicated in neuropathic pain following nerve injury (Narita *et al* 2005). In other neuronal injury animal models, such as axotomy-induced neuronal death, neurotoxin-induced neuronal injury, 6-hydroxydopamine-induced Parkinson's dopaminergic neuronal death, and in

ischemia-induced stroke, PDGF-CC protein or gene delivery protected different types of neurons from apoptosis in both the retina and brain (Tang *et al* 2010). In vitro study also showed the neuroprotective effect of PDGFs via anti-oxidative stress; the effect of PDGF-BB was more potent than that of PDGF-AA. This might be due to the activation and additive effects of two PDGFRs after PDGF-BB stimulation (Zheng *et al* 2010).

PDGF-B and PDGFR-β axis is involved in the development of vascular system, angiogenesis and blood vessel muturation. Hellström and colleagues found that PDGF-B and PDGFR-β critically contributes to the recruitment of vascular smooth muscle cells and pericytes during embryonic blood vessel formation in mouse (Hellstrom *et al* 1999). Battegay and colleagues found that PDGF-BB modulates endothelial proliferation and angiogenesis in vitro by activation of PDGFR-β, but not PDGF-AA and PDGFR-α (Battegay *et al* 1994). The different functions of PDGFR-α and PDGFR-β in angiogenesis is also determined in vivo study. Study from Zhang and colleagues compared the combination effect of FGF2 with PDGF-AA or PDGF-AB on angiogenic and vessel stability using in vivo angiogenesis and ishchemic hind-limb animal models. They found that the combination of FGF2 with PDGF-AB, but not PDGF-AA can stabilize newly formed vessels, suggesting that PDGFR-β is essential for angiogenesis and vascular stability (Zhang *et al* 2009).

Recent studies indicated that PDGFRs, especially PDGFR-α specifically orchestrates the disruption of the BBB (Shen *et al* 2011; Su *et al* 2008; Yao *et al* 2010). One study led by Su and colleagues has shown that PDGFs injection into the CSF of naïve mice increased the extravasation of Evans blue one hour after administration. Their study suggested that increase of cerebrovascular permeability led by PDGFs is through a

PDGFR-α dependent process (Su *et al* 2008). Yet another study led by Yao and colleagues recently found that cocaine-induced PDGF-BB increased vascular permeability and that administration of a PDGF-BB neutralizing antibody abolished this effect (Yao *et al* 2010). Pericytes play a critical role in supporting endothelial cell (EC) tube formation and stabilization and vascular maturation including basement membrane matrix deposition. In 2010, study from Armulik and colleagues determined the direct role of pericytes at BBB in vivo by using pericyte-deficient mice. Their results showed that pericyte deficiency increases the BBB permeability and a transcytosis route occurs to transport macromolecular across the BBB in pericyte-deficient vessels. The PDGFR antagonist, imatinib and PDGF-B retention motif knockout ($Pdgfb^{ret/ret}$) can preserve BBB integrity by arresting endothelial transcytosis (Armulik *et al* 2010). Earlier than these studies, an *in vitro* study reported that PDGF mediates tight junction and adherens junction protein redistribution and increases permeability in Madin-Darby canine kidney (MDCK) Cells (Harhaj *et al* 2002).

Principle for PDGF/PDGFRs Inhibition

Since PDGF/PDGFRs play important roles in the pathology of multiple diseases, it is essential to develop strategies to inhibit PDGF signaling. PDGF and PDGFR are functional only after dimerization. Therefore, any attempt to inhibit dimerization may potentially block PDGF/PDGFRs signaling (Andrae *et al* 2008). Neutralizing antibodies for PDGF ligands and receptors have been widely used to evaluate the function of PDGF signaling in multiple animal models mimicking different pathogenic processes. An oligonucleotide, (called aptamer) specifically binding target proteins has been developed

to block PDGFs functions in rodent disease models. Another efficient way is to generate drugs to inhibit the tyrosine kinase activity by acting on or near the ATP binding site of the kianse domain. Gleevec (imatinib mesylate, STI157), the most popular one of these drugs, blocks PDGFR-α, PDGFR-β and the bcr-abl fusion protein c-kit and Flt3 (Carroll *et al* 1997). Gleevec represents a new class of anticancer drugs and has been approved by Food and Drug Administration (FDA) for the therapy of chronic myelogenous leukemia and other cancers. It was regarded as a new gold standard for the treatment of chronic myeloid leukemia at all stages (Peggs and Mackinnon 2003). Currently a study found that a proximal 5'-flanking region of the human PDGF-A promoter contains one nuclease hypersensitive element (NHE) that is critical for PDGF-A gene transcription. Their study also established that ligand-mediated stabilization of G-quadruplex structures within the PDGF-A NHE can silence PDGF-A expression (Qin *et al* 2007).

History of Preclinical Models of Intracerebral Hemorrhage

Qingyi Ma[a]; Nikan Khatibi[b]; Hank Chen[a]; Jiping Tang[a]; John H. Zhang[a, b, c]

[a]Department of Physiology, Loma Linda University, Loma Linda, California, USA
[b]Department of Anesthesiology, Loma Linda University, Loma Linda, California, USA
[c]Department of Neurosurgery, Loma Linda University, Loma Linda, California, USA

Published: ***Acta Neurochir Suppl.*** 2011;111: 3-8.

Abstract

In order to understand a disease process, effective modeling is required that can assist scientist in understanding the pathophysiological processes that take place. Intracerebral hemorrhage (ICH), a devastating disease representing 15% of all stroke cases, is just one example of how scientists have developed models that can effectively mimic human clinical scenarios. Currently there were three models of hematoma injections that are being used to induce an ICH in subjects. They include the microballoon model introduced in 1987 by Dr. David Mendelow, the bacterial collagenase injection model introduced in 1990 by Dr. Gary Rosenberg, and the autologous blood injection model introduced by Dr. Guo-Yuan Yang in 1994. These models have been applied on various animal models beginning in 1963 with canines, followed by rats and rabbits in 1982, pigs in 1996, and mice just recently in 2003. In this review, we will explore in detail the various injection models and animals subjects that have been used to study the ICH process while comparing and analyzing the benefits and disadvantages of each.

Introduction

Intracerebral hemorrhage (ICH) is a devastating disease accounting for roughly 15% of all stroke types. As many as 50,000 individuals are affected annually in the United States with a large number of those individuals facing chronic morbidities and early mortalities.

Over the years, basic science research has focused on reducing and/or blocking the cascade of harmful events in ICH with the goal of improving clinical outcomes. But in order to effectively study the mechanisms behind these events, proper modeling is needed that can mimic pathophysiologic processes in humans. Studies on various animal models began in 1963 with canines, followed by rats and rabbits in 1982, pigs in 1996, and mice just recently in 2003. These animal subjects have been thoroughly studied individually and compared to human models looking for parallel between the two groups. As important as it is to find an animal subject that will mimic processes in the human brain, creating the actual hematoma is another challenge. Currently there are three models of injections that are being used to induce an ICH in subjects. They include the microballoon model introduced in 1987 by Dr. David Mendelow, the bacterial collagenase injection model introduced in 1990 by Dr. Gary Rosenberg, and the autologous blood injection model introduced by Dr. Guo-Yuan Yang in 1994 (Rosenberg *et al* 1990; Sinar *et al* 1987; Yang *et al* 1994).

In this retrospective review, the history behind the development of the ICH model will be presented and discussed. Furthermore, the advantages and disadvantages of each model type and animal subject will be evaluated.

Microballoon Model

In 1987, Sinar et al (Sinar *et al* 1987) made a microballoon insertion model in rats as a way to study the mass effects of ICH. A microballoon mounted on a No.25 blunted needle was inserted into the right caudate nucleus after a burr hole was created on the skull. The microballoon was inflated to 0.05 ml over a period of 20 seconds and was kept inflated for 10 minutes before being deflated. At the end of the study, the authors looked at brain histology, intracranial pressure, and cerebral blood flow. They found the microballoon model to be successful in producing an effective brain lesion with an extensive area of ischemic damage noted on the right caudate nucleus. Additionally there was a reduction in cerebral blood flow and an increase in intracranial pressure at the site of damage.

The advantage of the microballoon model is that it mimics the space-occupying aspect of the hematoma. The disadvantage is it fails to address the potential effects of blood and subsequent substances released by the clot formation. This could potentially be the reason why there is a smaller degree of ischemia in this model versus what would be expected with an equivalent volume of blood (Nath *et al* 1986; Yang *et al* 1994).

Collagenase Injection Model

Collagenases are proteolytic enzymes which degrade basement membrane and interstitial collagen (Harris and Krane 1974). Additionally, they have been shown through immunocytochemical studies to surround blood vessels (Montfort and Perez-Tamayo 1975). As a result, in 1990, Rosenberg et al made a new model for spontaneous ICH using bacterial collagenase injections directly in the brains of Sprague-Dawley rats

(Rosenberg *et al* 1990). In this model, male rats were placed in a stereotactic apparatus and 2 μl of saline containing 0.01-0.1 U bacterial collagenase (Type XI or VII) was infused into the left caudate nucleus over nine minutes. Bleeding occurred as early as ten minutes after collagenase injection, with edema also seen at the site of hemorrhage (Rosenberg *et al* 1990). Other modifications to this model were made, including: injection site changes, adjustments to collagenase concentration, injection rates/volumes, and heparinization. This model conceptually integrates small vessel breakdown to produce hemorrhage and allows a controllable amount of variability in hemorrhage size (James *et al* 2008). The advantage of this model is its ability to mimic spontaneous intraparenchymal bleeding in humans while avoiding the technical difficulties with handling blood (Andaluz *et al* 2002). It also mimics the hematoma expansion of continuous bleeding which occurs naturally in ICH patients (Fujii 1972; Kazui *et al* 1996). The disadvantages of this model are related to bacterial collagenase's ability to introduce a significant inflammatory reaction (Andaluz *et al* 2002).

Blood Injection Model

Blood injection ICH model has become the standard model for experimental ICH. The first recorded publication using arterial blood as a single injectable agent was conducted by Ropper et al in 1982 (Rohde *et al* 2002). Using a 27-gauge cannula, fresh blood from the ventricle of a donor rat was infused over one second into the right caudate nucleus of the subject ICH rat. This method did not account for key sources of variability. Hence in 1984, a variation of Ropper's model was performed by Bullock et al (Bullock *et al* 1984) to study the changes in intracranial pressure and cerebral blood flow. Instead of

using donor blood, Bullock used a 22-gauge needle that bridged the right caudate nucleus to the femoral artery. For the first time, the study was able to look at ICH under arterial pressure – thus, effectively evaluating the pathophysiology of ICH. One of the main disadvantages of this method was the lack of reproducibility due to the potential variations in blood pressure.

That is why in 1994, a study out of the University of Michigan by Yang et al (Yang *et al* 1994), discovered that the use of a microinfusion pump could address the concerning issues previous authors had run into. Using a microinfusion pump, a constant rate of autologous blood (extracted from the femoral artery) was infused into the right caudate nucleus, creating a controllable and reproducible hematoma. This single blood injection model has been applied to most of the recent ICH studies. Unfortunately, one of the major issues with Yang's technique was the reflux of blood up the needle tract and into the ventricular system or extension into the subdural space with a more rapid injection rate. Additionally, the inability of this technique to reproduce the systemic arterial pressure which can influence the hematoma size is also seen as a slight disadvantage. And finally, the use of the femoral artery created problems down the road when it came time to assess neurobehavioral deficits.

To address the concern of blood reflux up the needle tract, a double injection model was created just two years later. In 1996, a study led by Deinsberger et al (Deinsberger *et al* 1996) out of the Justus Liebig University in Germany, modified the single arterial blood injection model originally designed by Yang and instead used a double arterial blood injection model. What Deinsberger and his team proposed was injecting 5 µl of fresh autologous blood into the caudate nucleus and waiting ten minutes

to allow for clot formation. That way, when it was time to inject the rest of the autologous blood to mimic the hematoma, the chances of reflux would be minimized significantly. This was the main advantage of the double blood injection model over the single injection model-it minimized blood reflux through the needle tract. The disadvantages however, were the obvious difficulties with infusion and increase potential of clot formation because of the time lag between injections.

Large Animal Models

Monkeys

Chimpanzees and rhesus monkeys share over 90 % of their DNA with humans in addition to physiologic, structural and size similarities, making them ideal candidates for preclinical study. In 1982, Segal et al used macaque monkeys to demonstrate the effects of local therapy on hematoma formation using the thrombolytic urokinase. Their treatment was given after injection of 6 ml autologous blood into the right internal capsule. Additionally in 1988, Bullock et al (Bullock *et al* 1988)used adult Vervet monkeys to demonstrate and quantify a 90-120 minute decrease in the regional cerebral blood flow (rCBF) following an ICH. A key refinement to the primate model made by Bullock was the use of a catheter that infused blood directly from the femoral artery into the right caudate, thereby keeping the infusion pressure closer to arterial pressure and reducing complications from blood handling and delay.

The experiments using monkeys were costly and the various levels of restrictions and regulations were concerning. Hence, their use in ICH modeling was quickly discontinued.

Canines

Like monkeys, canines have long been the subject of medical research across the same range of fields, most notably having contributed to cardiovascular physiology (Fujii *et al* 1994). But like monkeys, use of canines in research involves similarly stringent criterion and cost. In 1963, Whisnant et al developed a model for experimental ICH by performing single injections of 0.5 to 1.5 ml of fresh autologous venous blood into the basal nuclei or deep white matter region in canines - producing varying sizes of ICH. In 1975, Sugi et al (Sugi *et al* 1975) used canines to develop a single autologous arterial blood injection model, noting lactate elevations in CSF after injection. In 1999, Qureshi et al (Qureshi *et al* 1999a) made single autologous blood injections (7.5 ml) over 20-30 minute under arterial pressure into the deep white matter adjacent to the basal ganglia of canines. The needle was pointed 20 degrees lateral to the vertical axis. The complications encountered in this study were the increased frequency of transtentorial herniation. Hence, they then used smaller injection volumes ranging from 2.8 to 5.5 mL which successfully induced formation of ICH with fewer complications (Qureshi *et al* 1999b). In 1999, Lee et al made use of an infusion pump for injection of 3-5 ml of non-heparinized autologous arterial blood into the temporo-parietal cortex (Lee *et al* 1999). This method took eight minutes in canine subjects and allowed for the formation of consistently-sized clots.

In 1985, the microballoon method was used by Takasugi et al (Takasugi *et al* 1985) who modified this method by injecting venous blood directly into the balloon as an attempt to minimize reflux. This model mimicked both the increased pressure and blood volume following ICH. Using this model, Takasugi was able to classify the chronological

stages after ICH and concluded that the increased repair time after ICH was correlated to the degree of histologic injury to the surrounding tissue, rather than to the size of the hematoma itself.

Pigs

Known for their large, gyrated brain and well-developed white matter, the large hematoma volume in pigs post-ICH enables a closer examination of the area compared to other animal species (Wagner *et al* 1996). In 1996, Wagner et al (Wagner *et al* 1996) developed a lobar hemorrhage model in pigs where 1.7 ml of autologous arterial blood was slowly injected using an infusion pump into the frontal white matter. The slow injection reduced the likelihood of ventricular rupture or leakage of blood along the needle track. Compared with rapid infusions at high pressures, this method more closely modeled ICH in humans where bleeding generally originates from small intraparenchymal arteries. In 2000, Kuker et al (Kuker *et al* 2000) injected 0.5 to 2.0 ml of venous blood with a blood reservoir into the anterior frontal lobe to study the characteristics of hematomas using magnetic resonance imaging. This study used Takasugi's method of prior microballoon catheter insertion to reduce needle pathway reflux. A different study in 2002 led by Rohde et al (Rohde *et al* 2002)modified this model into a double-injection procedure (with a main injection of 2 to 3 ml of autologous venous blood with blood reservoir in their study) to better prevent post-injection reflux. Pigs were also used in collagenase injection models. Collagenase infusions of 10 μl by micro-infusion pump over 20 to 30 minutes were made into the right somatosensory cortex by Mun-Bryce et al in 2001 (Mun-Bryce *et al* 2001). This study examined tissue

excitability following ICH and evaluated the outcomes using magnetic resonance imaging in addition to electro- and magneto-encephalography. Use of collagenase, which is released from injured cells (Nath *et al* 1986), does address the clinically relevant phenomenon of vasogenic edema following ICH. The levels of collagenase however, are far above those encountered in clinical ICH and therefore correlations must take this into account.

Small Animal Models

Rabbits

Rabbits were first used by Kaufman et al in 1985 (Kaufman *et al* 1985) in a single autologous blood injection model. The study failed to yield conclusive results and in fact, the rabbit died shortly after injection. A decade later, arterial blood was injected using an infusion pump by Koeppen et al (Koeppen *et al* 1995). Arterial blood extracted from the ear was injected into the right thalamus and to minimize reflux, needle withdrawal was delayed. The study found that subjects exhibited a reduction in neurobehavioral deficits. Compared to larger animal models, use of rabbits is less costly, meets a higher success rate, and allows for an extended period of study with less mortality. Qureshi et al in 2001 (Qureshi *et al* 2001) modified this model in order to look at patterns of cellular injury. In this model, a 30-gauge needle penetrated the brain, while autologous arterial blood was infused into the white matter of the left frontal lobe. Instead of using arterial blood, Gustafsson et al in 1999 (Gustafsson *et al* 1999) used autologous venous blood which was injected manually in the brain. Although a hematoma did form, the use of venous blood differs from what is seen in humans.

Rats

The earliest rat model using a single arterial blood injection method was conducted in 1982 by Ropper et al (Ropper and Zervas 1982). The study reported that blood and not the mass effect as was previous postulated, was responsible for the changes in regional cerebral blood flow. Unfortunately because of the nature of the design, certain outcomes could not be evaluated-the disadvantage of using donor blood introduces various immune reactions while the lack of arterial pressure fails to mimic a true human ICH experience. Additionally, variability in outcomes was an issue because of the potential for reflux up the needle tract and the potential for blood volume discrepancies. Several of these issues were addressed later by Bullock et al in 1984 (Bullock *et al* 1984). For instance, blood infusion was conducted more rapidly under arterial pressure, and in a smaller time window (10 sec); however, it was difficult to reproduce reliably. The blood pressure variations from animal to animal resulted in different injury volumes and the small time window required significant technical mastery. This was followed by development of a method which instead held the rate of infusion constant using microinfusion pumps (Yang *et al* 1994). The use of microinfusion pumps allowed production of a controllable and reproducible lesion with a slower injection rate and a lower pressure than in an arterial pressure model (100 mmHg). A remaining shortcoming was that a more rapid injection rate resulted in a variable reflux of blood along the needle track and poorly reproducible lesions.

To address the issue of needle tract reflux, the double injection method was developed by Deinsberger et al in 1996 (Deinsberger *et al* 1996). In this model, a smaller volume of blood was first infused, allowing for clot formation and a reduction in blood

reflux. While technically challenging, this technique met with great success in reproducibility and minimization of pathway reflux. The use of venous blood in the single blood injection model was addressed by Masuda et al in 1988 (Masuda *et al* 1988). While they described a significant success rate in the production of intraparenchymal hematomas, the use of venous blood did not faithfully replicate the conditions in the major form of clinical ICH, which involves rupture of an arterial vessel.

In 1990, Rosenberg et al established a new model for spontaneous ICH using bacterial collagenase infused directly into the brain in Sprague-Dawley rats (Rosenberg *et al* 1990). This model was especially popular because it was the closest mimicker of spontaneous ICH in human beings (Andaluz *et al* 2002).

Mice

The ICH model in mice was derived from experiments in rats. A single arterial blood injection into the right basal ganglia in mice was described by Nakamura et al in 2004 (Nakamura *et al* 2004). This study compared the effects of autologous arterial blood, donor whole blood, and saline injections to brain edema development. The study found that donor blood injection was associated with a significantly greater increase in edema in the ipsilateral cortex compared to an autologous blood injection model.

In 2003, Belayev et al (Belayev *et al* 2003) placed a cannula into the left striatum and injected 5 µl of heparinized cardiac blood from a donor mouse. Following the injection, seven minutes were given for clotting to occur, and a final injection of blood was given (10 µl). Double injection methods, such as this one in mice, were met with great success because of their consistency. Soon after, a triple injection method in mice

was developed using venous blood by Ma et al in 2006 (Dimitrijevic *et al* 2006). Two infusions of 5 µl of blood were separated by a seven minute pause for clot formation. After the second infusion, a one minute pause was given for additional formation, followed by a 20 µl infusion of blood. This method also produced consistent outcomes.

In 2008, Rynkowski et al (Rynkowski *et al* 2008) published a protocol for a modified double blood injection model in mice. In this model, 30 µl of autologous blood from the central tail artery was injected directly into the right stratium in two steps as previously described (Belayev *et al* 2003). In both the double and triple injection mouse models, potential immunoreactive blood from other mice was used, and although heparinized to minimize clot formation, it prevented proper study of pathologic processes associated with the hematoma formation.

In 1997, Choudri et al (Choudhri *et al* 1997) first utilized the previously established rat model for collagenase injection in mice by infusing 1 µl of bacterial collagenase into the right basal ganglia over four minutes. This was followed by Clark et al in 1998 (Clark *et al* 1998) who performed a two minute injection of 0.5 µl volume collagenase into the right caudate and globus pallidus, followed by a three minute delay to reduce tract reflux. Additionally, Clark's group performed a 28-point neurobehavioral evaluation at 24 and 48 hours. Neurobehavioral scoring has since been adopted by other groups as a way to follow functional differences with administration of various substances meant to worsen or improve the injury in ICH (Clark *et al* 1998; Thiex *et al* 2004).

Both rats and mice have been widely used in research because of their feasibility and ease with which to anesthetize compared to larger animals. Transgenic systems exist

primarily in mice, making this the optimal model for studying genomic effects on ICH and secondary mechanisms of injury. However, the relatively small size makes them difficult to implement techniques that are used in larger animals.

Conclusion

In this review, we looked at the three main models that have been developed to understand the physiology behind ICH-microballoon infusion, collagenase injection, and autologous blood injection model. Additionally, we compared the various animals species that have been used to conduct these experiments, including monkeys, canines, pigs, rabbits, mice, and rats. Although there are no ideal subjects or models that can mimic the natural process in humans, each model can be used to study certain aspects of the pathophysiological process behind an ICH. In the future, the ideal ICH model should have characteristic that can model spontaneous intracerebral hemorrhage in humans and allow for effective studies on physiology, procedural interventions, and mechanisms of secondary brain injury.

Specific Aims

The objective of our study is to determine the mechanisms by which inflammation and thrombin respectively lead to perihematomal brain edema in experimental ICH. We will investigate an inflammatory mediator, vascular adhesion protein-1 (VAP-1) and a thrombin pathway receptor, platelet derived growth factor receptor alpha (PDGFR-α). **Our central hypothesis is that the inhibition of an inflammatory mediator or a thrombin pathway receptor will attenuate brain edema, and improve neurological**

function in ICH mouse models. To verify the importance of these key factors, we will test our hypothesis with the two following specific aims.

Specific Aim 1 is to determine the role of VAP-1 in inflammation and brain edema in two ICH mouse models. Our specific hypothesis is that VAP-1 inhibition will attenuate brain edema via reduction of leukocytes infiltration and inflammatory mediators, thus improving neurological outcome in ICH mouse models.

Sub-aim 1A: Examine the effect of VAP-1 inhibition on brain edema and neurological deficits in a collagenase-injection ICH mouse model (cICH).

Sub-aim 1B: Confirm the role of VAP-1 in inflammation after ICH by modulating VAP-1 activity.

Sub-aim 1C: Examine the effect of VAP-1 inhibition on brain edema and neurological deficits in a blood-injection ICH mouse model (bICH).

Specific Aim 2 is to determine the role of PDGFR-α in ICH-induced brain injury in mice and its mechanism in BBB disruption. Our specific hypothesis is that suppression of the thrombin pathway receptor, PDGFR-α, will preserve BBB integrity, reduce brain edema and improve neurological function via p38 MAPK mediated MMP activation/expression in an ICH mouse model.

Sub-aim 2A: Determine the outcome of PDGFR-α suppression on BBB preservation and brain edema in a bICH mouse model.

Sub-aim 2B: Determine whether PDGFR-α disrupts BBB integrity via p38 MAPK mediated MMP activation in both bICH and naïve mice.

Sub-aim 2C: Investigate the role of thrombin in PDGFR-α activation in both bICH and thrombin injection model.

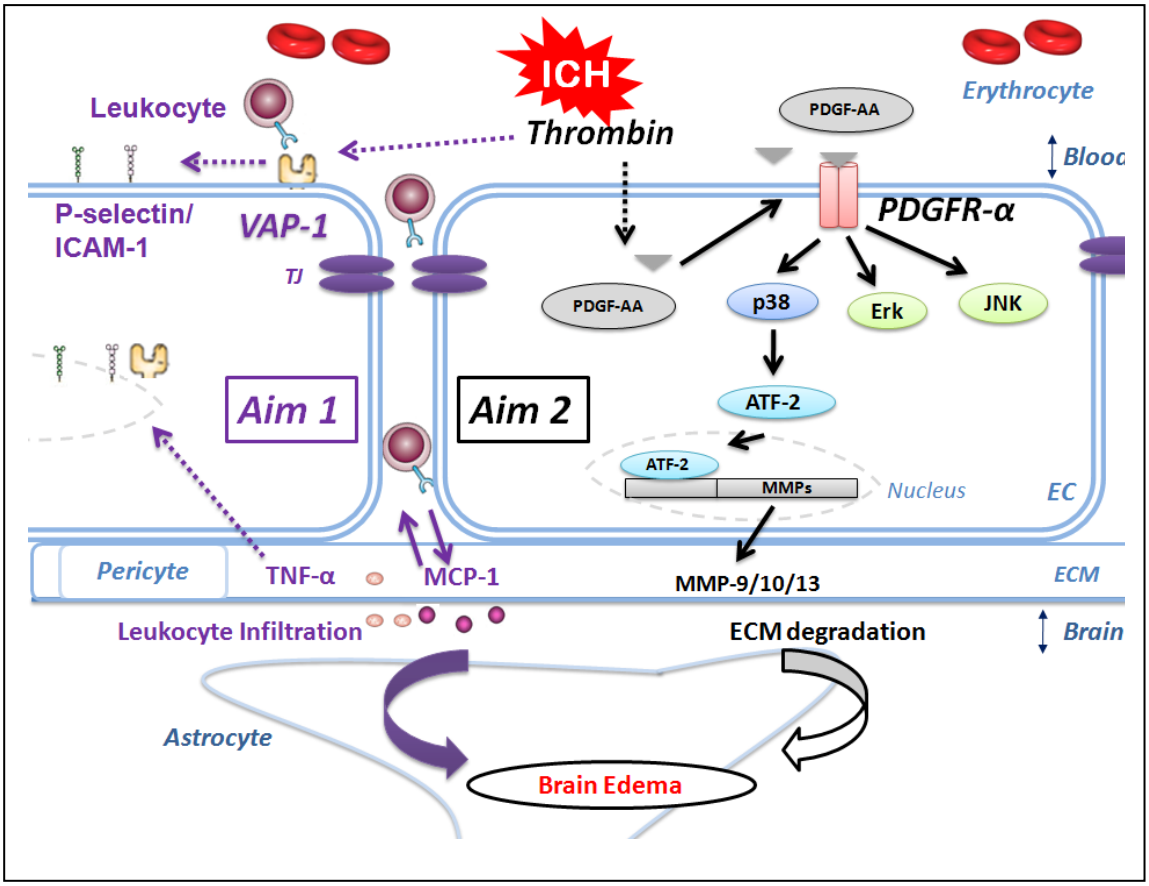

Figure 3 Schematic for the VAP-1 mediated leukocyte transmigration and PDGFR-α activation within the neurovascular unit following ICH. Thrombin is the potential upstream regulator of VAP-1 and PDGFR-α. **Aim 1:** VAP-1 mediates transmigration of leukocyte into brain parenchyma. Infiltrated leukocytes will release pro-inflammatory cytokines, enhance adhesion molecules expression and tight junction opening, finally lead to brain edema. **Aim 2;** Thrombin upregulates PDGF-AA expression and activates PDGFR-α which triggers the downstream MMPs activation/expression via p38-ATF-2 pathway. This ultimately leads to BBB disruption and brain edema.

CHAPTER TWO

VASCULAR ADHESION PROTEIN-1 INHIBITION PROVIDES ANTI-INFLAMMATORY PROTECTION FOLLOWING AN INTRACEREBRAL HEMORRHAGIC STROKE IN MICE

Qingyi Ma[a], Anatol Manaenko[a], Nikan H. Khatibi[b], Wanqiu Chen[a], John H. Zhang[a,b,c], Jiping Tang[a]

[a] Department of Physiology and Pharmacology, Loma Linda University

[b] Department of Anesthesiology, Loma Linda Medical Center

[c] Department of Neurosurgery, Loma Linda Medical Center

Published: ***J Cereb Blood Flow & Metab.*** 2011 Mar;31(3):881-93.

Abstract

The systemic immune response plays a vital role in propagating the damage of an intracerebral hemorrhage at the site of local injury. Vascular adhesion protein-1 (VAP-1), a semicarbazide-sensitive- amine-oxidase, was found in previous studies to play a role in migration of immune cells. In the present study, we hypothesize that VAP-1 inhibition may decrease brain injury by attenuating the transmigration of immune cells to the injury site, and by doing so, reduce cerebral edema and improve neurobehavioral function in mice. Two VAP-1 inhibitors, LJP1586 and semicarbazide (SCZ) were given 1 h after ICH induction by either collagenase or autologous blood-injection. VAP-1 siRNA, a VAP-1 gene silencer, and human recombinant AOC3 protein, a VAP-1 analogue, were delivered by intracerebroventricular injection. Post assessment included neurobehavioral testing, brain edema measurement, quantification of neutrophil infiltration and microglia/macrophage activation, and measurement of ICAM-1, P-selectin, MCP-1 and TNF-α expression 24 h after ICH, neurobehavioral testing and brain edema measurement also did at 72 h in cICH. We found that LJP1586 and SCZ reduced brain edema and neurobehavioral deficits 24 h after ICH induction. These two drugs were also found to decrease levels of ICAM-1, MCP-1, TNF-α, and inhibit neutrophilic infiltration and microglia/macrophage activation. We conclude that VAP-1 inhibition provided anti-inflammation effect by reducing adhesion molecule expression and immune cell infiltration after ICH.

Keywords: brain edema, inflammation, intracerebral hemorrhage (ICH), anti-inflammation, vascular adhesion protein-1 (VAP-1)

Introduction

Intracerebral hemorrhage (ICH) is a fatal stroke subtype that affects roughly 120,000 individuals in the United States each year (Ribo and Grotta 2006). Responsible for 10-15% of all strokes, ICH accounts for one of the highest morbidity and mortality rates, leaving those individuals who survive with lasting disabilities (Dennis *et al* 1993). As the population in the world continues to shift towards an aged majority, the incidence of ICH will be expected to grow and the demand for a better understanding of the pathophysiology will be expected.

The inflammatory response in an ICH is characterized by activation of local immune cells such as microglial cells. This local inflammatory reaction is partly responsible for the damages to the brain following injury. However, mounting evidence suggests that accumulation of systemic immune cells, specifically blood-derived leukocytes, are the primary orchestrators of this damage (Wang and Dore 2007). Infiltration of these systemic immune cells result in enhanced disruption of the blood-brain-barrier (BBB), causing an increase in cerebral edema formation, and subsequent deterioration in neurobehavioral function. As a result, studies have re-directed their attention to focus more on preventative measures that can decrease the accumulation of systemic immune cells to the site of injury. In focal ischemic stroke models, investigators found that systemic immune cell recruitment was mediated in part by the increase in adhesion molecule expression along the endothelial cell walls (Yilmaz and Granger 2008). As a result, these systemic immune cells propagated the local immune response by releasing pro-inflammatory cytokines at the site of injury, increasing cerebral edema and

worsening neurobehavioral function (Aronowski and Hall 2005; Barone and Feuerstein 1999; Emsley and Tyrrell 2002).

Vascular adhesion protein-1 (VAP-1), a cell-surface expressed glycoprotein, has recently emerged as a potential target for inflammatory regulation in the brain. Classified as a semicarbazide- sensitive-amine-oxidase (SSAO)(Salmi and Jalkanen 1992), VAP-1 can also function as an adhesion molecule, promoting leukocyte adhesion and transmigration. Under normal conditions, VAP-1 is expressed within cytosolic vesicles of endothelial cells where it remains dormant. However, under inflammatory conditions, VAP-1 migrates to the luminal surface of endothelial cells within the blood vessels where it mediates binding and transmigration of systemic immune cells into tissues, disrupting the BBB along with it (Salmi and Jalkanen 2005).

As a result in the present study, we investigated the role of VAP-1 in ICH-induced brain injury, specifically investigating its role in regulating the systemic immune response. We hypothesize that VAP-1 blockage will attenuate the infiltration of systemic immune cells by downregulating adhesion molecule expression and therefore, improve neurologic outcomes. In order to test this aim, we used a small molecule VAP-1 inhibitor, LJP1586 (O'Rourke *et al* 2008) to inhibit the VAP-1 activity. Additionally, since the SSAO enzyme activity is necessary for leukocyte transmigration (Koskinen *et al* 2004), another VAP-1 inhibitor, semicarbazide, was used as testament to the anti-inflammatory effects of LJP1586. Additionally, we injected VAP-1 siRNA, a VAP-1 gene silencer, to specify the inhibition of VAP-1, as well as recombinant AOC3 protein, a VAP-1 analogue, to neutralize the effect of LJP1586.

Materials and Methods

Animals

All procedures for this study were approved by the Animal Care and Use Committee at Loma Linda University and complied with the NIH Guide for the Care and Use of Laboratory Animals (National Institutes of Health Publication 85-23, revised 1985) and with Guidelines for the Use of Animals in Neuroscience Research by the Society for Neuroscience. Eight week old male CD1 mice (weight 35-45 grams, Charles River, MA, USA) were housed in a 12-hour light/dark cycle at a controlled temperature and humidity with free access to food and water. During surgery, body temperature was monitored and kept constant. Following surgery using one of the two established models, either the collagenase-ICH (cICH), or blood-ICH (bICH), the skull hole was closed with bone wax, the incision was closed with sutures, and the mice were allowed to recover. To avoid postsurgical dehydration, 0.5 ml of normal saline was given to each mouse by subcutaneous injection immediately following surgery.

Intracerebral Hemorrhage Mouse Models and Treatment (Figure 4)

ICH model was induced by collagenase injection (cICH) as previously described (Rosenberg *et al* 1990; Tang *et al* 2004; Tang *et al* 2005). Briefly, mice were anesthetized with ketamine (100 mg/kg) and xylazine (10 mg/kg) (2:1 v/v, intraperitoneal injection) and positioned prone in a stereotactic head frame (Kopf Instruments, Tujunga, CA). A cranial burr hole (1 mm) was drilled near the right coronal suture 1.4 mm lateral to the midline. A 27-gauge needle was inserted stereotactically into the right basal ganglia coordinates: 0.9 mm posterior to the bregma, 1.4 mm lateral to the midline, and 4 mm below the dura. Collagenase (VII-S, Sigma; 0.075 U in 0.5 ul of saline) was infused

into the brain over 2 min at a rate of 0.25 ul/min with a microinfusion pump (Harvard Apparatus, Holliston, MA). Sham-operated mice were subjected to needle insertion only. The needle was left in place for an additional 10 min after injection to prevent possible leakage of the collagenase solution.

Three experiments were carried out in the cICH model. 1. Mice were divided into four groups: sham (n=22), vehicle (ICH, n=32), LJP1586 treatment (3 mg/kg, 10 mg/kg, intraperitoneal injection, n=37) and semicarbazide treatment (100 mg/kg, 200 mg/kg, intraperitoneal injection, n=30). Both drugs were dissolved in phosphate-buffered saline (PBS, pH 7.4) and given 1 h after ICH induction. Both sham and vehicle animals received the same volume of PBS injection. 2. VAP-1 siRNA (Sigma Aldrich) was dissolved in sterilized water and given (100 pmol, 2 ul, intracerebroventricular injection) 48 h before ICH. The same volume of scramble siRNA (siGENOME Non-Targeting siRNA, Thermol Fisher Scientific) was administered as control. The animals were divided into five groups, sham (n=8), vehicle (ICH, n=8), siRNA plus sham (n=12), siRNA plus ICH (n=12), and scramble siRNA plus ICH groups (n=12). 3. Human recombinant AOC3 (VAP-1) protein (Abnova Co.) was given 10 min before ICH induction to neutralize the effects of LJP1586. Mice were divided into five groups: sham (n=8), vehicle (ICH, n=6), AOC3 (30 ng, 90 ng/animal, intracerebroventricular injection) plus LJP 1586 (10 mg/kg, intraperitoneal injection, n=22), AOC3 plus sham (n=6), and AOC3 plus ICH group (n=10).

ICH was induced using the autologous blood injection model (bICH) which was modified from previous descriptions (Belayev *et al* 2003; Rynkowski *et al* 2008; Wang *et al* 2008). Briefly, mice were anesthetized with ketamine (100 mg/kg) and xylazine (10

mg/kg) (2:1 v/v, intraperitoneal injection) and positioned prone in a stereotactic head frame (Kopf Instruments, Tujunga, CA). A scalp incision was made along the midline and a burr hole (1 mm) was drilled on the right side of the skull (0.2 mm anterior and 2.0 mm lateral of the bregma). The mouse tail was warmed with hot water for 2 min and then cleaned with 70% ethanol before cutting off 10 mm of the tail tip with sterilized surgical scissors. Next, 30 ul of autologous tail blood was collected in a capillary tube without heparin and blown into a 1cc insulin syringe. The syringe was fixed onto the microinjection pump while the needle was stereotaxically inserted into the brain through the burr hole. At first the needle was stopped at 0.7 mm above the target position and 5 ul of blood was delivered at a rate 2 μl/min. The needle was then advanced to the target position. After 7 min, the remaining 25 ul blood was injected at a rate of 2 μl/min. The needle was left in place for an additional 10 min after injection to prevent possible leakage and withdrawn slowly in 7 min.

Mice were treated with LJP1586 (10 mg/kg, intraperitoneal injection, n=6) or semicarbazide (200 mg/kg, intraperitoneal injection, n=6) 1 h after ICH induction. We also did sham (n=6) and vehicle group (n=7).

All animals were neurologically tested and sacrificed 24 h or 72 h after ICH induction. Evaluation of neurological function was carried out by a blind investigator. Brain samples were collected for measurement of brain water content, Western blot or immunohistochemistry.

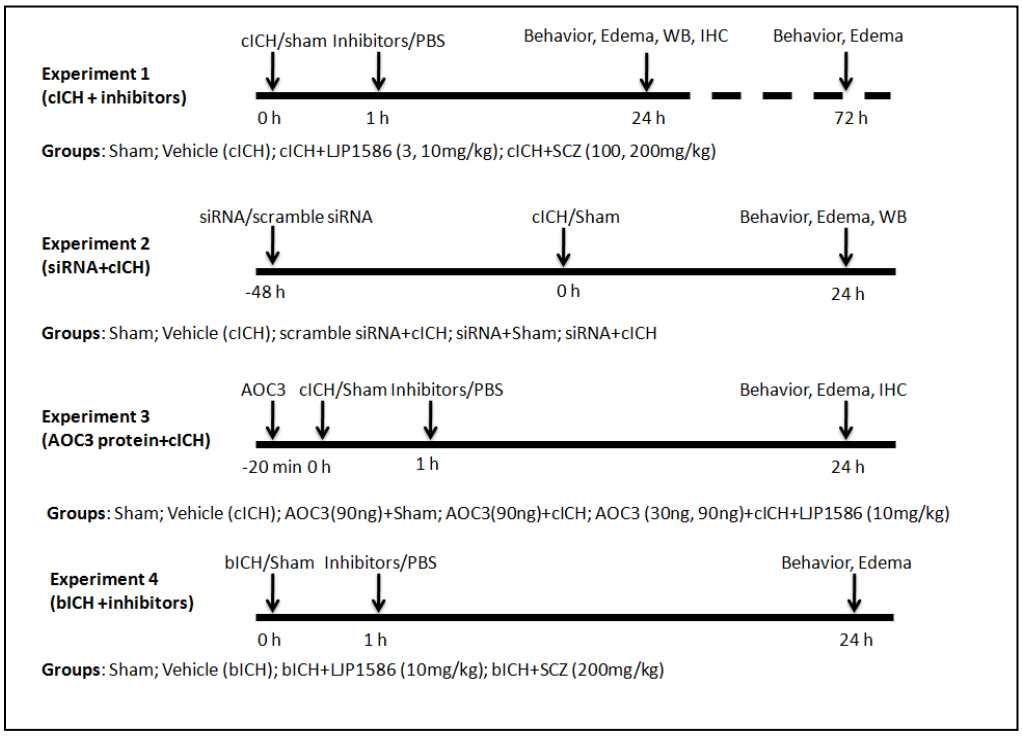

Figure 4: Experimental Design and Animal Group Classification

VAP-1 siRNA Injection

siRNA was administered by intracerebroventricular (ICV) injection to the mouse brain as previously described (Luo *et al* 2007). Briefly, mice were anesthetized with ketamine (100 mg/kg) and xylazine (10 mg/kg) (2:1 v/v, intraperitoneal injection) and positioned prone in a stereotactic head frame (Kopf Instruments, Tujunga, CA). A scalp incision was made along the midline and a burr hole (1 mm) was drilled in the right side of the skull (1.0 mm lateral of the bregma). According to the manufacture instructions, 2 ul (100 pmol) of VAP-1 siRNA (Sigma) suspended in sterile water or scramble siRNA was delivered into the ipsilateral ventricle with a Hamilton syringe over 2 min. The needle was left in place for an additional 5 min after injection to prevent possible leakage and then withdrawn slowly in 4 min. After the removal of the needle, the burr hole was sealed with bone wax, the incision was closed with sutures and the mice were allowed to recover. Intracerebral hemorrhage induced by collagenase injection was conducted 48 h later. Mice were sacrificed for edema measurement and VAP-1 protein expression 24 h after ICH. We did not measure the ICP because of the size challenges which mice impose. Furthermore, multiple invasive operations can affect study results quite unfavorably.

Human Recombinant AOC3 (VAP-1) Protein Injection

Human recombinant AOC3 (VAP-1) protein (Abnova Co.) was administered in the same manner as the VAP-1 siRNA injection described above. According to the manufacture's instruction, 1 µl (30 ng/mouse) or 3 µl (90 ng/mouse) protein solutions was delivered into the ipsilateral ventricle with a Hamilton syringe at a rate of 0.5 µl/min. The needle was left in place for an additional 5 min after injection to prevent possible leakage and withdrawn slowly in 4 min. After the removal of the needle, the burr hole

was sealed with bone wax. The collagenase was then injected into the ipsilateral basal ganglia to induce hemorrhage. Afterwards, the incision was closed with sutures and the mice were allowed to recover. Mice were sacrificed for edema measurement 24 h after ICH induction.

Hemorrhage Volume

Hemoglobin assay was used as previously described (Tang *et al* 2005). Briefly, mice were sacrificed 24 h after ICH and transcardially perfused with ice phosphate-buffered saline (PBS). Both ipsilateral and contralateral hemisphere were collected and kept in a -70 °C freezer. The ipsilateral hemisphere was homogenized for 60 sec in a tube with distilled water (total volume 3 mL). After centrifugation (12000 g, 30 min), 400 µl Drabkin's reagent (Sigma-Aldrich) was added into a 100 µl aliquots of the supernatant and allowed to react for 15 min. The absorbance of this solution was read with a spectrophotometer (540 nm) and the amount of blood in each brain was calculated using a standard curve generated with known blood volumes

Neurobehavioral Function Test

Neurobehavioral functions were evaluated by the modified Garcia test (Garcia *et al* 1995; Wu *et al* 2010). In the modified Garcia test, four items including side stroke, vibrissae touch, limb symmetry, and lateral turning were tested with a maximum neurological score able to be achieved at 12 (healthy animal). We also did performed the beam balance test (Zausinger *et al* 2000) and modified wire hanging test (Gerlai *et al* 2000) to further assess neurobehavior. The maximum score able to be reached per test

was 5 (data not shown). The behavior test was conducted at different time point after ICH induction by a blinded investigator.

Brain Water Content Measurement

Brain water content was measured as previously described (Tang *et al* 2004; Tang *et al* 2005; Tejima *et al* 2007). Briefly, mice were decapitated under deep anesthesia. Brains were immediately removed and cut into 4 mm sections. Each section was divided into four parts: ipsilateral and contralateral basal ganglia, ipsilateral and contralateral cortex. The cerebellum was collected as an internal control. Tissue samples were weighed on an electronic analytical balance (APX-60, Denver Instrument) to the nearest 0.1 mg to obtain the wet weight (WW). The tissue was then dried at 100°C for 24 h to determine the dry weight (DW). Brain water content (%) was calculated as [(WW - DW)/WW] x 100.

Western Blotting

Western Blotting was performed as described previously (Chen *et al* 2008; Ostrowski *et al* 2005). Animals were euthanized 24 h after ICH. Intracardiac perfusion with cold phosphate-buffered saline (PBS, pH 7.4) solution was performed, followed by removal of the brain and separation into ipsilateral and contralateral cerebrums. The brain parts were stored appropriately at -80°C immediately until analysis. Protein extraction from whole-cell lysates were obtained by gently homogenizing them in RIPA lysis buffer (Santa Cruz Biotechnology, Inc, sc-24948) with further centrifugation at 14,000 g at 4°C for 30 min. The supernatant was used as whole cell protein extract and the protein concentration was determined using a detergent compatible assay (Bio-Rad, Dc protein

assay). Equal amounts of protein (50 μg) were loaded on an SDS-PAGE gel. After being electrophoresed and transferred to a nitrocellulose membrane, the membrane was blocked and incubated with the primary antibody overnight at 4°C. The primary antibodies were goat polycolonal anti-ICAM-1 (Santa Cruz Biotechnology, 1:500), goat ploycolonal anti-P-selectin (Santa Cruz Biotechnology, 1:500), rabbit polyclonal anti-MCP1 (Abcam 1:1000), and rabbit polycolonal anti-TNF-alpha (Millipore, 1:1000). Nitrocellulose membranes were incubated with secondary antibodies (Santa Cruz Biotechnology) for 1h at room temperature. Immunoblots were then probed with an ECL Plus chemiluminescence reagent kit (Amersham Biosciences, Arlington Heights, IL) and visualized with the imagine system (Bio-Rad, Versa Doc, model 4000). The data were analyzed by the software Image J.

Assessment of Histology

At 24 h after ICH, mice were perfused under deep anesthesia with cold phosphate-buffered saline (PBS, pH 7.4), followed by infusion of 4% paraformaldehyde. The brains were then removed and fixed in formalin at 4°C for a minimum of 3 days. The brains were then dehydrated with 30% sucrose in phosphate-buffered saline (PBS, pH 7.4) and the frozen coronal slices (10 μm thick) were then sectioned in cryostat (CM3050S; Leica Microsystems). Immunohistochemistry was performed (Titova *et al* 2008) using the following primary antibodies: rabbit anti-Iba-1 antibody (Wako Chemicals USA, Inc) and rabbit anti-human myeloperoxidase polyclonal antibody (1:300; Dako Cytomation Inc.). The positive cell numbers were counted as previous described (Wang and Dore 2008). The number of immunoreactive cells from 12 locations per mouse (3 sections per

mouse, 4 fields per section, n=4, microscopic field 20x) were averaged and expressed as positive cells per field.

Statistical Analysis

Data were expressed as means ± s.e.m. Statistical difference between two groups was analyzed using the t-test. Multiple comparisons were statistically analyzed with one-way analysis of variance (ANOVA) followed by Tukey multiple comparison post-hoc analysis or Student-Newman-Keuls test. A p-value of less than 0.05 was considered statistically significant. For the rating scale data (neurobehavioral test), data were expressed as median ± 25th-75th percentiles. We used the Kruskal-Wallis One Way Analysis of Variance on Ranks, followed by the Steel-Dwass multiple comparisons tests. For the western blot data, we used the Kruskal-Wallis One Way Analysis of Variance on Ranks, followed by the Student-Newman-Keuls Method for Pairwise Multiple Comparison Procedures.

Results

VAP-1 Inhibition Had no Effect on Hemorrhagic Volume

Hemorrhagic volume was estimated at 24 h after collagenase injection by hemoglobin assay with spectrophotometry (Tang *et al* 2005). There was no statistical difference observed between cICH vehicle mice and 10 mg/kg LJP1586 treated mice (38.712 ± 2.35 µl, n=8 and 39.03 ± 2.32 µl, n=8, respectively; t_{14}= -0.0969, P=0.924; Figure 5A).

Neurobehavioral Deficits Improve with VAP-1 Inhibitors.

Two VAP-1 inhibitors were applied after cICH. LJP1586 is a selective, novel small molecule inhibitor of rodent and human VAP-1 activity with relative little effects on other monoamine oxidases. Its anti-inflammation effects have been studied in LPS-induced lung inflammation (O'Rourke *et al* 2008). Semicarbazide, a reference compound for inhibiting SSAO activity, was the other VAP-1 inhibitor (Mercier *et al* 2007).

To evaluate the sensorimotor deficits after cICH, the modified Garcia test was conducted at both 24 h and 72 h post-cICH. The results showed that vehicle mice presented with severe neurobehavioral deficits compared to sham mice ($P<0.05$ versus Sham). However, following treatment with high-dose LJP1586 (10 mg/kg) and high-dose semicarbazide (10 mg/kg), a significant improvement in neurobehavioral function was seen with the modified Garcia test at both 24 h and 72 h ($P<0.05$ versus Vehicle, Figure 5B). For the beam balance test, a significant improvement in neurobehavioral function was seen following treatment with high-dose LJP1586 and high-dose semicarbazide at both 24 h and 72 h ($P<0.05$ versus Vehicle, data not shown); however, in the wire hanging test, high-dose LJP1586 (10 mg/kg) dramatically improved neurobehavioral function compared to vehicle group at both 24 h and 72 h ($P<0.05$ versus Vehicle, data not shown), while high-dose semicarbazide significantly improved neurobehavioral function only at 72 h ($P<0.05$ versus Vehicle, data not shown).

Overall, it was found that VAP-1 inhibitors could improve neurobehavioral functions in a cICH model at both acute and delayed stages.

Brain water content was also measured 24 h and 72 h post-cICH (Figure 5C, D). Following treatment with low-dose (3 mg/kg) and high-dose (10 mg/kg) LJP1586, brain edema was found to be significantly reduced in the ipsilateral basal ganglia compared to

vehicle groups (Ipsilateral basal ganglia: 24 h, 3 mg/kg, 80.53 ± 0.30 vs. Vehicle, 81.82 ± 0.32, $P<0.05$; 10 mg/kg, 80.41 ± 0.27 vs. Vehicle, 81.82 ± 0.32, $P<0.01$; 72 h, 10 mg/kg, 80.92± 0.17 vs. Vehicle, 82.96 ± 0.21, $P<0.05$). In the ipsilateral cortex, high-dose LJP1586 (10 mg/kg) significantly reduced brain edema compared to vehicle (Ipsilateral cortex: 24 h, 10 mg/kg, 79.21 ± 0.15 vs. Vehicle, 80.31 ± 0.29, $P<0.05$; 72 h, 79.70 ± 0.12 vs. Vehicle, 80.37 ± 0.18, $P<0.05$). With high-dose semicarbazide treatment (200 mg/kg), brain edema decreased in the ipsilateral basal ganglia compared to vehicle at both 24 h and 72 h (ipsilateral basal ganglia: 24 h, 200 mg/kg, 80.68 ± 0.16 vs. Vehicle, 81.82 ± 0.32, $P<0.05$; 72 h, 81.17 ± 0.24 vs. Vehicle, 82.96 ± 0.21, $P<0.05$), however, in the ipsilateral cortex, only post-treatment at 72 h significantly reduced brain water content (Ipsilateral cortex: 200 mg/kg, 79.76 ± 0.10 vs. Vehicle, 80.37 ± 0.18, $P<0.05$).

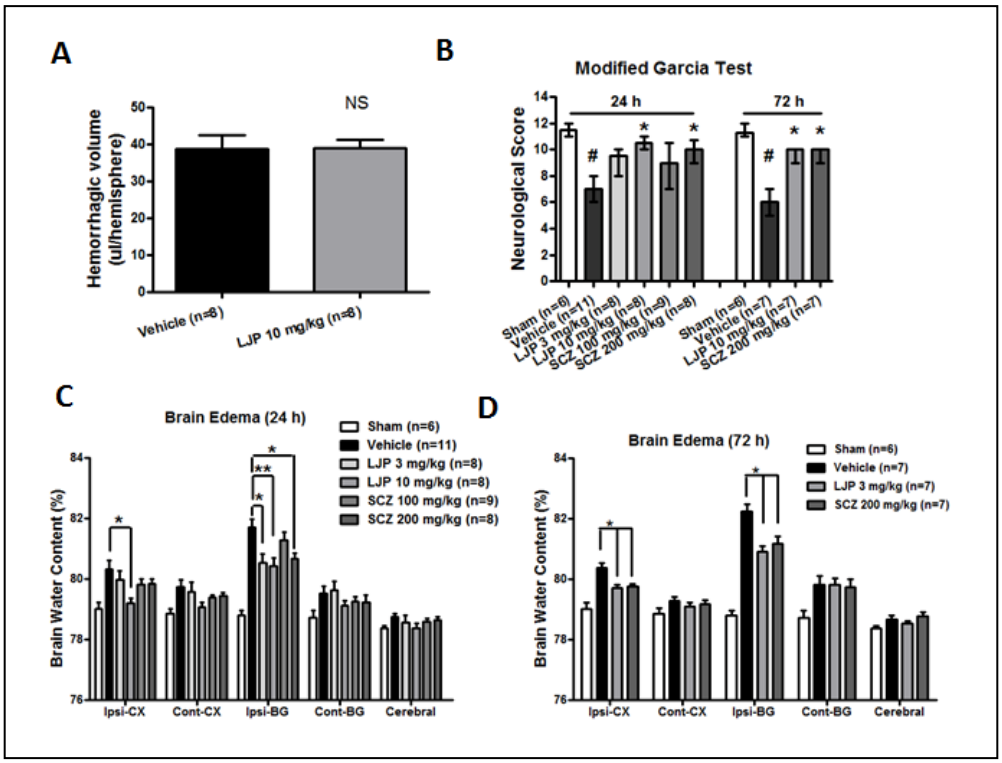

Figure 5. Effect of VAP-1 inhibitors, LJP1586 and semicarbazide (SCZ) on hemorrhagic volume, neurological score and brain water content at 24 h and 72 h after cICH in mice. ***A***, Result of hemoglobin assay for hemorrhagic volume in vehicle and LJP1586 (10 mg/kg) treated mice (n=8). NS, not significant. ***B***, The neurological score for the modified Garcia test (healthy animal: 12) at 24 h and 72 h in Sham, ICH and ICH with treatments. ***C***, LJP1586 and SCZ reduced brain water content at 24 h after cICH in mice. Brain samples were collected from Sham, ICH and ICH with treatments. ***D***, The neurological score for the modified Garcia test (healthy animal: 12) at 72 h in Sham, ICH and ICH with treatments. Brain sections (4 mm) were divided into four parts: ipsilateral basal ganglia (Ipsi-BG), ipsilateral cortex (Ipsi-CX), contralateral basal ganglia (Cont-BG), contralateral cortex (Cont-CX). Cerebellum (Cerebel) is the internal control. # $P<0.05$ versus Sham. * $P<0.05$ versus Vehicle. ** $P<0.01$ versus Vehicle.

VAP-1 Inhibitors Down-Regulate Levels of ICAM-1, MCP-1, and TNF-α after ICH Injury

In an *in vitro* study, VAP-1 was found to produce biologically active mediators that could act as signals to induce expression of E- and P-selectins, as well as intercellular adhesion molecule-1 (ICAM-1) in endothelial cells (Jalkanen *et al* 2007). As a result, we investigated whether VAP-1 activity had any effect on the expression of adhesion molecules, i.e. ICAM-1, P-selectin, 24 h post-ICH injury. Additionally, in the development of choroidal neovascularization (CNV), the expression of a number of inflammatory molecules such as TNF-α and MCP-1 was suppressed after VAP-1 blockade (Noda *et al* 2008). As a result, we also studied the effect of VAP-1 inhibition on cytokine expression, looking specifically at MCP-1 and TNF-α.

Our results demonstrated that cICH injury produced a significant increase in the expression of P-selectin ($P<0.05$ versus Sham, Figure 6A) and ICAM-1 ($P<0.01$ versus Sham, Figure 6B). Treatment with high-dose LJP1586 (10 mg/kg) and semicarbazide (200 mg/kg) significantly decreased the expression of P-selectin ($P<0.05$ versus Sham, Figure 6A) and ICAM-1($P<0.05$ versus Vehicle, Figure 5B). Levels of the pro-inflammatory cytokines MCP-1 and TNF-α were significantly increased 24 h post-cICH (MCP-1, $P<0.01$; TNF-α, $P<0.05$ versus Sham, Figure 6C,D). Treatment with high-dose LJP1586 (10 mg/kg) and semicarbazide (200 mg/kg) markedly reduced the level of MCP-1 and TNF-α ($P<0.05$ versus Vehicle, Figure 6C,D).

VAP-1 Inhibition Blocks Migration of Systemic Neutrophils and Microglia/Macrophage Activation.

In order to determine the effect VAP-1 had on inflammatory cells, we checked neutrophilic infiltration by MPO staining and microglia/macrophage activation by Iba-1 staining. At the same time, quantification of both the MPO and Iba-1 positive cells in the perihematomal area were determined. The results demonstrated that post-treatment with LJP1586 at 24 h showed a significant reduction in the MPO positive cell numbers (11.89 ± 2.57, n=4 and 25.03 ± 1.31, n=4 respectively; t_6=4.547, P=0.01; Figure 7A,C) while the microglia/macrophage activation was also attenuated in the perihematomal area compared with vehicle mice (4.23 ± 0.57, n=4 and 7.81 ± 0.50, n=4 respectively; t_6=4.731, P=0.003; Figure 7D,E).

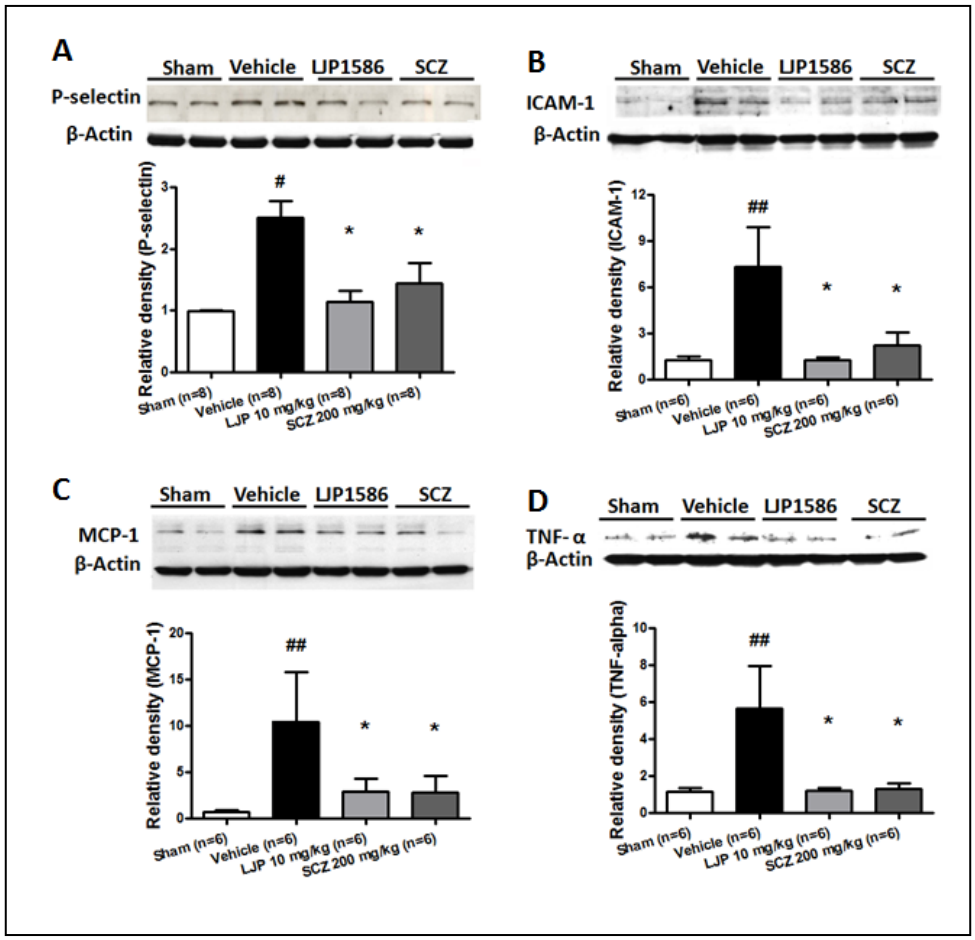

Figure 6: Adhesion molecules and pro-inflammatory cytokine levels were increased in vehicle group and decreased by VAP-1 inhibitors 24 h after cICH in mice. ***A***, Analysis of P-selectin level in ipsilateral hemisphere at 24 h following ICH by Western blot. NS, not significance. ***B***, Analysis of ICAM-1 level in ipsilateral hemisphere at 24 h following ICH by Western blot. ***C***, Analysis of MCP-1 level in ipsilateral hemisphere at 24 h following ICH by Western blot. ***D***, Analysis of TNF-α level in ipsilateral hemisphere at 24 h following ICH by Western blot. All the brain samples were ipsilateral hemisphere collected from Sham, ICH and ICH with treatments (LJP1586: 10 mg/kg; SCZ: 200 mg/kg). ## P < 0.01 versus Sham group. # *P*<0.05 versus Sham. * *P*<0.05 versus Vehicle, n=6-8.

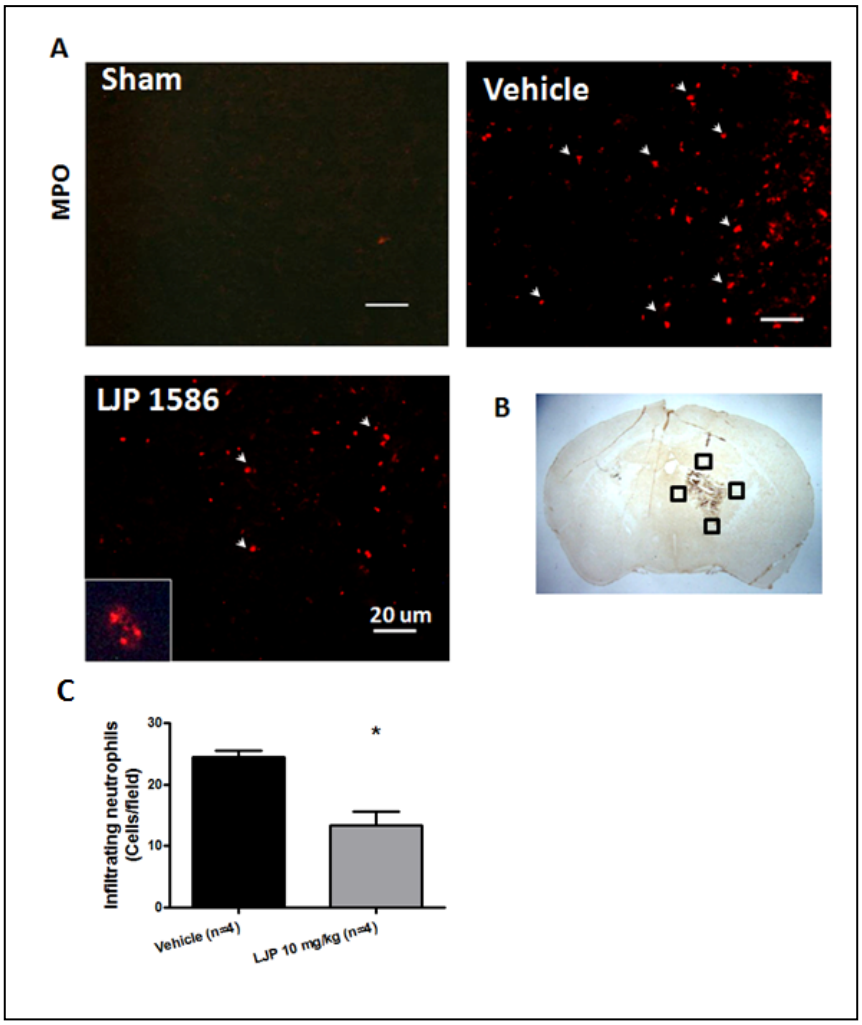
A
MPO
Sham
Vehicle
LJP 1586
20 um
B
C
Infiltrating neutrophils (Cells/field)
30
20
10
0
*
Vehicle (n=4)
LJP 10 mg/kg (n=4)

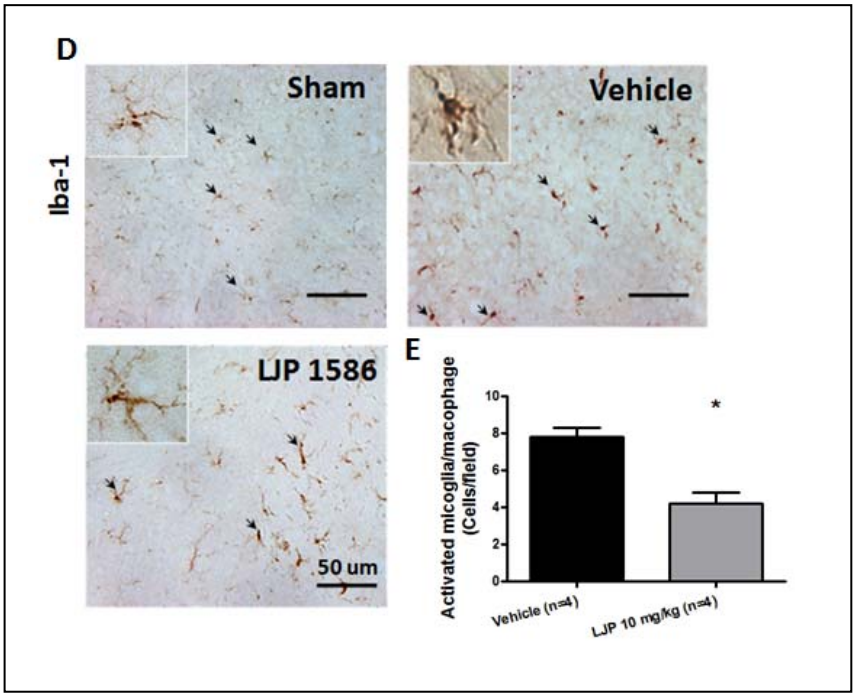
D
Iba-1
Sham
Vehicle
LJP 1586
50 um
E
Activated microglia/macophage (Cells/field)
10
8
6
4
2
0
*
Vehicle (n=4)
LJP 10 mg/kg (n=4)

Figure 7: Effect of VAP-1 inhibitor, LJP1586 on neutrophils infiltration and microglia/macrophage activation in the perihematomal region 24 h after cICH in mice. ***A***, Represented photograph of immunofluorescence staining for myeloperoxidase (MPO) showing that the MPO positive cell were increased in vehicle group and decreased in LJP1586 treatment (10 mg/kg) group at 24 h after ICH. Sections from mice brain were probed with anti-MPO antibody and rabbit TX Red secondary antibody (red). Scale bars, 20 μm. ***B***, The schematic diagram shows the four areas (black squares) for the MPO positive cells counting in the perihematomal region. ***C***, Bar graph illustrating the quantification of MPO positive cells in the perihematomal region at 24 h in Sham, Vehicle and LJP 1586 treatment (10 mg/kg) (12 fields/brain). It showed that inhibition of VAP-1 significantly reduced the number of MPO positive cells. ***D***, Represented photograph of immunohistochemistry staining for Iba-1 positive cells showed that the activated microglia/macrophage was increased in vehicle group and decreased in LJP1586 treatment (10 mg/kg) group 24 h after ICH. Sections from mice brain were probed with rabbit anti-Iba1 antibody and goat anti-rabbit secondary antibody. Scale bars, 50 μm. ***E***, Bar graph illustrating the quantification of Iba-1 positive cells in vehicle and LJP 1586 treatment (10 mg/kg) in the perihematomal region (12 fields/brain). The data revealed that VAP-1 inhibition by LJP1586 significantly reduced the number of activated Iba-1 positive cells. * $P<0.05$ versus Vehicle group, n=4.

VAP-1 siRNA Decreases VAP-1 Levels after ICV Injection.

To examine the specificity of the anti-inflammatory effects of VAP-1 inhibitors, VAP-1 siRNA as well as scramble siRNA (nontargeting siRNA) was given 48 h prior to cICH induction. Protein levels of VAP-1 where then detected in the ipsilateral hemisphere by western blot at 24 h. In sham mice, siRNA injection significantly reduced VAP-1 levels ($P<0.05$, Figure 8A). Compared with scramble siRNA injection, VAP-1 levels in cICH mice were significantly decreased with siRNA injection ($P<0.05$, Figure 8A). Additionally, neurobehavioral functions and brain edema were evaluated 24 h post-cICH induction. Compared with cICH mice, the siRNA injected mice showed an improvement in neurobehavioral functions ($P<0.05$ versus Vehicle, Figure 8B). Moreover, brain edema in the ipsilateral basal ganglia was also significantly reduced (Ipsilateral basal ganglia: siRNA+ICH, 81.73±0.23 vs. ICH, 82.75 ± 0.27, $P<0.05$, Figure 8C).

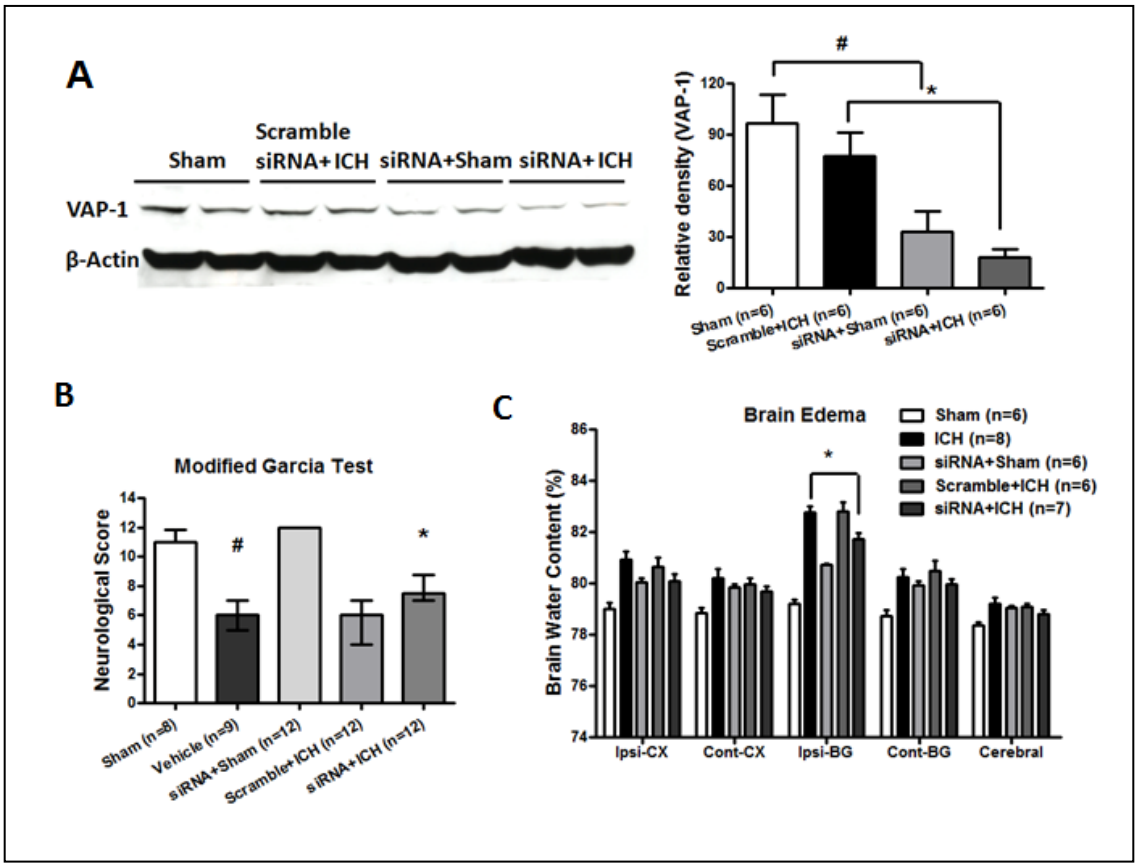

Figure 8: Effect of VAP-1 siRNA on neurological score and brain water content at 24 h after cICH in mice. VAP-1 siRNA was injected 48 h before ICH and brain samples were collected 24 h after ICH from Sham, siRNA+Sham, scramble siRNA+ICH and siRNA+ICH. VAP-1 siRNA was injected 48 h before ICH while neurobehavioral function and brain water content were evaluated 24 h after ICH. VAP-1 siRNA improved neurobehavioral functions and decreased brain water content 24 h after collagenase-induced ICH in mice. ***A,*** Western blotting with rabbit anti-VAP-1 antibody showed that the VAP-1 level in the ipsilateral hemisphere was reduced 72 h after VAP-1 siRNA injection in a collagenase-induced intracerebral hemorrhage. ***B,*** The neurological score for the modified Garcia test (healthy animal: 12) at 24 h in Sham, siRNA+Sham, ICH, non+ICH and siRNA+ICH. ***C***, VAP-1 siRNA reduced brain water content 24 h after ICH. Brain samples were collected from Sham, siRNA+Sham, ICH, nontargeting siRNA+Sham and siRNA+ICH. Brain sections (4 mm) were divided into four parts: ipsilateral basal ganglia (Ipsi-BG), ipsilateral cortex (Ipsi-CX), contralateral basal ganglia (Cont-BG), contralateral cortex (Cont-CX). Cerebellum (Cerebel) is the internal control. "non+ICH" presented nontargeting (scramble) siRNA+ICH. # $P<0.05$ versus Sham group. * $P<0.05$ versus Vehicle group. For western blot, * $P<0.05$ versus Scramble siRNA +ICH group.

Human Recombinant AOC3 (VAP-1) Protein Abolishes the Anti-inflammatory Effects of the VAP-1 Inhibitor

The human recombinant AOC3 (VAP-1) protein was given as a neutralizer for LJP1586. The recombinant protein (30 ng/mouse, 90 ng/mouse) was given by ICV injection 10 min before cICH induction. High-dose LJP1586 (10 mg/kg) was then administered 1 h after cICH. Both neurobehavioral function and brain edema were evaluated 24 h post-cICH.

In the modified Garcia test, both the low-dose (30 ng/mouse) and high-dose (90 ng/mouse) AOC3 protein markedly reversed the protective effects of LJP1586 treatment ($P<0.05$, Figure 9A). For the wire hanging and beam balance tests, high dose AOC3 injected mice demonstrated a more severe neurobehavioral deficit than the ICH group alone. Compared with LJP1586 treated mice, neither low-dose nor high-dose AOC3 protein attenuated the effects of LJP1586 ($P<0.05$ versus ICH+LJP, data not shown). With regards to brain edema, the data showed that in the ipsilateral basal ganglia, high-dose AOC3 protein in cICH mice resulted in a markedly higher accumulation of edema than cICH mice alone (ipsilateral basal ganglia: 90 ng/mouse+ICH, 84.07 ± 0.39 vs. ICH, 82.32 ± 0.30, $P<0.05$, Figure 9B). Both low-dose and high-dose AOC3 reversed the edema lowering effects of LJP1586 (Ipsilateral basal ganglia: 30 ng/mouse+ICH+LJP1586, 82.57 ± 0.29 vs. ICH+LJP1586, 80.94 ± 0.32, $P<0.01$; 90 ng/mouse+ICH+LJP1586, 82.81 ± 0.30 vs. ICH+LJP1586, 80.94 ± 0.32, $P<0.01$, Figure 6B). In the ipsilateral cortex, there was no statistical significance found between the cICH mice group and the cICH plus AOC3 protein group. And finally, high-dose AOC3 protein (90 ng/mouse) significantly increased brain edema compared to the mice treated

with LJP1586 (Ipsilateral cortex: 90 ng/mouse+ICH+LJP1586, 80.672 ± 0.21 vs. ICH+LJP1586, 79.58 ± 0.20, $P<0.05$, Figure 9B).

Recombinant AOC3 Protein Reversed the Effect of VAP-1 Inhibition on Migration of Systemic Neutrophils and Activation Microglia/Macrophage

In order to further confirm the role of VAP-1 in inflammation, we evaluated the neutrophilic infiltration by MPO staining and microglia/macrophage activation by Iba-1 staining following recombinant AOC3 protein injection with LJP1586. Additionally, quantification of both the MPO and Iba-1 positive cells in the perihematomal area were determined. Our results showed that there was no statistically significant difference in MPO positive cell numbers between recombinant AOC3 protein administration with LJP1586 post-treatment mice and vehicle mice (24.48 ± 3.2, n=4 and 25.27 ± 1.92, n=4, respectively; t_6= 0.424, P=0.69; Figure 9C,D); while the microglia/macrophage activation failed to show a difference in the perihematomal area compared with vehicle mice (5.98 ± 0.83, n=4 and 7.06 ± 0.86, n=4, respectively; t_6= 0.905, P=0.40; Figure 9E,F).

VAP-1 Inhibitors Improved Neurobehavioral Functions and Reduced Brain Edema in an Autologous Blood Injection ICH Model

Our results have suggested thus far that VAP-1 inhibition can significantly reduce brain edema and improve neurobehavioral functions in a cICH model. To strengthen these results, the autologous blood injection ICH model (bICH) was also applied to confirm the anti-inflammatory effects of VAP-1 inhibition. Both VAP-1 inhibitors, LJP1586 and semicarbizade, were administered 1 h after bICH induction in high concentrations (LJP1586, 10 mg/kg; semicarbizde, 200 mg/kg). Both neurobehavioral

functions and brain edema were evaluated at 24 h. The results showed that treated mice performed markedly better in the modified Garcia test compared with vehicle mice ($P<0.05$, Figure 10A). Additionally, compared with vehicle mice, both treatment groups had significantly reduced brain edema accumulations in the ipsilateral basal ganglia (ipsilateral basal ganglia: 10 mg/kg LJP1586, 80.59±0.28 vs. Vehicle, 81.49±0.15, $P<0.05$; 200 mg/kg SCZ, 80.58 ± 0.10 vs. Vehicle, 81.49±0.15, $P<0.05$, Figure 10B).

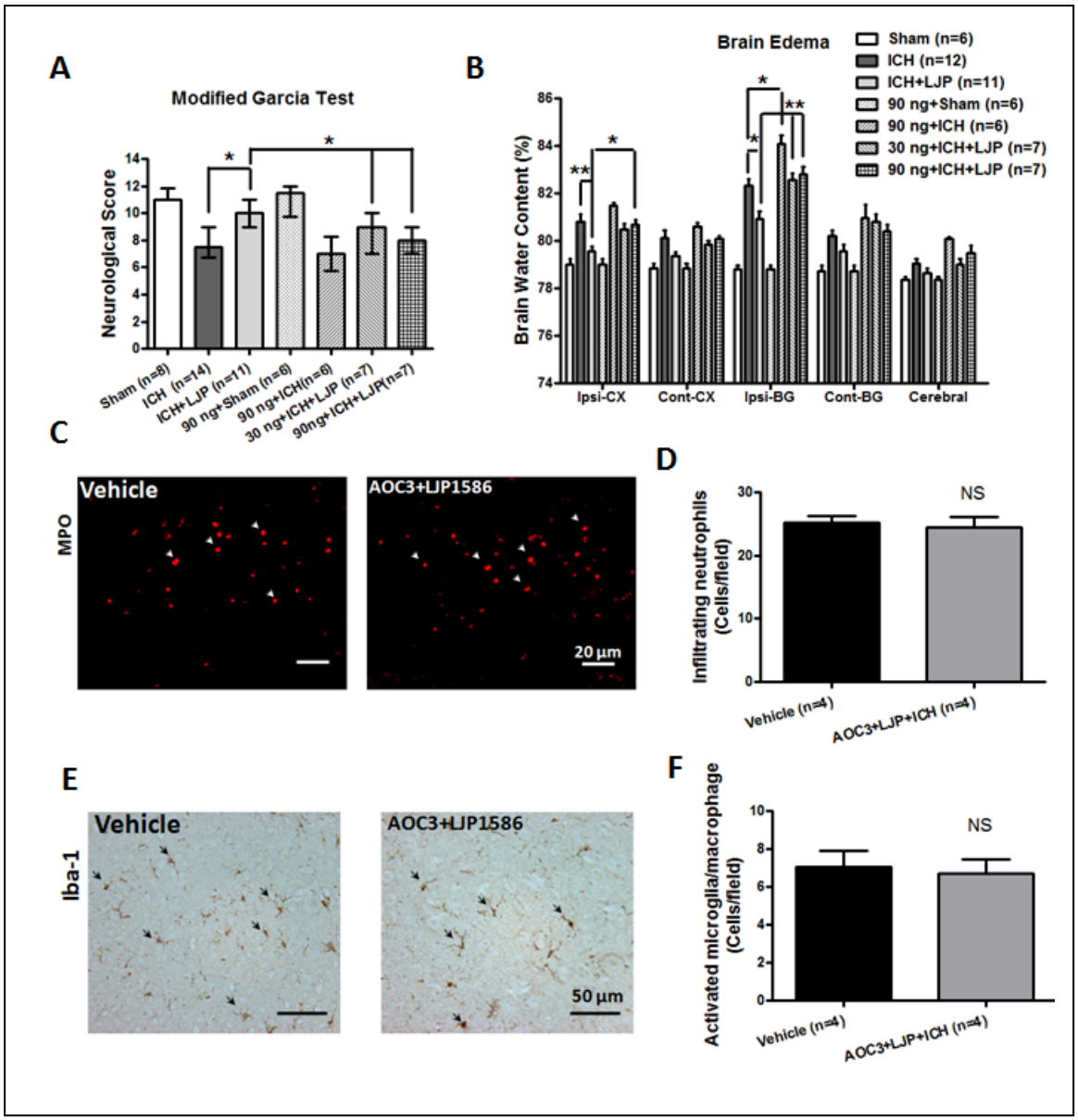
A
Modified Garcia Test
Neurological Score
Sham (n=8)
ICH (n=14)
ICH+LJP (n=11)
90 ng+Sham (n=6)
90 ng+ICH(n=6)
30 ng+ICH+LJP (n=7)
90ng+ICH+LJP(n=7)
B
Brain Edema
Brain Water Content (%)
Sham (n=6)
ICH (n=12)
ICH+LJP (n=11)
90 ng+Sham (n=6)
90 ng+ICH (n=6)
30 ng+ICH+LJP (n=7)
90 ng+ICH+LJP (n=7)
Ipsi-CX
Cont-CX
Ipsi-BG
Cont-BG
Cerebral
C
MPO
Vehicle
AOC3+LJP1586
20 μm
D
Infiltrating neutrophils (Cells/field)
NS
Vehicle (n=4)
AOC3+LJP+ICH (n=4)
E
Iba-1
Vehicle
AOC3+LJP1586
50 μm
F
Activated microglia/macrophage (Cells/field)
NS
Vehicle (n=4)
AOC3+LJP+ICH (n=4)

Figure 9: Effect of recombinant AOC3 (VAP-1) protein on neurological score, brain water content and neutrophils infiltration and microglia/macrophage activation at 24 h after cICH in mice. Recombinant AOC3 protein was injected 10 min before ICH induction. ***A***, The neurological score for the modified Garcia test (healthy animal: 12) at 24 h after ICH in Sham, ICH, ICH+LJP1586 (10 mg/kg), ICH+LJP1586 (10 mg/kg)+VAP-1 protein (30 ng/animal, 90 ng/animal), Sham+VAP-1 protein (90 ng/animal) and ICH+VAP-1 protein (90 ng/animal). ***B***, Recombinant AOC3 protein reduced brain water content at 24 h after ICH. Brain samples were collected from Sham, ICH, ICH+LJP1586 (10 mg/kg), ICH+LJP1586 (10 mg/kg)+VAP-1 protein (30 ng/animal, 90 ng/animal) , Sham+VAP-1 protein (90 ng/animal) and ICH+VAP-1 protein (90 ng/animal). ***C***, Represented photograph of immunofluorescence staining for myeloperoxidase (MPO) MPO positive cell in vehicle group and recombinant AOC3+LJP1586 treatment (10 mg/kg) group at 24 h after ICH. Sections from mice brain were probed with anti-MPO antibody and rabbit TX Red secondary antibody (red). Scale bars, 20 μm. ***D***, Bar graph illustrating the quantification of MPO positive cells in the perihematomal region at 24 h in Vehicle and recombinant AOC3+LJP1586 treatment (10 mg/kg) (12 fields/brain). It showed that recombinant AOC3 abolished the effect of LJP1586 on reducing the number of MPO positive cells. ***E***, Represented photograph of immunohistochemistry staining for Iba-1 positive cells in vehicle group and recombinant AOC3+LJP1586 treatment (10 mg/kg) group 24 h after ICH. Scale bars, 50 μm. ***F***, Bar graph illustrating the quantification of Iba-1 positive cells in vehicle and recombinant AOC3+LJP1586 treatment (10 mg/kg) group in the perihematomal region (12 fields/brain). * **P*<0.01, * *P*<0.05, NS, not significant.

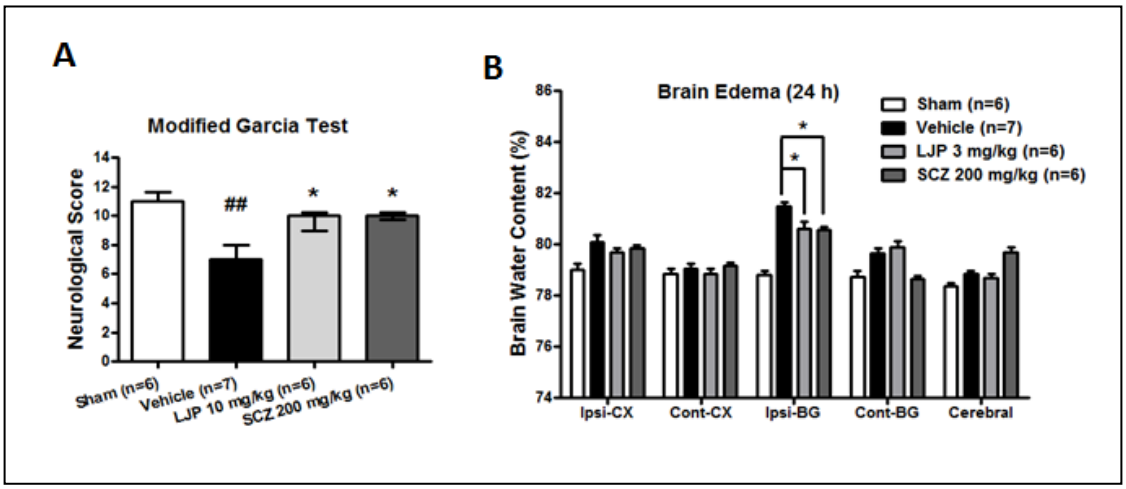

Figure 10: VAP-1 inhibitors, LJP1586 and semicarbazide improved neurological score and decreased brain water content 24 h after bICH in mice. ***A***, The neurological score for the modified Garcia test (healthy animal: 12) at 24 h in Sham, ICH and ICH with treatments (LJP1586: 10 mg/kg; SCZ: 200 mg/kg). ***B***, VAP-1 inhibitors, LJP1586 and semicarbazide reduced brain water content at 24 h after autologous blood induced ICH in mice. Brain samples were collected from Sham, ICH and ICH with treatments (LJP1586: 10 mg/kg; SCZ: 200 mg/kg). Brain sections (4 mm) were divided into four parts: ipsilateral basal ganglia (Ipsi-BG), ipsilateral cortex (Ipsi-CX), contralateral basal ganglia (Cont-BG), contralateral cortex (Cont-CX). Cerebellum (Cerebel) is the internal control. ## $P< 0.01$ versus Sham group. * $P<0.05$ versus Vehicle group.

Discussion

Intracerebral hemorrhage is a fatal stroke subtype that currently has no effective treatment option. In the present study, we investigated the effects of VAP-1 inhibition on ICH-induced brain injury. Specifically investigating the potential of this inhibition to reduce the migration of systemic immune cells to the site of injury and prevent the propagation of further parenchymal damage.

ICH is induced in mice by either one of two paradigms: by injection of autologous tail blood into the basal ganglia, or by injection of a clostridial bacterial collagenase into the basal ganglia (James *et al* 2008). In the cICH model, formation of the hematoma is generated by direct disruption of blood vessels, mimicking a spontaneous ICH in humans (MacLellan *et al* 2008). However, bacterial collagenase has been known to induce an exaggerated inflammatory response in the brain; although *in vitro* studies have refuted this hypothesis (Matsushita *et al* 2000). As a result, to avoid the possible interference of bacterial collagenase in the normal inflammatory response after ICH, the autologous blood injection model was also employed to verify the anti-inflammatory properties of VAP-1 inhibition.

VAP-1 is a homodimeric protein molecule present in a wide variety of cell types, including endothelial cells. Specifically, VAP-1 supports leukocyte adhesion by binding to and oxidatively deaminating a primary amino group presented on the leukocyte surface, resulting in the formation of a temporary bond between the two cell types (Salmi *et al* 2001). Thus, blocking of VAP-1 would be expected to inhibit leukocyte migration. In our study, we found that VAP-1 inhibition down-regulated the adhesion molecule ICAM-1 and reduced the infiltration of systemic immune cells, specifically neutrophils, to the site

of injury. Additionally, with the reduction in systemic immune cells accumulating at the injury site, there was a marked reduction in pro-inflammatory cytokines, TNF-α and MCP-1, and a reduction in activation of microglial/macrophages. This prevented further propagation of the local immune response. Clinically this translates into a significant reduction in cerebral edema accumulation and marked improvement in neurobehavioral function which was the case at both 24 h and 72 h post-ICH.

VAP-1's involvement in leukocyte infiltration has been studied in various experimental models. Most have implicated this protein as the key player in adhesion and transmigration of circulating systemic immune cells to the site of local injury. In ischemic models, VAP-1 has been shown to mediate leukocyte adhesion/infiltration in diabetic OVX females given chronic estrogen-replacement therapy (Xu *et al* 2006). Studies on VAP-1 knockout mice found that absence of VAP-1 led to abnormal leukocyte trafficking and attenuation of the inflammatory response in peritoneal infection (Stolen *et al* 2005). Additionally, *in vitro* studies have directly implicated VAP-1 in inducing E/P-selectin and ICAM-1 expression during inflammatory conditions in endothelial cells (Jalkanen *et al* 2007). Studies investigating the relationship between VAP-1 and ocular inflammation found VAP-1 to be involved in leukocyte extravasations (Noda *et al* 2008). Specifically, noting that VAP-1 inhibition reduced the expression of ICAM-1 and macrophage recruitment, while decreasing the secretion of pro-inflammatory markers TNF-α and MCP-1 to the choroidal tissue. In our study, we were able to show using immunohistochemistry that there was a strong presence of infiltrated neutrophils and activated microglia/macrophages around the hematoma region 24 h after the cICH injury. Additionally, treatment with the VAP-1 blocker LJP1586 significantly decreased the

MPO-positive cell numbers and activated microglia/macrophages numbers, implying that VAP-1 mediates the infiltration of these systemic immune cells and propagation.

To strengthen our hypothesis that VAP-1 inhibition could provide anti-inflammatory effects in ICH, we injected VAP-1 siRNA to knockdown VAP-1 expression. Our data showed that VAP-1 protein level in sham and cICH operated mice were significantly reduced after VAP-1 siRNA injection, and also cICH operated mice showed a lower VAP-1 level than sham. The same phenomenon has been reported in human ischemic stroke models (Airas *et al* 2008). The study by Airas and colleagues showed that in the acute phase of ischemic stroke, VAP-1 positive vessels were strongly diminished in the ipsilateral hemisphere, but the VAP-1 levels in the serum were significantly increased. Additionally, we introduced human recombinant AOC3 protein to neutralize the effects of LJP1586. Our data showed that both low-dose and high-dose exogenous VAP-1 protein delivery counteracted the effect of VAP-1 inhibitor. It produced a worse performance in cICH mice with VAP-1 inhibition, and restored brain edema back to the level of the cICH mice. We also found that the administration of exogenous VAP-1 protein exacerbated neurobehavioral deficits and brain edema in cICH mice and only slightly worsened it in sham mice.

One limitation of our study is the injection pattern of siRNA and human recombinant VAP-1 protein. Although we have no direct evidence that siRNA and recombinant protein may cross the BBB, previous studies have shown that following cICH, there is a marked increase in BBB permeability by 30 min which is maintained from 5h to 7 days, with normal permeability being restored by day 14 (Rosenberg *et al* 1993).

In conclusion, this study shows that VAP-1 inhibition ameliorates ICH-induced brain damage in adult male mice by attenuating the adhesion and transmigration of circulating systemic immune cells to the site of local injury. By doing so, VAP-1 inhibition prevents the propagation of the local inflammatory process and in turn, reduces cerebral edema, improves neurobehavioral function and may act as a potential therapeutic target for future clinical direction.

CHAPTER THREE

PDGFR-A INHIBITION PRESERVES BLOOD-BRAIN BARRIER AFTER INTRACEREBRAL HEMORRHAGE

Qingyi Ma, MS,[1] Bin Huang, MD,[1] Nikan Khatibi, MD,[2] William Rolland II, BS,[1]

Hidenori Suzuki, MD, PhD,[1] John H. Zhang, MD, PhD,[1,2,3] and Jiping Tang, MD[1]

[1] Department of Physiology and Pharmacology, Loma Linda University, Loma Linda, California, USA
[2] Department of Anesthesiology, Loma Linda Medical Center, Loma Linda, California, USA
[3] Department of Neurosurgery, Loma Linda Medical Center, Loma Linda, California, USA

Published: ***Ann Neurol.*** 2011 (*In press*)

Abstract

Objective: Perihematomal edema results from disruption of the blood-brain barrier (BBB) by key mediators, such as thrombin, following intracerebral hemorrhage (ICH). Platelet derived growth factor receptor alpha (PDGFR-α), a tyrosine kinase receptor, was found in previous studies to play a role in orchestrating BBB impairment. In the present study, we investigated the role of PDGFR-α following ICH-induced brain injury in mice, specifically investigating its effect on BBB disruption.

Methods: Brain injury was induced by autologous arterial blood (30 μl) or thrombin (5 U)-injection into mice brains. A PDGFR antagonist (Gleevec) or agonist (PDGF-AA) was administered following ICH. PDGF-AA was injected with a thrombin inhibitor, hirudin in ICH mice. Thrombin-injected mice were given Gleevec or PDGF-AA neutralizing antibody. A p38 MAPK inhibitor, SB203580 was delivered with PDGF-AA in naïve animals. Post-assessment included neurological function tests, brain edema measurement, Evans blue extravasation, immunoprecipitation, western blot and immunohistology assay.

Results: PDGFR-α suppression prevented neurological deficits, brain edema and Evans blue extravasation at 24-72 hours following ICH. PDGFR-α activation led to BBB impairment and this was reversed by SB203580 in naïve mice. Thrombin inhibition suppressed PDGFR-α activation and exogenous PDGF-AA increased PDGFR-α activation, regardless of thrombin inhibition. Animals receiving a PDGF-AA neutralizing antibody or Gleevec showed minimized thrombin injection-induced BBB impairment.

Interpretation: PDGFR-α signaling may contribute to BBB impairment via p38 MAPK mediated MMP activation/expression following ICH and thrombin may be the key

upstream orchestrator. The therapeutic interventions targeting the PDGFR-α signaling may be a novel strategy to prevent thrombin-induced BBB impairment following ICH.

Introduction

Spontaneous intracerebral hemorrhage (ICH) is the result of small vessel bleeds within the brain parenchyma and the subsequent formation and expansion of the hematoma. This process represents the deadliest and least treatable stroke subtype, accounting for close to 15-20% of all strokes (Ribo and Grotta 2006). One of the main reasons for its devastating nature is the formation of perihematomal cerebral edema, a consequence that occurs from disruption of the blood-brain barrier (BBB). To this date, many factors have been implicated in orchestrating the disruption including thrombin, inflammatory mediators, hemoglobin degradation products (He *et al* 2010), and matrix metalloproteinases (MMPs) (Keep *et al* 2008). Yet the mechanism to explain how the process is carried out still remains to be elucidated.

Platelet derived growth factor receptors (PDGFRs) are a subfamily of tyrosine kinase receptors including two members, PDGFR-α and PDGFR-β, expressed throughout various cell-types in the brain, including astrocytes, neurons (Heldin and Westermark 1999), and capillary endothelial cells (Marx *et al* 1994). These receptors have extracellular domains which ligands, platelet derived growth factors (PDGFs) can bind to initiate downstream signaling pathways. Recently, several lines of evidence have suggested that PDGFRs, especially PDGFR-α may be involved in the stroke process, specifically orchestrating the disruption of the BBB (Su *et al* 2008; Yao *et al* 2010). In one study the authors observed that PDGFR-α agonists injection into the CSF of naïve

mice significantly increased Evans blue extravasation compared to just PBS injected animals (Su *et al* 2008).

As a result in the present study, we investigated the role of the PDGFR-α following an ICH-induced brain injury in mice, specifically investigating its position as a key orchestrator of BBB disruption. We hypothesize that PDGFR-α signal may contribute to BBB impairment via a p38 MAPK pathway mediated MMPs activation/expression following ICH injury and thrombin, an established mediator of BBB injury in ICH, may be the upstream regulator of PDGFR-α activation. In order to test this aim, first we investigated the expression of PDGFR-α and its` ligand, PDGF-AA in brain following ICH. We next used both a PDGFR antagonist (Gleevec) and agonist (PDGF-AA) to manipulate PDGFR-α activation, and measured the phosphorylation level of the PDGFR-α while observing the pre-determined outcomes. We also gave a p38 MAPK inhibitor known as SB 203580 hydrochloride, to potentially reverse the BBB disruption induced by PDGFR-α activation. Because of our hypothesis that thrombin may act as the key upstream orchestrator, hirudin, a thrombin specific inhibitor was also administered into animals with or without PDGFR-α agonist injection following ICH. Furthermore, in an established thrombin injection model, PDGFR-α antagonist or PDGF-AA neutralizing antibody was introduced to determine the role of thrombin in activating and/or inhibiting the PDGFR-α pathway.

Materials and Methods

Animals

All procedures for this study were approved by the Institutional Animal Care and Use Committee (IACUC) at Loma Linda University. Please see details in Supplementary Text.

Intracerebral Hemorrhage Mouse Model

ICH was induced using the autologous arterial blood injection model (bICH) which was modified as previously described (Rynkowski *et al* 2008). Please see details in Supplementary Text.

Injection of Thrombin into Basal Ganglia

Animals were fixed in the same manner as the autologous blood injection model described above with the same coordinates used. Thrombin (Sigma) was dissolved in sterilized PBS and delivered into the right basal ganglia (5 U/5 μl per mouse). Control animals were given 5 μl of PBS.

Experimental Design

Four separate experiments were conducted (Fig 11, experiment 1-4) in two models. Experiment 1: Gleevec was administered (intraperitoneal injection) at three doses 1 hour following bICH. Post-assessment included western blot, zymography (6 hours), neurological deficits, brain edema and Evans blue extravasation (24 and 72 hours). Experiment 2: PDGF-AA was co-injected with blood into right basal ganglia. Neurological deficits and brain edema were determined at 24 hours; PDGF-AA was

injected with or without a p38 MAPK inhibitor into right basal ganglia in naïve animals. Evans blue extravasation was detected at 1 and 24 hours.

Experiment 3: The thrombin specific inhibitor, hirudin with or without PDGF-AA was injected with blood into right basal ganglia. Post-assessment included western blot (6 hours), neurological deficits and Evans blue extravasation (24 hours).

Experiment 4: Gleevec was administered (intraperitoneal injection) 1 hour following thrombin injection. PDGF-AA antibody was co-injected with thrombin into right basal ganglia. Post-assessment included western blot, zymography (6 hours) and Evans blue extravasation (24 hours). Please see details in Supplementary Text.

Neurobehavioral Function Test

Neurobehavioral functions were evaluated by modified Garcia test (Garcia *et al* 1995; Wu *et al* 2010) and corner turn test (Hua *et al* 2002). Please see details in Supplementary Text.

Brain Water Content Measurement

Please see details in Supplementary Text.

BBB Permeability

BBB permeability was evaluated with Evans blue staining (250 μl of 4% solution in saline) as previously described (Seiffert *et al* 2004). Please see details in Supplementary Text.

Immunoprecipitation

Please see details in Supplementary Text.

Western Blotting

Please see details in Supplementary Text.

Gelatin Zymography

MMP-2/9 activity was measured by gelatin zymography modified from previous study (Chen *et al* 2009). Please see details in Supplementary Text.

Immunofluorescence

Please see details in Supplementary Text.

Statistics

Data was expressed as mean ± standard error of the mean. Analysis was performed using GraphPad Prism software. For the rating scale data (modified Garcia test), data were expressed as median ± 25th-75th percentiles. Please see details in Supplementary Text.

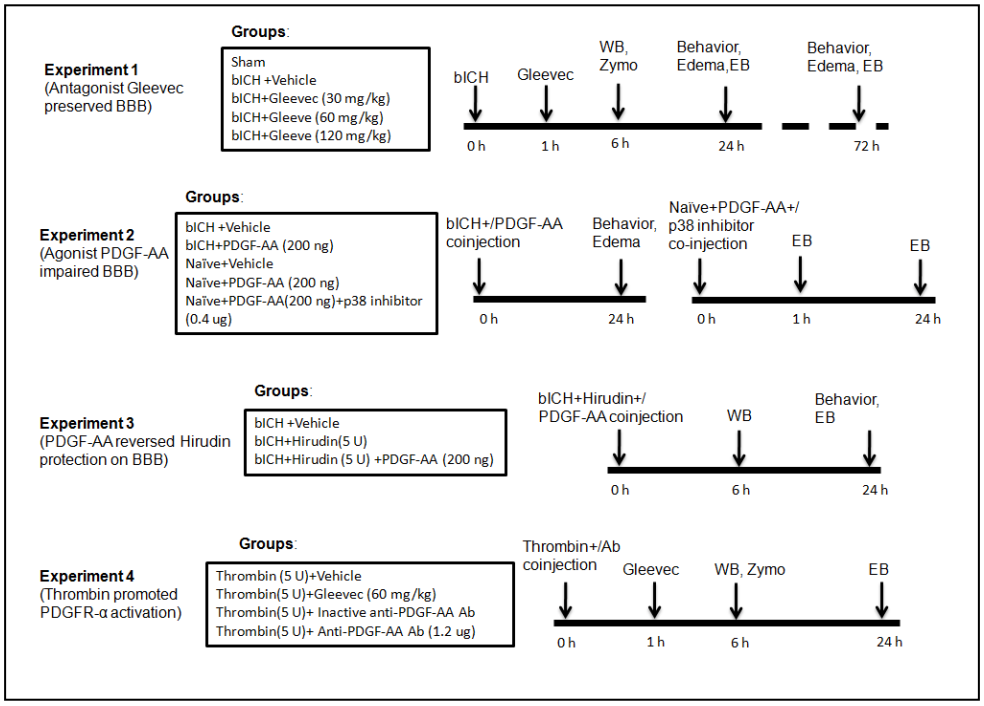

Figure 11: Experimental design and animal groups classification. bICH = autologous arterial blood-induced intracerebral hemorrhage; Zymo = zymography assay; WB = western blotting; EB = Evans blue assay; Anti-PDGF-AA Ab = Anti-PDGF-AA antibody.

Results

PDGFR-α and PDGF-AA Were Upregulated Following bICH Injury

Western blot was performed to determine the profile of PDGFR-α at 3, 6, 12, 24 and 72 hours and endogenous PDGF-AA level at 6 hours following bICH. Western blot results revealed that PDGFR-α level (Fig 12A, B) was increased 3 hours post bICH and reached a peak around 6 hours in which the PDGFR-α level was almost six times more than sham animals ($p < 0.05$). Following this peak, the level of PDGFR-α declined at 12 hours ($p < 0.05$) and 24 hours, returning close to normal level by 72 hours. Endogenous PDGF-AA (Fig 12C, D), a specific PDGFR-α ligand/agonist was significantly increased in the ipsilateral hemisphere (Ipsi) 6 hours post bICH compared to both contralateral (Contra) hemisphere ($p < 0.05$) and sham animals ($p < 0.05$). The double immunofluorescence staining revealed that the PDGFR-α immunoreactivity was mainly found on the neurovascular structure, including perivascular related astrocytes and the endothelial cells (Fig 12E).

PDGFR-α Suppression Improved Neurobehavioral Functions, Reduced Brain Edema, and Preserved BBB Integrity

A PDGFR-α antagonist, Gleevec was administered at three doses (30, 60, and 120 mg/kg) by intraperitoneal injection 1 hour following bICH. Neurobehavioral functions, brain edema and BBB permeability were evaluated at 24 and 72 hours following bICH. The results at 24 hours revealed that vehicle animals demonstrated severe deficits compared to sham animals in both modified Garcia test ($p < 0.01$; Fig 13A) and corner turn test ($p < 0.01$; Fig 13B). Following Gleevec administration at medium (60 mg/kg; $p < 0.01$) and high doses ($p < 0.05$; 120 mg/kg), there was a significant improvement in

neurological score in modified Garcia test. With regards to corner turn test, the medium dose (60 mg/kg) significantly improved neurobehavioral function compared to vehicle animals ($p < 0.05$). We also evaluated neurobehavioral function at the delayed stage (72 hours) post bICH using the medium dose Gleevec treatment. The results demonstrated that the medium dose treatment could significantly improve neurobehavioral function following both modified Garcia test and corner turn test at 72 hours compared to vehicle animals ($p < 0.05$).

At 24 hours post bICH, the medium (60 mg/kg) and high-dose (120 mg/kg) treatment significantly decreased brain edema in the ipsilateral basal ganglia (ipsi-BG) compared to vehicle group (ipsi-BG: 60 mg/kg, 80.82 ± 0.30 vs vehicle, 81.88 ± 0.23, $p < 0.05$; 120 mg/kg, 80.92 ± 0.34 vs vehicle, 81.88 ± 0.23, $p < 0.05$; Fig 3C). In the ipsilateral cortex (ipsi-CX), brain edema was significantly increased in the vehicle group compared to sham group (ipsi-CX; vehicle, 80.22 ± 0.26 vs sham, 79.12 ± 0.21, $p < 0.05$). Although following Gleevec treatment the brain edema showed a trend towards reduction, there was no statistical significance reached. With regards to the 72 hours post bICH medium-dose (60 mg/kg) treatment, we found a significant reduction in brain edema in the ipsilateral basal ganglia compared to the vehicle group (ipsi-BG: 60 mg/kg, 81.75 ± 0.20 vs vehicle, 83.29 ± 0.23, $p<0.05$; Fig 3D). Evans blue extravasation (Fig 3E) was significantly increased at both 24 hours and 72 hours compared to sham groups ($p < 0.01$), and significantly reduced after medium-dose (60 mg/kg) Gleevec treatment ($p < 0.05$).

PDGFR-α Suppression Inhibited MMP Activity and MMP-10/13 Expression through Orchestration of The p38 MAPK Pathway Post bICH

Phosphorylated PDGFR-α (Fig 14A, B) was significantly increased compared to sham animals (about seven times; $p < 0.05$) while Gleevec treatment (60 mg/kg) significantly reduced PDGFR-α phosphorylation level ($p < 0.05$) 6 hours post bICH. Gleevec treatment (60 mg/kg) also significantly reduced the active MMP-9 level ($p < 0.05$) but not MMP-2 compared to vehicle animals (Fig 14C-E), and reduced MMP-10 ($p < 0.05$; Fig 14F, G) and MMP-13 expression ($p < 0.05$; Fig 4H, I). The results also revealed that phosphorylated p38 MAPK was significantly reduced following Gleevec treatment ($p < 0.05$) yet, did not reduce the phosphorylation level of Erk1/2 and JNK1/2 (Fig 14J, K). Additionally, we also found that phosphorylated ATF-2, the substrate of p38 was also significantly reduced ($p < 0.05$; Fig 14L, M). Additionally, the cellular localization of PDGFR-α downstream mediators was determined by double immunofluorescence staining. Similar to the PDGFR-α, MMP-9, MMP-13 and phosphor-p38 immunoreactivity were mainly found in the neurovascular structure, including astrocytes and the endothelial cells, and MMP-10 was only found in the endothelial cells (Supplemental Fig 1).

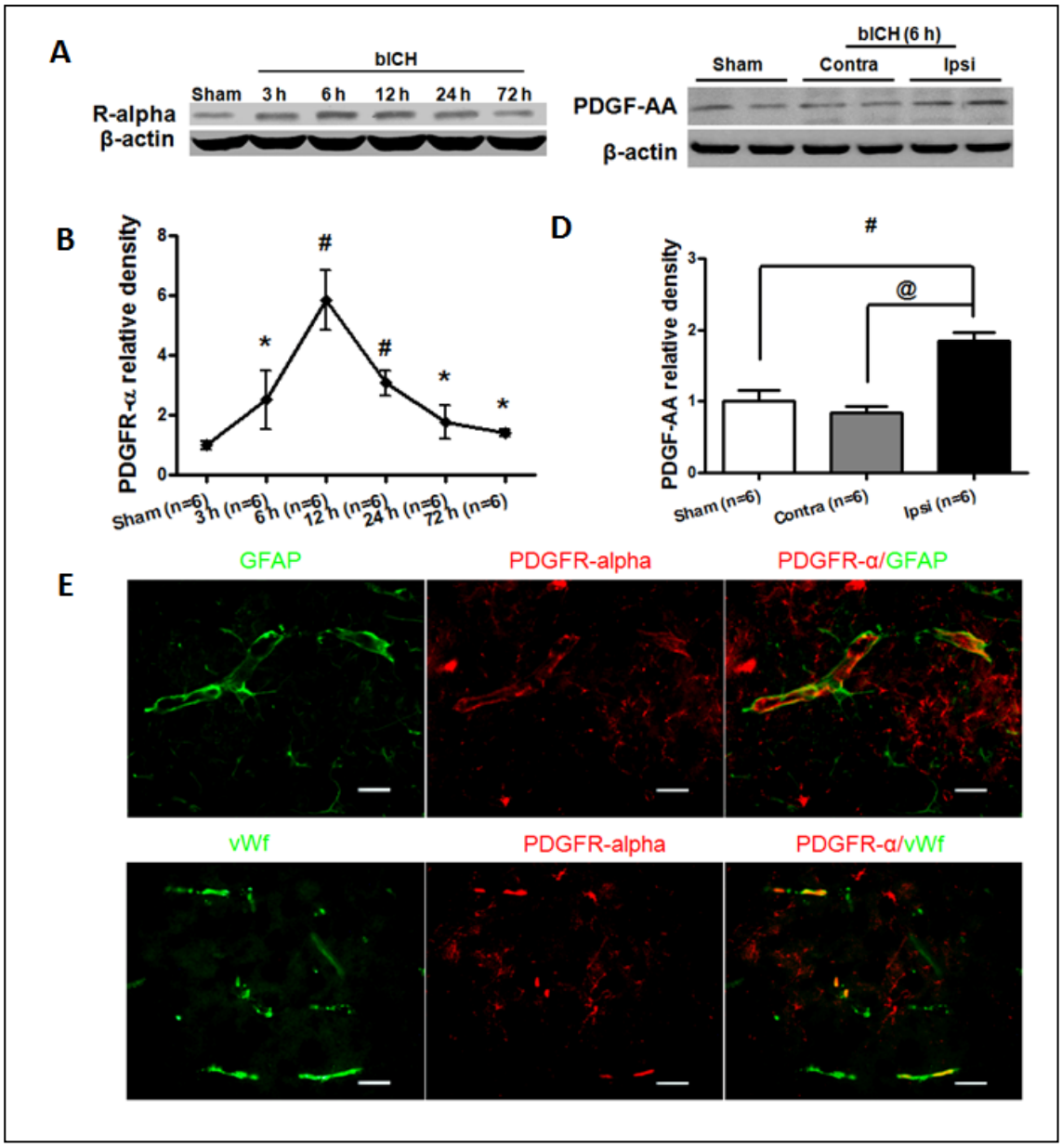

Figure 12: Expression of PDGFR-α and PDGF-AA after autologous arterial blood induced intracerebral hemorrhage (bICH). (A) Western blot assay for the profiles of PDGFR-α expression in the ipsilateral hemisphere in sham and bICH mice 3, 6, 12, 24 and 72 hours following operation. (C) Western blot assay for PDGF-AA expression in sham, ipsilateral (Ipsi) and contralateral (Contra) hemisphere in bICH mice 6 hours following operation; (E) Representative photographs of immunofluorescence staining for PDGFR-α (red) expression in astrocytes (GFAP, green) and endothelial cells (vWf, green) in the perihematomal area 6 hours following bICH. Scale bar: 50 μm. Quantification of A and C is shown in B and D, respectively. n = 6 mice per group and per time point. Error bars represent mean ± standard error of the mean. # $p < 0.05$ vs Sham; * $p < 0.05$ vs bICH (6 h); # $p < 0.05$ vs Sham; @ $p < 0.05$ vs Contra.

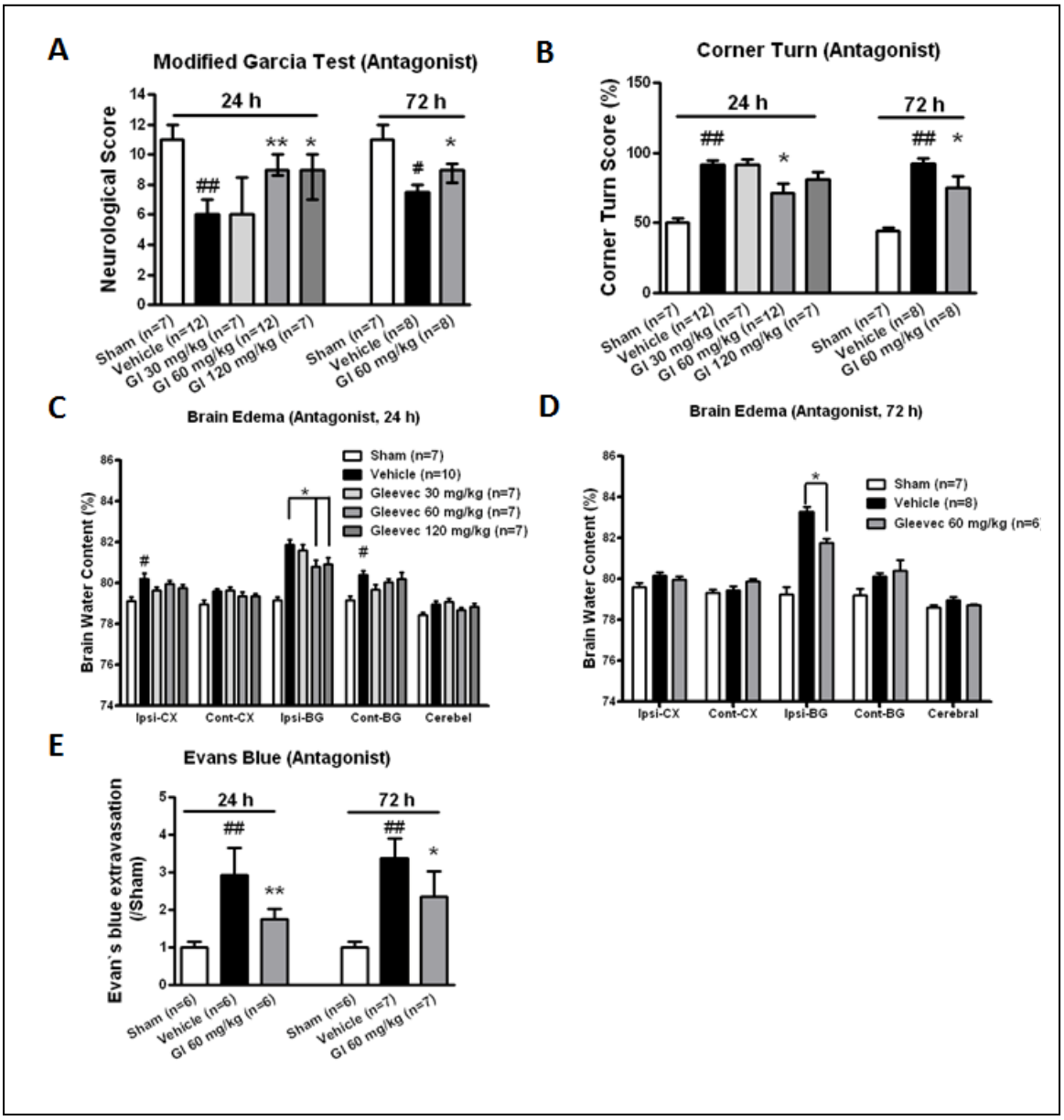
A
Modified Garcia Test (Antagonist)
Neurological Score
24 h
72 h
Sham (n=7)
Vehicle (n=12)
GI 30 mg/kg (n=7)
GI 60 mg/kg (n=12)
GI 120 mg/kg (n=7)
Sham (n=7)
Vehicle (n=8)
GI 60 mg/kg (n=8)
B
Corner Turn (Antagonist)
Corner Turn Score (%)
24 h
72 h
C
Brain Edema (Antagonist, 24 h)
Brain Water Content (%)
Sham (n=7)
Vehicle (n=10)
Gleevec 30 mg/kg (n=7)
Gleevec 60 mg/kg (n=7)
Gleevec 120 mg/kg (n=7)
Ipsi-CX
Cont-CX
Ipsi-BG
Cont-BG
Cerebel
D
Brain Edema (Antagonist, 72 h)
Brain Water Content (%)
Sham (n=7)
Vehicle (n=8)
Gleevec 60 mg/kg (n=6
Ipsi-CX
Cont-CX
Ipsi-BG
Cont-BG
Cerebral
E
Evans Blue (Antagonist)
Evan`s blue extravasation (/Sham)
24 h
72 h
Sham (n=6)
Vehicle (n=6)
GI 60 mg/kg (n=6)
Sham (n=6)
Vehicle (n=7)
GI 60 mg/kg (n=7)

Figure 13: PDGFR-α suppression improved neurological functions, reduced brain edema and Evans blue extravasation at 24 and 72 hours following bICH. PDGFR-α antagonist, Gleevec was administered 1 hour following bICH. Modified Garcia test (A) and corner turn (B) at 24 and 72 hours following operation in sham, vehicle and Gl treatment groups (24 hours: 30, 60 and 120 mg/kg; 72 hours: 60 mg/kg). Brain edema at 24 hours (C) and 72 hours (D) following operation in sham, vehicle and Gl treatment groups (24 hours: 30, 60 and 120 mg/kg; 72 hours: 60 mg/kg). Brain sections (4 mm) were divided into four parts: ipsilateral basal ganglia (Ipsi-BG), ipsilateral cortex (Ipsi-CX), contralateral basal ganglia (Cont-BG), contralateral cortex (Cont-CX). Cerebellum (Cerebel) is the internal control. (E) Evans blue extravasation at 24 and 72 hours in the ipsilateral hemisphere following operations in sham, vehicle and Gl treatment groups (60 mg/kg). n = 6-12 mice per group. Error bars represent median ± 25th-75th percentiles (A) or mean ± standard error of the mean (B, C, D and E). # $p < 0.05$ vs Sham; ## $p < 0.01$ vs Sham; * $p < 0.05$ vs Vehicle; ** $p < 0.01$ vs Vehicle.

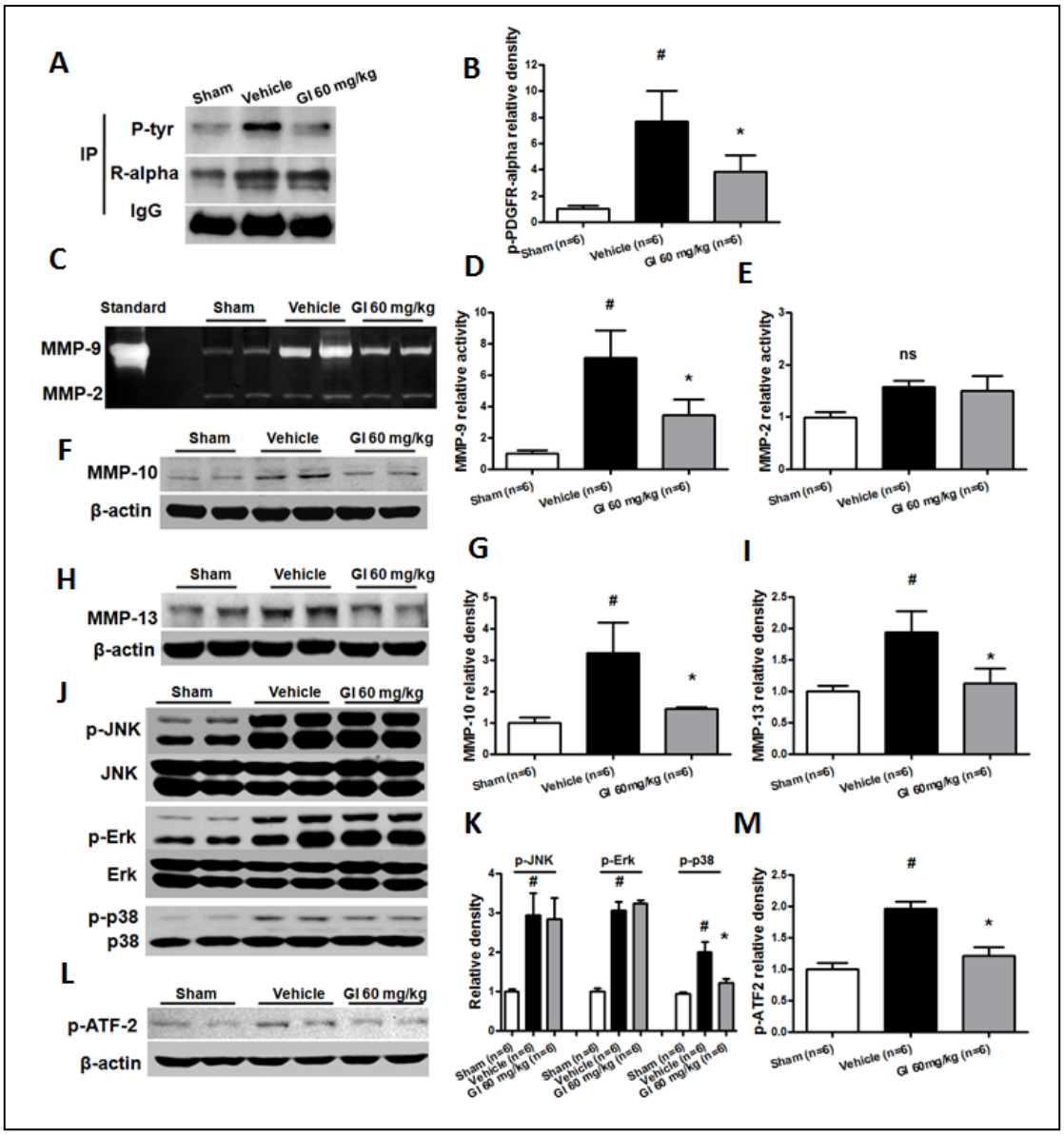

Figure 14: Characterization of PDGFR-α pathway at 6 hours following bICH in mice. PDGFR-α antagonist, Gleevec (60 mg/kg) was administered 1 hour following bICH. (A) Immunoprecipitation assay (IP) for phosphor-PDGFR-α level with phosphotyrosine-specific antibody (P-tyr) in the ipsilateral hemisphere in sham, vehicle and Gl treatment (60 mg/kg) mice. The precipitated protein was also visualized with PDGFR-α-specific antibodies (R-alpha). IgG was visualized as a loading control. (C) Gelatin zymography assay for MMP-9 and MMP-2 activity in the ipsilateral hemisphere in sham, vehicle and Gl treatment (60 mg/kg) mice; Western blot assay for MMP-10 (F), MMP-13 (H), JNK/p-JNK, Erk/p-Erk and p38/p-p38 (J), p-ATF-2 (L) in the ipsilateral hemisphere in sham, vehicle and G1 treatment (60 mg/kg) mice. Quantification of A, C, F, H, J, and L is shown in B, D, E, G, I, K, and M, respectively, n = 6 mice per group. Error bars represent mean ± standard error of the mean. # $p < 0.05$ vs Sham; * $p < 0.05$ vs Vehicle; ns indicates not significant.

PDGFR-α Activation Increased Brain Edema Post bICH

At 24 hours post PDGF-AA delivery, neurobehavioral deficits were evaluated using modified Garcia test (Supplemental Fig 2A) and corner turn test (Supplemental Fig 2B). Our results revealed no difference in deficit severity compared to vehicle treatment animals, although two out of nine animals with PDGF-AA injection died in 24 hours. We also found that the brain edema in the ipsilateral basal ganglia was significantly increased compared to vehicle animals (ipsi-BG: PDGF-AA, 82.59 ± 0.24 vs Vehicle, 81.87 ± 0.23, $p < 0.05$; Supplemental Fig 2C) 24 hours after PDGF-AA delivery.

PDGFR-α Activation Impaired BBB Integrity But Was Reversed Using a p38 MAPK Inhibitor in Naïve Mice

At 24 hours following PDGF-AA injection, Evans blue extravasation was significantly increased in the ipsilateral hemisphere compared to just PBS injection mice ($p < 0.01$). BBB permeability was also detected 1 hour following PDGF-AA injection. The results showed that the Evans blue extravasation was also increased compared to just PBS injection ($p < 0.05$; Fig 15A). A p38 MAPK inhibitor, SB 203580 hydrochloride was co-injected with PDGF-AA into the right basal ganglia of naïve mice. 24 hours later, we found that the Evans blue extravasation was significantly diminished compared to PDGF-AA injection animals ($p < 0.05$; Fig 15B).

Thrombin Inhibition Preserved BBB Integrity, While Suppressing PDGFR-α Activation and PDGF-AA Expression Post bICH

Thrombin inhibitor, hirudin was co-injected with autologous arterial blood into the right basal ganglia of mice. 24 hours following hirudin injection, Evans blue extravasation (Fig 16A) was significantly reduced in hirudin injected animals compared

to vehicle animals ($p < 0.05$). Hirudin treatment also significantly improved neurological scores following modified Garcia test ($p < 0.05$; Supplemental Fig 13A), but failed to show improvement with corner turn test (Supplemental Fig 3B). Our results demonstrated that level of phosphorylated PDGFR-α (Fig 6B, C) and PDGF-AA (Fig 16D, E) were both significantly decreased in hirudin treated animals compared to vehicle animals ($p < 0.05$) 6 hours post bICH.

PDGFR-α Activation Reversed the Protective Effects of Thrombin Inhibition on BBB Integrity Post bICH

Our results demonstrated that Evans blue extravasation was significantly increased compared to only hirudin treated mice ($p < 0.05$) 24 hours following hirudin and PDGF-AA co-injection (Fig 17A). The protection asserted by hirudin on neurobehavioral function was reversed following PDGF-AA administration in modified Garcia test ($p < 0.05$; Supplemental Fig 4A) but not in corner turn test (Supplemental Fig 4B) 24 hours after injection. Additionally, we also observed that the level of phosphorylation of PDGFR-α significantly increased by PDGF-AA compared to just hirudin treated mice ($p < 0.05$) 6 hours after injection (Fig 17B, C).

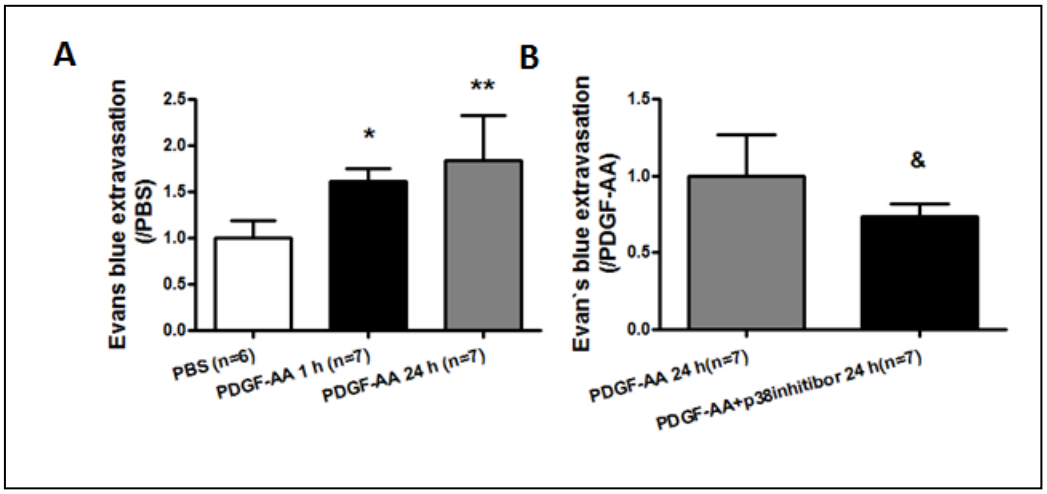

Figure 15: PDGFR-α activation by exogenous PDGF-AA increased Evans blue extravasation in naïve mice. (A) Evans blue extravasation in the ipsilateral hemisphere at 1 and 24 hours following PDGF-AA injection or 24 hours following PBS injection in naïve mice; (B) Evans blue extravasation in the ipsilateral hemisphere at 24 hours in PDGF-AA or PDGF-AA+p38 inhibitor co-injection naïve mice. n = 6-7 mice per group. Error bars represent mean ± standard error of the mean. * $p < 0.05$ vs PBS; ** $p < 0.01$ vs PBS; & $p < 0.05$ vs PDGF-AA (24 hours).

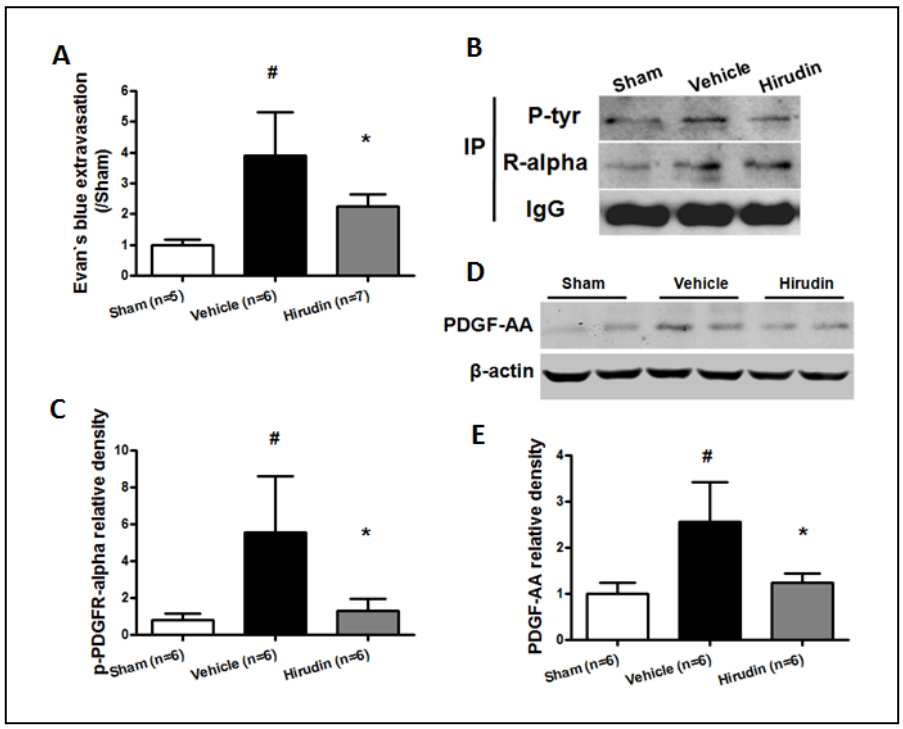

Figure 16: Thrombin inhibition reduced Evans blue extravasation, phosphor-PDGFR-α and PDGF-AA levels following bICH injury. Thrombin inhibitor, hirudin (5 U) was co-injected with autologous arterial blood. (A) Evans blue extravasation in the ipsilateral hemisphere 24 hours following operation in sham, vehicle and hirudin treatment (5 U) mice; (B) Immunoprecipitation assay (IP) for phosphor-PDGFR-α level with phosphotyrosine-specific antibody (P-tyr) in the ipsilateral hemisphere 6 hours following operation in sham, vehicle and hirudin treatment (5 U) mice. The precipitated protein was also visualized with PDGFR-α-specific antibodies (R-alpha). IgG was visualized as a loading control. (D) Western blot assay for PDGF-AA level in the ipsilateral hemisphere 6 hours following operation in sham, vehicle and hirudin treatment (5 U) mice. Quantification of B and D is shown in C and E, respectively, n = 5-7 mice per group. Error bars represent mean ± standard error of the mean. # $p < 0.05$ vs Sham; * $p < 0.05$ vs Vehicle.

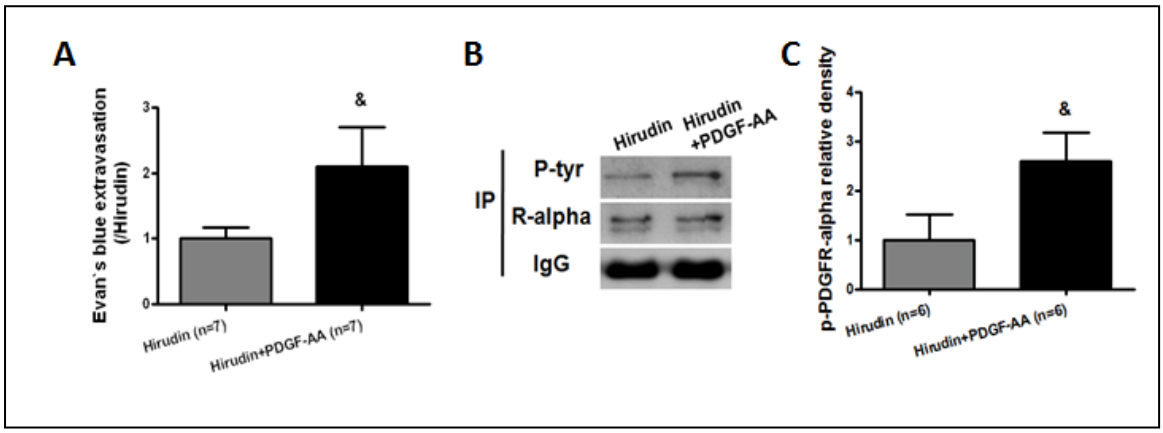

Figure 17: Activation of PDGFR-α by PDGF-AA reversed thrombin inhibition by hirudin following bICH. Thrombin inhibitor, hirudin (5 U) with or without PDGF-AA (200 ng) was co-injected with autologous arterial blood. (A) Evans blue extravasation in the ipsilateral hemisphere 24 hours following bICH in hirudin (5 U) and hirudin (5 U) + PDGF-AA (200 ng) mice; (B) Immunoprecipitation assay (IP) for phosphor-PDGFR-α level with phosphotyrosine-specific antibody (P-tyr) in the ipsilateral hemisphere 6 hours after bICH in hirudin (5 U) and hirudin (5 U) + PDGF-AA (200 ng) mice. The precipitated protein was also visualized with PDGFR-α-specific antibodies (R-alpha). IgG was visualized as a loading control. Quantification of B is shown in C. n = 6-7 mice per group. Error bars represent mean ± standard error of the mean. & $p < 0.05$ vs Hirudin.

PDGFR-α Suppression Reduced Thrombin-Induced BBB Impairment through the PDGFR-α/ p38/MMPs Pathway

Our results showed that Gleevec treatment significantly diminished Evans blue extravasation compared to thrombin injected animals ($p < 0.05$; Fig 18A). Phosphorylated PDGFR-α was significantly increased 6 hours following thrombin injection and significantly reduced in the Gleevec treated mice compared to just thrombin injected mice ($p < 0.05$; Fig 18B, C). Gleevec treatment significantly reduced MMP-9 level ($p < 0.05$) but not MMP-2 (Supplemental Fig 5A-C) 6 hours following thrombin injection. Similarly, MMP-10 (Supplemental Fig 5D, E) and MMP-13 (Supplemental Fig 5F, G) expression were also significantly reduced after treatment ($p < 0.05$). Additionally, Gleevec treatment significantly diminished the phosphorylation level of p38 MAPK ($p < 0.05$; Supplemental Fig 5H, I) as well as p38 MAPK substrate, ATF2 ($p < 0.05$; Supplemental Fig 5J, K) compared to just thrombin injected mice.

Neutralization of PDGF-AA with Anti-PDGF-AA Antibody Reduced Thrombin-Induced BBB Impairment

PDGF-AA level was significantly increased 6 hours in ipsilateral hemisphere following thrombin injection compared to contralater hemisphere and sham ($p < 0.05$; Fig 18D, E). 24 hours after PDGF-AA antibody injection, Evans blue extravasation level was significantly diminished compared to either control (Thrombin+inactive antibody) or just thrombin injected mice ($p < 0.05$; Fig 18F).

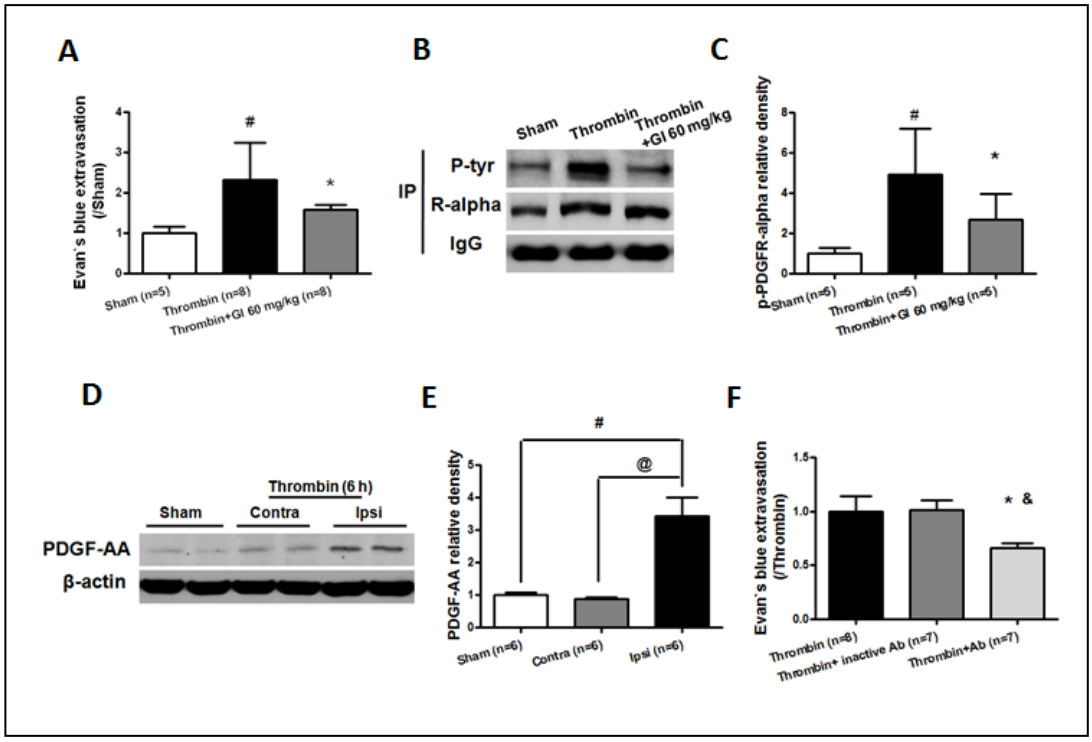

Figure 18: Gleevec and PDGF-AA neutralizing antibody reduced Evans blue extravasation 24 hours following thrombin injection in mice. PDGFR-α antagonist, Gleevec (60 mg/kg) was administered 1 hour following thrombin (5 U) injection. Inactive PDGF-AA antibody (PDGF-AA Ab) or PDGF-AA antibody (PDGF-AA Ab, 1.2 μg) was co-injected with thrombin (5 U) into right basal ganglia. (A) Evans blue extravasation in the ipsilateral hemisphere 24 hours following operation in sham, thrombin (5 U) and Gl treatment (60 mg/kg) groups; (B) Immunoprecipitation assay (IP) for phosphor-PDGFR-α level with phosphotyrosine-specific antibody (P-tyr) in the ipsilateral hemisphere 6 hours following thrombin injection in sham, thrombin (5 U) and Gl treatment (60 mg/kg) mice. The precipitated protein was also visualized with PDGFR-α-specific antibodies (R-alpha). IgG was visualized as a loading control. (D) Western blot assay for PDGF-AA in Sham, ipsilateral (Ipsi) and contralateral (Contra) hemisphere in thrombin injection mice 6 hours following operation; (F) Evans blue extravasation in the ipsilateral hemisphere 24 hours following operation in thrombin (5 U), thrombin (5 U)+inactive PDGF-AA antibody (PDGF-AA Ab), and PDGF-AA antibody (PDGF-AA Ab, 1.2 μg) mice. Quantification of B and D is shown in C and E, respectively. n = 5-8 mice per group. Error bars represent mean ± standard error of the mean. # $p < 0.05$ vs Sham; * $p < 0.05$ vs Thrombin; @ $p < 0.05$ vs Contra; & $p < 0.05$ vs Thrombin+inactive Ab.

Discussion

Intracerebral hemorrhage is a fatal stroke subtype that currently has no effective treatment option. Even if patients survive the initial attack, the growing hematoma triggers a series of life threatening events leading to accumulation of cerebral edema, progression of neurobehavioral deficits, and possibly death (Strbian *et al* 2008). In the present study, we investigated the effects of the PDGFR-α and its ability to orchestrate BBB disruption following an ICH injury. Our findings suggest that therapeutic interventions targeting the PDGF-AA/PDGFR-α system may be a novel strategy to prevent BBB impairment and thus attenuate the subsequent accumulation of brain edema responsible for both structural and functional damage following ICH injury.

In order to determine the role of PDGFR-α on BBB disruption in ICH, a PDGFR antagonist, Gleevec was used to suppress PDGFR-α activity, which has showed protective effect on BBB integrity in ischemic stroke model (Strbian *et al* 2008). Gleevec represented a new class of anticancer drugs and has been approved by US Food and Drug Administration for the therapy on chronic myelogenous leukemia and other cancers by inhibition of several tyrosine kinase, including PDGFR-α. It was regarded as a new gold standard for treatment of chronic myeloid leukemia at all stages (Peggs and Mackinnon 2003) while some dose-related adverse events have been observed in some patients during Gleevec therapy, such as nausea, vomiting, diarrhea, and fluid retention etc. (Deininger *et al* 2003; O'Brien *et al* 2003). In our study, we observed a dose-dependent effect of Gleevec treatment on neurological function improvement after ICH. The medium dose (60 mg/kg) significantly improved neurological function while the low dose (30 mg/kg) or high dose (120 mg/kg) did not.

Increased BBB permeability following PDGF administration is not a new concept. Previous study led by Su and colleagues has suggested just that – specifically showing that PDGF injections into the CSF of naïve mice could increase the Evans blue extravasation compared to just PBS injections (Su *et al* 2008). Yet another study led by Yao and colleagues recently found that cocaine-induced PDGF could increase vascular permeability and that administration of a PDGF neutralizing antibody could abolish this effect (Yao *et al* 2010). Similar to these studies, we found that ICH injury resulted in a transient increase in PDGFR-α/PDGF-AA levels, peaking at 6 hours and returning to baseline by 72 hours. This resulted in a significant increase in brain edema accumulation and BBB disruption which we measured at 24 hours. To our surprise, there was no simultaneous decline in neurological functions with further brain edema accumulation in the bICH with exogenous PDGFR-α agonist group compared to the bICH vehicle group. We attributed this unexpected outcome to the inability of neurological function test to pick up subtle changes in edema accumulation that occurred between the vehicle and agonist group.

With regards to mechanics, we now discuss the potential downstream signaling of PDGF-AA/ PDGFR-α which we hope will explain the mediation of the BBB disruption. MAPK pathway has been established as one of the downstream effectors of PDGFR-α signaling (Dibb *et al* 2004). There are several subfamilies of MAPKs including the extracellular signal-regulated kinases (ERK1/2), ERK5, the Jun amino-terminal kinases (JNK1–3) and the p38 kinases (Gehart *et al* 2010). Generally, p38 and JNK are detrimental in stroke models, with previous research showing that p38/MAPK2 is involved in control of the tight junctional closures among astrocytes (Zvalova *et al* 2004)

and plays a key role in orchestrating BBB disruption and vasogenic edema formation following focal cerebral ischemia and reperfusion (Nito *et al* 2008). In our study, we found that p38 MAPK level, and not Erk or JNK level, were significantly decreased following Gleevec treatment - and that phosphorylated ATF2 (activating transcription factor 2), a substrate of p38 and JNK, was also markedly decreased. Moreover, the p38 MAPK inhibitor, SB 203580 hydrochloride, which was administered with PDGF-AA in naïve animals, was found to reverse the PDGF-AA induced BBB impairment. These findings suggest that PDGF-AA/ PDGFR-α system may orchestrate the damage to the BBB integrity through a p38 MAPK signaling pathway.

The detrimental role of matrix metalloproteinases, especially MMP-9 and MMP-2 has been well documented in the literature with regards to their effects on BBB integrity following ICH injury (Power *et al* 2003; Rosenberg and Navratil 1997; Tang *et al* 2004). Current studies suggested that MMP-10 and 13 were upregulated in both animal and human brain infarcted tissue following ischemic stroke damage (Cuadrado *et al* 2009; Rosell *et al* 2005). Similar to other members in the MMP family, MMP-13 (collagenase-3) can breakdown collagen and gelatin structures and in previous *in vitro* studies has been shown to cleave pro-MMP-9 to active MMP-9 (Knauper *et al* 1997) – which can occur following MMP-10 as well (Nakamura *et al* 1998). With regards to this study, we found that PDGFR-α suppression significantly reduced MMP-9 activity but not MMP-2. We also observed that the expression of MMP-10 and MMP-13 were significantly decreased following PDGFR-α suppression. All of which resulted in preservation of the BBB integrity. In all, taken together MMPs may be the direct downstream proteins of PDGFR-α/p38 pathway and direct mediators of BBB impairment following ICH.

Now that we've discussed downstream orchestrators of PDGFR-α induced BBB damage, we wanted to investigate who was responsible for the upstream regulation of PDGFR-α signaling following ICH injury. Previous literature has alluded to the notion that thrombin regulates the expression of PDGF-AA through a PAR-1 receptor found in endothelial cells (Chandrasekharan *et al* 2004). Therefore in the present study, two different mice models were conducted to investigate the potential relationship between thrombin and PDGF-AA. First in the autologous arterial blood-induced ICH model, we found that PDGF-AA expression was significantly down-regulated following the delivery of hirudin, a thrombin specific inhibitor. We also found that the effects of hirudin on BBB preservation were reversed by exogenous PDGF-AA injection. In the thrombin injection model, we first found the increase of phosphorylated PDGFR-α level as well as its downstream signals, p38 MAPK and MMPs, and the diminishment following PDGFR-α suppression by Gleevec treatment. In this case, we also found that the PDGF-AA level was significantly upregulated in the ipsilateral hemisphere. Additionally, a PDGF-AA neutralizing antibody given with thrombin markedly reduced BBB permeability. Taken together, these findings demonstrated that thrombin is an essential upstream regulator of PDGF-AA/PDGFR-α system.

Why not just block thrombin? The dual role of thrombin in ICH has been well described in previous studies. On one hand, thrombin itself can directly damage the BBB and cause brain edema formation following ICH; while on the other hand, it can act as an essential element in the coagulation cascade to stop bleeding. The concentration of thrombin generated in the brain following ICH has been calculated. Normally, 1 ml of whole blood can provide roughly 260 to 360 units of thrombin from prothrombin. That

means that about 15 U of thrombin is generated following a 50 µl blood injection (about 30 µl plasma) (Lee *et al* 1996). A number of studies have regarded thrombin generated during blood clotting and hematoma formation as a major cause of brain edema formation (Lee *et al* 1997; Xi *et al* 1998). One study led by Xi et al. revealed that thrombin is also responsible for prolonged brain edema following ICH (Xi *et al* 1998).

Mounting evidence that thrombin infusion into the brain produces the same amount of BBB disruption suggested that thrombin could be directly responsible for the breakdown (Yang *et al* 1994). Moreover, thrombin can cleave its receptors and induce downstream protein production, such as vascular endothelial growth factor (VEGF) which can lead to increased endothelial cell permeability (Sarker *et al* 1999). Therefore, antithrombin therapy using intravenous is considered as a way to prevent brain tissue damage during invasive procedure including surgical removal of hematomas and possibly even direct infusion of thrombin inhibitors into hematomas (Matsuoka and Hamada 2002). Unfortunately, a series of studies showed that the thrombin inhibitors, such as argatroban and hirudins, can provide protective effects in animal models (Kitaoka *et al* 2002; Xue *et al* 2009) but, while in phase 1 clinical trials hemorrhagic transformations and increased hemorrhages were major adverse effects that occurred in patients (Hursting *et al* 1997; Matsuoka and Hamada 2002). As a result, it is very reasonable to develop a therapy strategy that can disrupt downstream thrombin mediators following ICH because they provide fewer side effects than direct thrombin inhibition.

It is also important to note that in addition to PDGF-AA, thrombin also regulates the expression of other PDGFs, such as PDGF-BB (Stenina *et al* 2001) which has led to BBB disruption in previous study (Su *et al* 2008). Although in our study we hypothesized

that PDGFR-α activation may be responsible for BBB impairment, our study cannot rule out the possibility that other PDGFs may be involved in BBB disruption and thus remains one of the main limitations of this study.

Since the PDGF signals expressed transiently and peaked 6 hours after ICH, one of the limitations of our study was the potential narrow therapeutic time window. Previous study showed that BBB permeability in the perihematomal region increased markedly 8 to 12 hours after ICH, and continued to rise for 48 hours(Yang *et al* 1994). And the early BBB disruption is associated with the thrombin which is generated by the hematoma (Lee *et al* 1997). Our study was based on the pathophysiology of intracerebral hemorrhage and brain edema formation and may provide insight in understanding the mechanism of BBB disruption and clue on brain edema therapy. In the present study, Gleevec was administered 1 hour after ICH. However, the profile of PDGFR-α expression showed that at 12 hours and 24 hours after ICH, the PDGFR-α level was still 3.08 times and 1.76 times higher than that of sham animals respectively, therefore, a delayed treatment will be conducted in our future study to further establish the therapeutic time window.

In conclusion, our findings suggest that PDGFR-α may contribute to BBB impairment and brain edema formation induced by ICH. Thrombin may in fact be the upstream regulator of PDGFR-α signaling that regulates PDGF-AA expression (potential mechanisms see Supplemental Fig 5). Targeting the PDGFR-α signaling may provide an alternative treatment to thrombin-induced BBB injury following ICH.

Supplementary Text

Animals

All procedures for this study were approved by the Institutional Animal Care and Use Committee (IACUC) at Loma Linda University. Eight-week old male CD1 mice (weight about 30 g, Charles River, MA, USA) were housed in a 12 hours light/dark cycle at a controlled temperature and humidity with free access to food and water. Following surgery the skull hole was closed with bone wax, the incision was closed with sutures, and the mice were allowed to recover. To avoid postsurgical dehydration, 0.5 ml of normal saline was given to each mouse by subcutaneous injection immediately following surgery.

Intracerebral Hemorrhage Mouse Model

ICH was induced using the autologous arterial blood injection model (bICH) which was modified from previous descriptions (Rynkowski *et al* 2008). Briefly, mice were anesthetized with ketamine (100 mg/kg) and xylazine (10 mg/kg) (2:1 v/v, intraperitoneal injection) and positioned prone in a stereotactic head frame (Kopf Instruments, Tujunga, CA). A scalp incision was made along the midline and a burr hole (1 mm) was drilled on the right side of the skull (0.2 mm anterior and 2.0 mm lateral of the bregma). The mouse tail was cleaned with 70% ethanol before a penetration into the tail central artery with a sterilized 27 G needle was done. Next, 30 ul of autologous tail arterial blood was collected in a capillary tube without heparin and blown into a 500 ul Hamilton syringe. The syringe was fixed onto the microinjection pump while the needle was stereotaxically inserted into the brain through the burr hole. At first the needle was stopped at 0.7 mm above the target position and 5 ul of blood was delivered at a rate of 2

μl/min. This allowed for a small clot to form which would prevent reflux of the remaining blood to be injected back up the needle tract. The remaining 25 ul blood was injected at the appropriate target site at a rate of 2 μl/min after 5 min. The needle was left in place for an additional 10 min after injection to prevent possible leakage and withdrawn slowly in 5 min.

Experimental Design

Experiment 1-3 was conducted in autologous arterial blood injection model and experiment 4 was conducted in thrombin injection model.

Experiment 1: The PDGFR-α antagonist, Gleevec was dissolved in PBS and administered (intraperitoneal injection) at three different dosages (30, 60, 120 mg/kg) 1 hour following bICH. Vehicle animals were given the same volume injection, but with PBS. Western blot and zymography were conducted at 6 hours after ICH; Neurological deficits, brain edema and Evans blue staining for BBB permeability were performed at 24 and 72 hours.

Experiment 2: PDGF-AA protein (Abcam) was simultaneously injected with autologous blood into the right basal ganglia. Neurological deficits and brain edema were determined at 24 hour; PDGF-AA (200 ng/2 ul PBS per mouse) was also injected into naïve animals with SB 203580 hydrochloride (0.4 ug/2 ul PBS per mouse), a p38 MAPK inhibitor, or PBS. Vehicle groups received the same volume of PBS injection. Evans blue extravasation was detected at 1 and 24 hours in the PDGF-AA with PBS groups and at 24 hours for the PDGF-AA with SB 203580 hydrochloride group.

Experiment 3: The thrombin specific inhibitor, hirudin (Sigma) was dissolved in sterilized PBS and injected (5 U/5ul PBS per mouse) into the basal ganglia with autologous blood. Hirudin, PDGF-AA and autolougous blood were injected into the basal

ganglia in others. Western blot was conducted at 6 hours following injection. Neurological deficits, brain edema and Evans blue extravasation were detected at 24 hours after injection.

Experiment 4: The PDGFR-α antagonist, Gleevec (60 mg/kg) was administered (intraperitoneal injection) 1 hour following thrombin injection. The PDGF-AA antibody (1.2 ug/mouse, Millipore) was injected with thrombin into the right basal ganglia. The control animals were given thrombin with the same dose of inactive PDGF-AA antibody boiled for 5 min in a 95 °C water bath. Western blot and zymography were conducted 6 hours following injection. Evans blue extravasation was detected at 24 hours after injection.

Neurobehavioral Function Test

Neurobehavioral functions were evaluated by the modified Garcia test (Garcia *et al* 1995; Wu *et al* 2010) and corner turn test (Hua *et al* 2002). In the modified Garcia test, four items including side stroke, vibrissae touch, limb symmetry, and lateral turning were tested with a maximum neurological score able to be achieved at 12 (healthy animal). In the corner turn test, animals were allowed to enter into a corner with a 30 ºC angel. The animals will try to exit the corner with either a right turn or left turn. Ten trials were performed for each animal. The outcome was presented with the percentage of right turn to 10 trials. All neurobehavioral function tests were conducted at different time point following bICH induction by a blinded investigator.

Brain Water Content Measurement

Brain water content was measured as previously described (Rynkowski *et al* 2008) with slight modifications. Briefly, mice were decapitated under deep anesthesia. Brains were immediately removed and cut into 4 mm sections around the needle track. Each section was divided into four parts: ipsilateral and contralateral basal ganglia, ipsilateral and contralateral cortex. The cerebellum was collected as an internal control. Each part was weighed on an electronic analytical balance (APX-60, Denver Instrument) and then dried at 100 °C for 24 h to determine the dry weight (DW). Brain water content (%) was calculated as [(WW - DW)/WW] x 100.

BBB Permeability

To evaluate BBB permeability mice were intraperitoneally injected with Evans blue (250 ul of 4% solution in saline, Sigma, St. Louis, MO) as previously described following a slight modification (Seiffert *et al* 2004). After three hours circulation, mice were perfused under deep anesthesia with cold phosphate-buffered saline (PBS, pH 7.4) until the outflow was clear. Then the brain was removed and separated into ipsilateral and contralateral cerebrums and stored appropriately at -80 °C immediately until analysis. The ipsilateal parts of the brains were homogenized in PBS and centrifuged (15000 g, 4 °C, 30 min). The supernatant was collected and mixed with equal volume of Trichloroacetic acid (TCA) overnight. After centrifugation (15000 g, 4 °C, 30 min), Albumin–Evans blue complex concentrations were measured spectrophotometerically at a wavelength of 610 nm.

Sample Preparation

Mice were euthanized 6 hours following bICH. Perfusion with cold phosphate-buffered saline (PBS, pH 7.4) solution was performed, followed by removal of the brain and separation into ipsilateral and contralateral cerebrums. The brain parts were stored appropriately at -80 °C immediately until analysis. Protein extraction was obtained by gently homogenizing them in RIPA lysis buffer (Santa Cruz) with phosphatase inhibitors (Sigma) with further centrifugation at 14,000 g at 4 °C for 30 min. The supernatant was collected and the protein concentration was determined using a detergent compatible assay (Bio-Rad, Dc protein assay). Samples were stored at -80 °C for immunoprecipitation, western blot or zymography.

Immunoprecipitation

Immuonprecipitation for phosphorylated PDGFR-α was carried out according to the manufacture instructions. Equal amounts of protein (200 ug) was mixed with anti-PDGFR-α (1:100, cell signaling) in microcentrifuge tube and incubated for 2 hours at 4 °C. Then protein A/G PLUS-Agarose (Santa Cruz) was added and left to shake overnight at 4 °C. The mixture was washed 3 times with the centrifuge (1000 g, 5 min, 4 °C). The pellet was collected and re-suspended in equal volumes of loading buffer. Samples were run on SDS-PAGE gels and probed with antibodies to PDGFR-α and p-PDGFR-α.

Western Blotting

Western Blotting was performed as previously described (Chen *et al* 2008). After samples preparation, equal amounts of protein were run on an SDS-PAGE gel. After

being electrophoresed and transferred to a nitrocellulose membrane, the membrane was blocked and incubated with the primary antibody overnight at 4°C. The primary antibodies were anti-phospho-JNK1/2 (1:1000, cell signaling), anti-JNK1/2 (1:1000, cell signaling), anti-phospho-ERK1/2 (1:1000, cell signaling), anti-ERK1/2 (1:1000, Santa Cruz), anti-phospho-p38 (1:1000, cell signaling), anti-p38 (1:1000, cell signaling), anti-phospho-ATF2 (1:1000, Abcam), anti-PDGF-AA (1:1000, Millipore), anti-MMP-13 (1:1000, Abcam), anti-MMP-10 (1:1000, Santa Cruz), and p-Tyr (PY99) (1:1000, Santa Cruz). Nitrocellulose membranes were incubated with secondary antibodies (Santa Cruz) for 1 hour at room temperature. Immunoblots were then probed with an ECL Plus chemiluminescence reagent kit (Amersham Biosciences, Arlington Heights, IL) and visualized with the image system (Bio-Rad, Versa Doc, model 4000). All data was analyzed using the software Image J.

Gelatin Zymography

MMP-2/9 activity was measured by gelatin zymography modified from previous studies (Chen *et al* 2009). Equal amounts of protein was mixed with zymography sample buffer and loaded on a 10% gelatin zymogram gels (invitrogen). Gels were then washed with denature buffer (Bio-Rad) for 1 hour and incubated in development buffer for 72 hours at 37 °C. Gels were stained with 0.5% coomassie blue G-250 for 1 hour and destained with the same buffer without G-250 till the clear bands were seen on the blue background. Human MMP-9 (Chemicon) was used as gelatinase standard. The gel image was taken and later calculated using the image J software.

Immunofluorescence

Six hours following bICH, mice were perfused under deep anesthesia with cold phosphate-buffered saline (PBS, pH 7.4), followed by infusion of 10% paraformaldehyde. Brains were then removed and fixed in formalin at 4 °C for a minimum of 3 days. Samples were then dehydrated with 30% sucrose in phosphate-buffered saline (PBS, pH 7.4) and the frozen coronal slices (10 μm thick) were then sectioned in cryostat (CM3050S; Leica Microsystems). Double immunofluorescence was performed as previously described (Chen *et al* 2009). Anti-PDGFR-α antibody (1:100, R&D), anti-MMP-9 (1:50, Santa Cruz), anti-MMP-13 (1:50, Abcam), anti-MMP-10 (1:50, Santa Cruz) and anti-phospho-p38 (1:50, Cell signaling) were incubated separately with primary antibodies: anti-GFAP antibody (1:200, Dako), anti-vWF antibody (1:100, Millipore) overnight at 4 °C, followed by incubation with appropriate fluorescence conjugated secondary antibodies (Jackson Immunoresearch, West Grove, PA). The slices were visualized underneath a fluorescence microscope (Olympus BX51, Olympus Optical Co. Ltd, Japan), and pictures were taken with software MagnaFire SP 2.1B (Olympus, Melville, NY).

Statistics

Data was expressed as mean ± standard error of the mean. Analysis was performed using GraphPad Prism software. Statistical differences between two groups were analyzed using Student`s unpaired, two-tailed t-test. Multiple comparisons (without rating scale data) were statistically analyzed with one-way analysis of variance (ANOVA) followed by Student-Newman-Keuls test. Statistically significance was defined as $p < 0.05$. For the rating scale data (modified Garcia test), data were expressed as median ±

25th-75th percentiles. We used the Kruskal-Wallis One Way Analysis of Variance on Ranks, followed by the Steel-Dwass multiple comparisons tests.

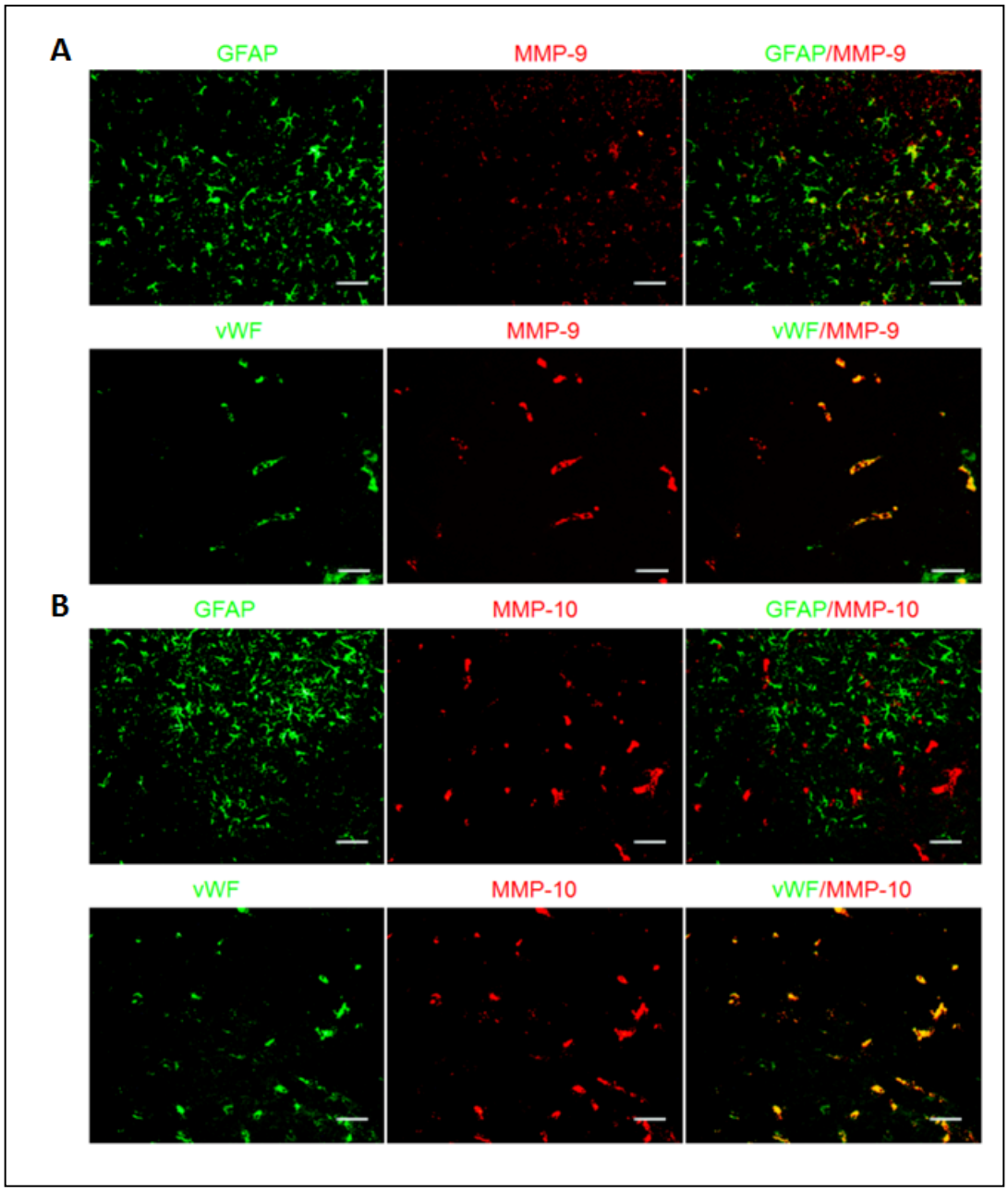

Supplemental figure 1. Immunofluorescence for the expression of MMP-9, MMP-10, MMP-13 and phospho-p38 MAPK in the astrocytes and endothelial cells in the perihematomal area 6 hours following bICH. Representative photographs of immunofluorescence staining revealed that MMP-9 (A), MMP-13

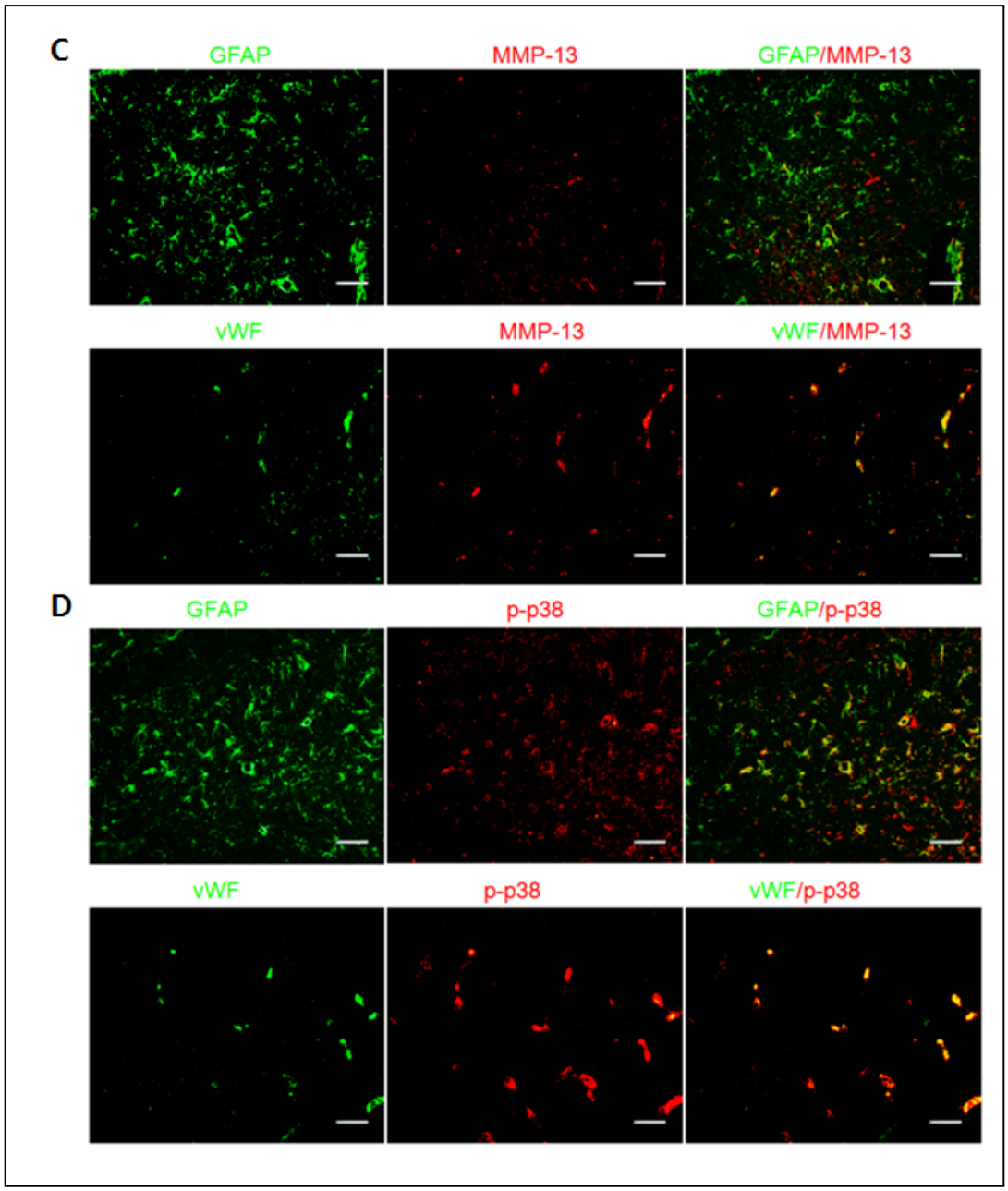

Supplemental figure 1, *Continued.* (C) and phosphor-p38 (D) (red) expressed in astrocytes (GFAP, green) and endothelial cells (vWf, green), and MMP-10 (B) expressed in endothelial cells (vWf, green). Scale bar: 50 µm.

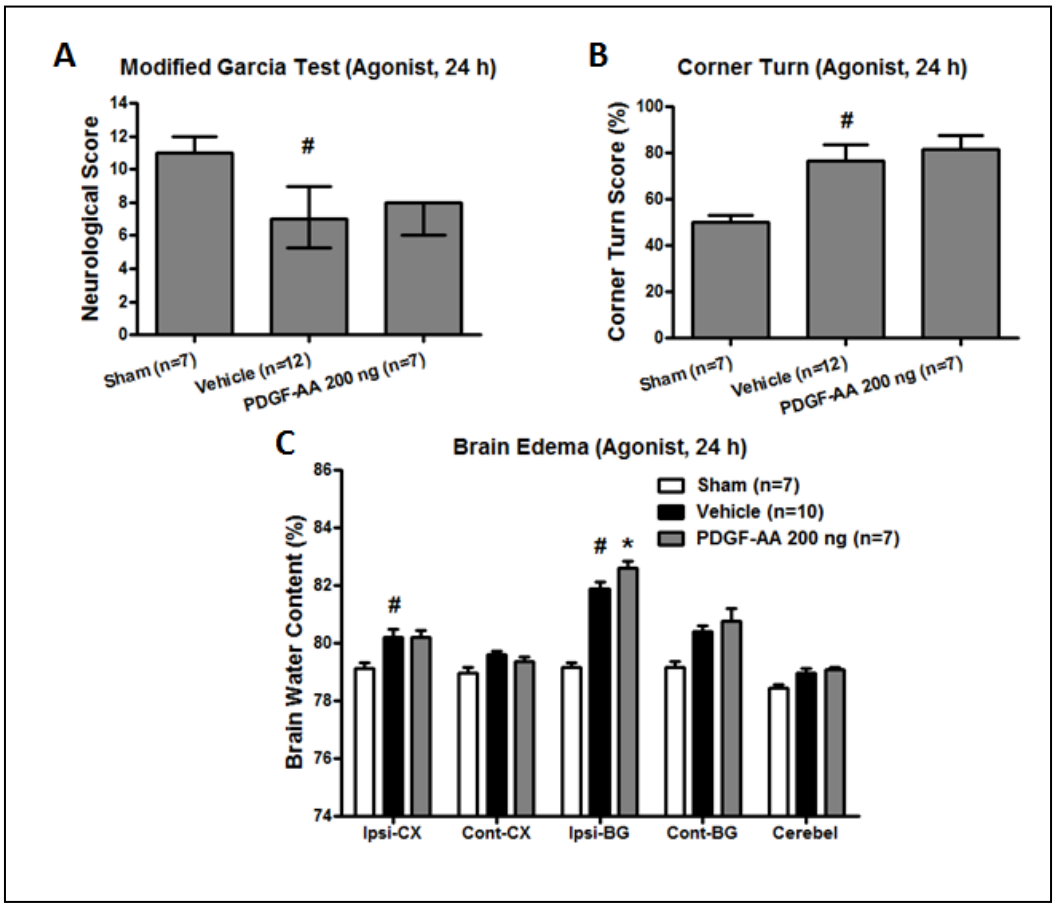

Supplemental figure 2: PDGFR-α activation failed to exacerbate neurobehavioral functions (A, B), but increased brain edema in bICH mice (C). Modified Garcia test (A) and corner turn (B) at 24 hours following operation in sham, vehicle and PDGF-AA treatment (200 ng) mice; (C) Brain edema 24 hours following operation in sham, vehicle and PDGF-AA treatment (200 ng) mice; # $p < 0.05$ vs Sham; * $p < 0.05$ vs Vehicle. n = 7-12 mice per group. Error bars represent median ± 25th-75th percentiles (A) or mean ± standard error of the mean (B and C). # $p < 0.05$ vs Sham; * $p < 0.05$ vs Vehicle.

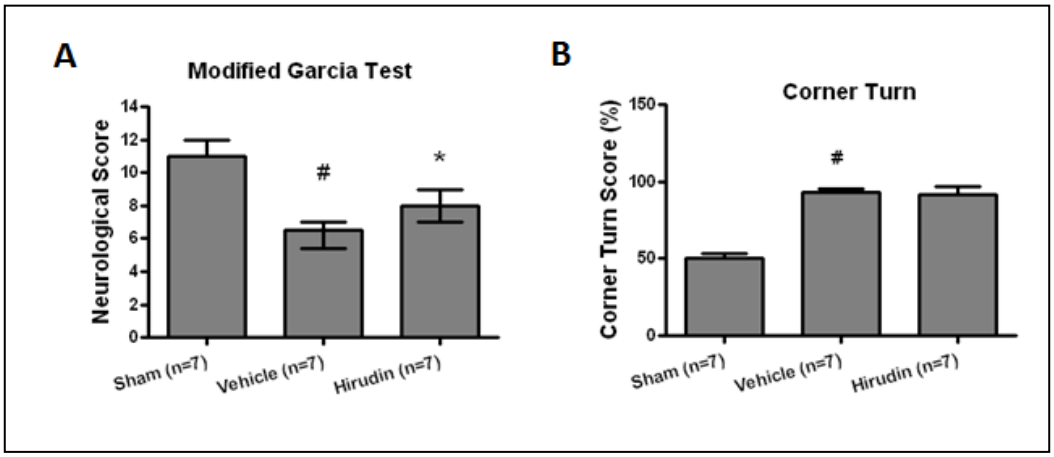

Supplemental Figure 3: Thrombin inhibition improved neurobehavioral functions following bICH injury. Modified Garcia test (A) and corner turn (B) 24 hours following operation in sham, vehicle and hirudin treatment (5 U) mice. n = 7 mice per group. Error bars represent median ± 25th-75th percentiles (A) or mean ± standard error of the mean (B). # $p < 0.05$ vs Sham; * $p < 0.05$ vs Vehicle.

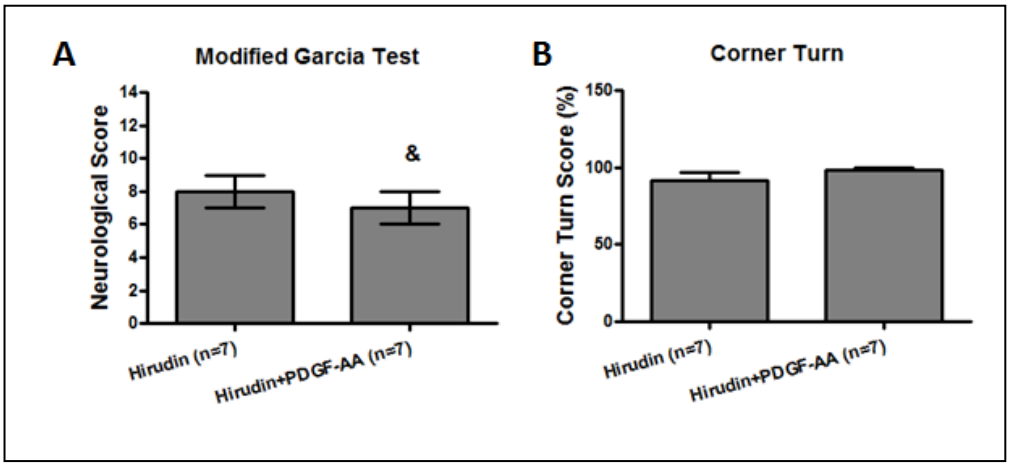

Supplemental Figure 4: Activation of PDGFR-α by PDGF-AA reversed thrombin inhibition by hirudin following bICH. Modified Garcia test (A) and corner turn (B) 24 hours after bICH in hirudin (5 U) and hirudin (5 U)+PDGF-AA (200 ng) mice. n = 7 mice per group. Error bars represent median ± 25th-75th percentiles (A) or mean ± standard error of the mean (B). & $p < 0.05$ vs Hirudin.

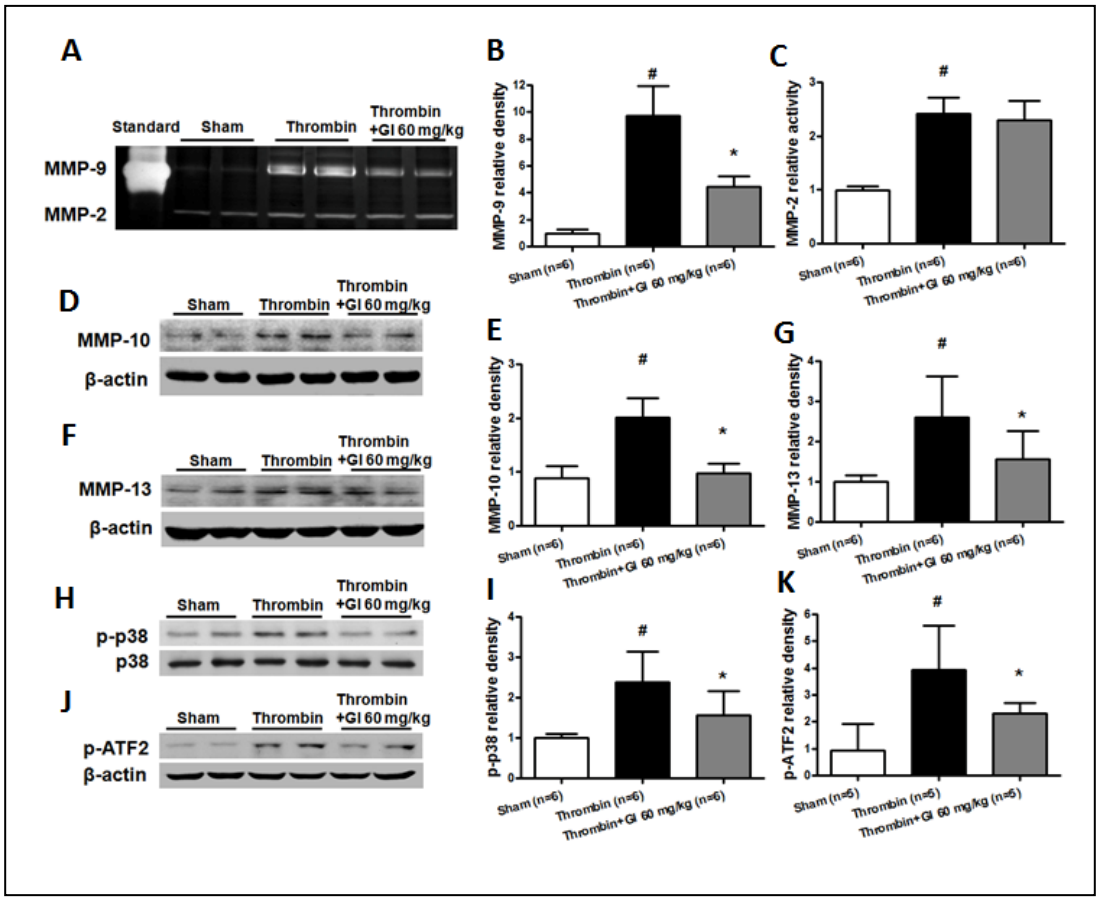

Supplemental Figure 5: Characterization of the PDGFR-α downstream pathway at 6 hours following thrombin injection in mice. (A) Zymography assay for MMP-9 and MMP-2 activity in the ipsilateral hemisphere in sham, thrombin and Gl treatment (60 mg/kg) mice; Western blot assay for MMP-10 (D), MMP-13 (F), and p38/p-p38 (H), p-ATF-2 (J) in the ipsilateral hemisphere in sham, thrombin and Gl treatment (60 mg/kg) mice. Quantification of A, D, F, H and J is shown in B, C, E, G, I and K, respectively, n = 5-8 mice per group. Error bars represent mean ± standard error of the mean. # $p < 0.05$ vs Sham; * $p < 0.05$ vs Thrombin.

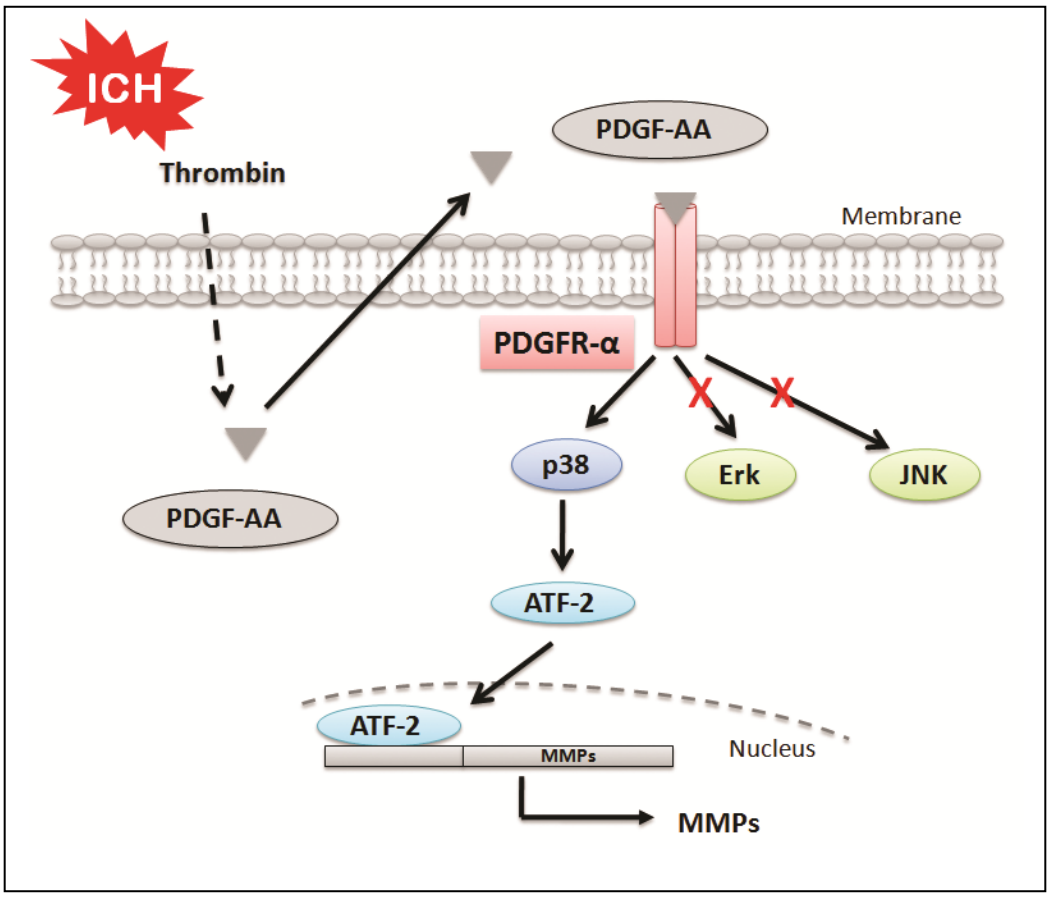

Supplemental Figure 6: Schematic of PDGFR-α signaling pathway triggered by thrombin post-ICH. Thrombin promotes PDGFR-α activation via upregulation of PDGF-AA, leading to p38 MAPK signaling but not ERK or JNK MAPKs signaling, and subsequent activation of downstream transcription factor, ATF-2. Activation of ATF-2 results in expression of MMPs which degrade extracellular matrix and finally lead to BBB disruption.

CHAPTER FOUR

SUMMARY AND CONCLUSION

Our data presented in the previous chapters indicated that the inhibition of VAP-1 mediated inflammatory response or PDGFR-α mediated BBB permeability reduced brain edema and improved neurological function in ICH mouse models. Furthermore, we explored the underlying mechanisms and found: (1) VAP-1 inhibition downregulated the level of other adhesion molecules, such as ICAM-1, P-selectin, pro-inflammatory factors, such as MCP-1 and TNF-α, and also inhibited the leukocyte infiltration and macrophage/microglia activation, (2) PDGFR-α was transiently upregulated in ipsilateral hemisphere following ICH injury and orchestrated blood-brain barrier permeability via p38-ATF2-MMPs pathway. Thrombin was the upstream regulator of PDGFR-α activity. Thus, our study developed new therapeutic strategies for brain edema treatment by targeting an inflammatory mediator, VAP-1 and a BBB orchestrator, PDGFR- α.

Significance of Anti-inflammation and BBB Damage in ICH

Multiple factors have been suggested to induce BBB damage following ICH, including the inflammatory response (immune cells and their products, cytokine and chemokine), thrombin and MMPs.

The earliest report of antileukocyte therapy was from Mendelow`s lab. They made a global depletion of circulating leucocytes and platelets by whole body irradiation in a rodent ICH model and found protection against both cerebral ischemia and edema

formation (Kane *et al* 1992). Recently Zhao and colleagues injected 15-Deoxy-Delta(12,14)-prostaglandin J2 (15d-PGJ2), a physiologic agonist for PPAR gamma into striatal hematoma and found a restriction of neutrophil infiltration as well as the reduction of neurobehavioral deficits and neuronal damage (Zhao *et al* 2006). Some studies focused on the inhibition of MMPs. Wang and colleagues showed that the administration of MMPs inhibitor GM6001 (100 mg/kg) ameliorated dysregulation of gelatinase activity, neutrophil infiltration, production of oxidative stress, brain edema and degeneration of neurons (Wang and Tsirka 2005a). From the same group another study reported that the tripeptide macrophage/microglial inhibitory factor (MIF), Thr-Lys-Pro inhibited microglial activation and macrophage infiltration, reduced brain edema and improved the neurological function (Wang and Tsirka 2005b). In 2003, Power and colleagues applied minocycline one hour after a collagenase-induced ICH in rat. They found that minocycline suppressed monocytoid cell activation as well as MMP-12 expression after 7 days of treatment. The apoptotic cell death was reduced and functional recovery was also observed (Power *et al* 2003). Aside from the immune cells inhibition, treatment focused on the cellular components of inflammation has also been investigated. TNF-α-specific antisense oligodeoxynucleotide (Mayne *et al* 2001b) and adenosine A_{2A} receptor agonists (Mayne *et al* 2001a) have been applied following ICH. Reduced cell death and improved neurological functions were also observed. Application of IL-1ra was a promising way to affect IL-1. Masada and colleagues have applied an adenovirus vector for IL-1ra and found reduction of brain edema in an autologous blood model of ICH in rat (Masada *et al* 2001). Additionally, Wu and colleagues found that caspase-1 inhibitor, Ac-YVAD-CMK protected BBB integrity by reducing IL-1β expression in a collagenase-

injection ICH mouse model (Wu *et al* 2010). Studies by Titova and colleagues targeted CD-18, an integrin on brain injury in a collagenase-induced ICH in CD-18 knockout mice. Twenty four hours later, the numbers of infiltrated neutrophils were markedly reduced. And CD-18 knockout mice also show a reduced brain edema and improved neurological functions (Titova *et al* 2008).

Currently, there are no effective therapeutic strategies to prevent ICH induced BBB disruption in human although a large number of investigations have been conducted. In experimental animal models, studies mainly focused on mediators which have been shown to be upregulated following ICH injury or compounds related to BBB permeability, such as inflammatory cytokines, thrombin and MMPs (Abbott *et al* 2006; Power *et al* 2003). MMPs were upregulated following ICH and can lead to BBB damage and hemorrhage by degradation of extracellular matrix (ECM) components (Alvarez-Sabin *et al* 2004; Rosenberg *et al* 1993). TIMP-2, an endogenous MMPs inhibitor reduced extracellular matrix proteolysis and protected BBB (Rosenberg *et al* 1992). Some MMPs inhibitors, such as BB-1101 and GM6001, have been found to preserve BBB integrity, reduce brain edema and neurological deficits (Power *et al* 2003; Rosenberg and Navratil 1997). Therefore, targeting inflammatory response or BBB impairment orchestrators are essential for the development of alternative therapeutic strategies for ICH induced brain injury.

Mechanism of VAP-1 in Anti-Inflammation

In 1992, Salmi and Jalkanen discovered VAP-1, a 90 Kilodalton endothelial cell molecule in synovial vessels from arthritis patients. They also found that VAP-1 antibody

reduced the binding of lymphocyte to high endothelial venules (Salmi and Jalkanen 1992). Since then, the roles of VAP-1 in inflammatory response have been widely investigated both *in vitro* and in inflammatory disease animal models.

In vitro studies, Yoong and colleagues reported that VAP-1 and ICAM-1 mediated, tethering and firm adhesion steps respectively, in T cell infiltration in human hepatocellular carcinoma and VAP-1 antibody inhibited T cell binding to endothelium in an *in vitro* tissue binding assay (Yoong *et al* 1998). Another study suggested that the enzymatic activity of VAP-1 was responsible for both transmigration and adhesion. VAP-1 antibody resulted in a 50% reduction of lymphocyte binding to TNF-α treated HSE cells (Hepatic sinusoidal endothelial) while inhibition of VAP-1 amine oxidase activity reduced both adhesion and transmigration of lymphocytes to a level similar to that seen with the use of VAP-1 antibody (Lalor *et al* 2002). VAP-1 function has also been verified in various inflammatory animal models. In peritoneal inflammation models in rabbit, Tohka and colleagues observed an increase in granulocyte rolling velocity and reduced firm bound and extravsasion leukocytes and indicated that VAP-1 functions as a molecular brake during granulocyte rolling and mediates the firm adhesion and recruitment (Tohka *et al* 2001). In an age-related mouse macular degeneration (AMD) model, VAP-1 suppression diminished the expression of pro-inflammatory cytokines, including TNF-α, MCP-1 as well as adhesion molecule, ICAM-1 (Noda *et al* 2008). Since VAP-1 are involved in the inflammatory response as shown by above evidences, studying the role of VAP-1 in ICH-induced inflammation and the underlying mechanisms is critically important for stroke therapy.

For the first time, we studied the functions of VAP-1 in ICH-induced inflammatory response in mouse models. In our study, we used small VAP-1 molecular inhibitors, LJP 1586 (O'Rourke et al., 2008) as well as a reference compound, semicarbazide to inhibit the VAP-1(SSAO) activity. The administration of a small molecular VAP-1 inhibitor, LJP1586 reduced brain edema and improved neurological function in both collagenase and blood-induced ICH mouse models. Moreover, we found that the protective effect was achieved by anti-inflammation since, VAP-1 inhibition downregulated adhesion molecules and pro-inflammatory factors expression as well as neurophils infiltration and microglia activation. With regards to mechanism, VAP-1 siRNA or human recombinant AOC3 protein was also applied to validate the neuroprotective role of LJP1586 by VAP-1 inhibition as well. All our data showed that the inhibition of VAP-1 provided neuroprotection by anti-inflammatory effect in ICH models.

Our study investigated the function of VAP-1 in both callagenase injection and autologous blood injection models which are the most widely used rodent ICH models (Andaluz et al., 2002). With the collagenase injection model (cICH), the strength is that the formation of the hematoma was generated by direct disruption of blood vessels, mimicking a spontaneous ICH in humans (MacLellan et al., 2008). Additionally, the amount of collagenase injected correlates well with the final size of the hematoma. However, bacterial collagenase has been known to induce an exaggerated inflammatory response in the brain. Although *in vitro* study showed that the concentration of collagenase used *in vivo* cannot cause apoptosis, higher doses of collagenase induces neuronal damage (Matsushita et al., 2000). Autologous blood injection model (bICH)

closely mimics the clinical manifestation of ICH partly because it lacks an exaggerated inflammatory response. However, bICH does not allow an opportunity to evaluate re-bleeding or the effects of microvascular breakdown. In order to avoid the limitation of each model and the possible interferes of bacterial collagenase in the inflammatory response after ICH, we investigated the anti-inflammation effect of VAP-1 blockade in both models. Our results showed that the inhibition of VAP-1 in autologous blood injection ICH model also provided neuroprotective effect.

VAP-1 was called inflammatory inducible protein, however, the underlying mechanism and mediators inducing VAP-1 expression or translocation were still unclear. In 1997, Salmi and colleagues used an organ culture technique for the investigation of the regulation of VAP-1 expression in a more physiological micromilieu microenvironment. After treatment with inflammatory mediators in human tonsillar tissue, IL-1 and TNF-α upregulated VAP-1 expression but thrombin did not (Arvilommi *et al* 1997). As the authors mentioned VAP-1 upregulation was organ-specific and may be induced by the combination of multiple factors, and *in vitro* studies do not completely reflect the pathophysiological condition, therefore, this result cannot rule out the possibility that thrombin may regulate VAP-1 expression or translocation in other organs during inflammation. Thrombin has multiple functions during inflammation. It played a role in leukocyte extravasation (Kaur *et al* 2001; Lorant *et al* 1991) and regulate cytokines expression, including TNF-α (Hua *et al* 2006). It has been reported that thrombin regulates adhesion molecules expression and translocation in endothelial cells, including P-selectin, E-selectin, ICAM-1 and VCAM-1 (Kaplanski *et al* 1998; Lorant *et al* 1991; Minami and Aird 2001; Rahman *et al* 1999; Sugama *et al* 1992). VAP-1 was determined

to be a molecular brake during granulocyte rolling and mediates recruitment *in vivo* (Tohka *et al* 2001) and also regulates the expression of other adhesion molecule. Based on these observations, it is rational to suggest that the thrombin may regulate VAP-1 expression and translocation in brain tissue during inflammation.

Dual Roles of PDGF/PDGFRs

As a growth factor the functions of PDGF/PDGFR system during development have been well established, however, a high level of PDGF expression in tissue may change the function in an unfavorable local environment. In 1995, Kim and colleagues found that the serum-deprived normal rat kidney fibroblast (NRK) cells treated with PDGF-AA or PDGF-BB homodimers presented with apoptotic cell death. Epidermal growth factor also induced apoptotic cell death under identical conditions. The potential mechanism was that the inability to transit the G1/S checkpoint determined the direction of the PDGF signal to apoptosis (Kim *et al* 1995). Studies in 1997, based on previous studies showed that a p53-independent apoptotic pathways existed following irradiation, the same group found that the activation of PDGF signaling led to apoptotic cell death in mutant p53-containing, hormone-independent, highly metastatic prostate carcinoma cells following irradiation (Morris *et al* 1997).

However, the anti-apoptotic cell death function of PDGFs was also reported in several cell types, including smooth muscle cells, fibroblasts and cardiomyocytes (Harrington *et al* 1994; Romashkova and Makarov 1999; Vantler *et al* 2005; Vantler *et al* 2010). In 2004, Egawa-Tsuzuki reported that the infusion of PDGF-B reduced lesion size in a hypoxia ischemia animal model. And the PDGFR-β signaling was found to protect

against NMDA-induced CNS injury (Egawa-Tsuzuki *et al* 2004). A novel PDGF ligand, PDGF-CC was found to protect different types of neurons from apoptosis in both the retina and brain animal models, including axotomy-induced neuronal death, neurotoxin-induced neuronal injury, 6-hydroxydopamine-induced Parkinson's dopaminergic neuronal death and ischemia-induced stroke (Tang *et al* 2010).

PDGF/PDGFRs are also involved in the development of BBB structure and stabilization. It is well known that pericytes play a critical role in supporting endothelial cell (EC) tube formation and stabilization and vascular maturation including basement membrane matrix deposition. In 2010, study from Stratman and colleagues reported that endothelial-derived PDGF-BB was required to control pericyte motility, proliferation, and recruitment along the EC tube. The combined inhibition of PDGF-BB and HB-EGF-induced signaling in quail embryos with soluble receptor traps or antibodies reduced pericyte recruitment to EC tubes, decreased basement membrane matrix deposition, and increased vascular hemorrhage phenotypes *in vivo* (Stratman *et al* 2010). Currently, Raines and colleagues studied the role of pericyte in the transport of insulin across the endothelial cell layer and found that PDGF-B deficiency enhanced hepatic vascular transendothelial transport and insulin sensitivity (Raines *et al* 2011).

In contrast, Su and colleagues found that tPA therapy induced hemorrhagic transformation was mediated by its substrate, PDGF-CC, an endogenous agonist of PDGFR-α. Their finding suggests that BBB disruption induced by PDGF was a PDGFR-α dependent process since the injection of different PDGFs into the CSF of naïve mice could increase the extravasation of Evans blue one hour following administration (Su *et al* 2008). Yet another study led by Yao and colleagues recently found that cocaine-

induced PDGF-BB could increase vascular permeability and that administration of a PDGF-BB neutralizing antibody could abolish this effect (Yao *et al* 2010). Earlier studies, reported that PDGF mediated tight junction and adherens junction protein redistribution and increased permeability in Madin-Darby canine kidney (MDCK) cells (Harhaj *et al* 2002). All the data suggests that PDGF/PDGFR may play a multifaceted role under different stimulus conditions.

Mechanism of PDGF/PDGFRs on BBB Damage

The mechanisms about PDGFs/PDGFRs regulation on BBB integrity are still unclear. Previous study from Su and colleagues reported a PDGFR-α dependent pathway in tPA therapy caused BBB impairment. In our study, we proposed that another protease, thrombin was responsible for PDGFR-α activation.

Mounting evidences indicated that thrombin might be an upstream regulator of PDGF ligands. In 1988, Kavanaugh investigated PDGF ligands expression after treatment with several compounds in microvascular endothelial cells, and found that thrombin stimulated B chain transcription and had little or no effect on A chain transcription (Kavanaugh *et al* 1988). Three years later, Shankar reported that both PDGF-AA and BB expression were stimulated with thrombin via GTP gamma S in human endothelial cells (Shankar *et al* 1992). In 1995, Kanthou and colleagues treated human vascular smooth muscle cells (HVSMC) with a thrombin receptor agonist/activating peptide (TRAP) or thrombin. Their data revealed that thrombin and to a lesser extent TRAP induced PDGF-AA protein expression (Kanthou *et al* 1995). In lung and airway epithelial cells, it has been reported that thrombin stimulated PDGF expression via its PAR-1 receptor and not

PAR-3 or PAR-4 receptor (Shimizu *et al* 2000). In 2005, Narita investigated if PAR-1 PDGF pathway in spinal cord injury could contribute to the development of a neuropathic pain-like state in a sciatic nerve ligation mice model. They found that hirudin, PDGFR-α/Fc chimera protein or a PDGFR-dependent tyrosine kinase inhibitor suppressed thermal hyperalgesia and tactile allodynia induced by sciatic nerve ligation (Narita *et al* 2005). All these previous reports supported our hypothesis that thrombin will result in BBB impairment possibly via the activation of PDGFR-α.

In our study, we hypothesized that PDGFR-α activation may contribute to BBB impairment via p38 MAPK mediated MMP activation/expression following ICH and that thrombin may be the upstream regulator. We found that ICH-induced brain injury transiently upregulates PDGFR-α level and markedly increased PDGF-AA level mainly in endothelial cells and perivascular related astrocytes. For the role of PDGFR-α in orchestrating BBB disruption after ICH, PDGFR-α antagonist, Gleevec which showed protective effect on BBB integrity in a mouse ischemic stroke model was used one hour after ICH. We used three different doses and observed a dose-dependent effect of Gleevec treatment on the improvement of neurological function after ICH. While some dose-related adverse events reported in some patients during Gleevec therapy, such as nausea, vomiting, diarrhea, and fluid retention etc. (Deininger *et al* 2003; O'Brien *et al* 2003) do not occur. Moerover, We attempted to invetigate the downstream signals of PDGFR-α and found that PDGFR-α agonist, PDGF-AA induced BBB disruption and was reversed by a p38 inhibitor in naïve mice. MMPs were evaluated as potential downstream mediators of PDGFR-α on BBB disruption. Base on previous studies that thrombin led to BBB damage and regulated PDGFs expression, thus we proposed that thrombin may be

responsible for PDGFR-α activation. Our data showed that PDGF-AA reversed the effect of thrombin inhibitor, hirudin on BBB disruption and indicated that thrombin was the upstream regulator of PDGFR-α regulator. Furthermore, in our thrombin injection model, animals receiving a PDGF-AA neutralizing antibody or Gleevec, the PDGFR-α antagonist, showed minimized thrombin-induced BBB impairment. Therefore, we concluded that PDGFR-α signaling may contribute to BBB impairment following ICH and that thrombin may be the key upstream orchestrator.

In summary, our study investigated the mechanisms of brain edema development from two directions: inflammatory response and BBB orchestrators leading to direct BBB disruption. We found that the inhibition of inflammatory mediator, VAP-1 or a BBB orchestrator, PDGFR-α reduced brain edema and improved neurological function. Therefore, targeting VAP-1 or PDGFR-α signaling may provide potential therapy treatments to ICH-induced brain injury.

Future Studies

Our study just focus on PDGFR-α signaling, however, PDGFR-β signaling may also be involved in BBB impairment since thrombin also regulates the expression of PDGF-BB (Stenina *et al* 2001) which is the agonist of both PDGFR-α and PDGFR-β and increases BBB permeability (Su *et al* 2008). Gleevec is a tyrosine kinase antagonist, which not only inhibits PDGFR-α but also inhibits PDGFR-β. Thus we do not deny the potential effect of PDGFR-β on BBB disruption. Therefore, a further study is warranted to explore the role of PDGFR-β on BBB damage in ICH. Measuring the activation of PDGFR-β after ICH will be helpful to clarify the role of PDGFR-β BBB damage. PDGF-

BB + PDGFR-α neutralizing antibody can be injected to test the effect on BBB permeability. If PDGF-BB plus PDGFR-α neutralizing antibody increases BBB permeability, PDGFR-β may also be responsible for BBB damage.

REFERENCES

Abbott NJ, Ronnback L, Hansson E (2006) Astrocyte-endothelial interactions at the blood-brain barrier. *Nat Rev Neurosci* 7:41-53

Airas L, Lindsberg PJ, Karjalainen-Lindsberg ML, Mononen I, Kotisaari K, Smith DJ, Jalkanen S (2008) Vascular adhesion protein-1 in human ischaemic stroke. *Neuropathol Appl Neurobiol* 34:394-402

Alvarez-Sabin J, Delgado P, Abilleira S, Molina CA, Arenillas J, Ribo M, Santamarina E, Quintana M, Monasterio J, Montaner J (2004) Temporal profile of matrix metalloproteinases and their inhibitors after spontaneous intracerebral hemorrhage: relationship to clinical and radiological outcome. *Stroke* 35:1316-22

Alvarez RH, Kantarjian HM, Cortes JE (2006) Biology of platelet-derived growth factor and its involvement in disease. *Mayo Clin Proc* 81:1241-57

Andaluz N, Zuccarello M, Wagner KR (2002) Experimental animal models of intracerebral hemorrhage. *Neurosurg Clin N Am* 13:385-93

Andrae J, Gallini R, Betsholtz C (2008) Role of platelet-derived growth factors in physiology and medicine. *Genes Dev* 22:1276-312

Antoniades HN, Scher CD, Stiles CD (1979) Purification of human platelet-derived growth factor. *Proc Natl Acad Sci U S A* 76:1809-13

Arai T, Miklossy J, Klegeris A, Guo JP, McGeer PL (2006) Thrombin and prothrombin are expressed by neurons and glial cells and accumulate in neurofibrillary tangles in Alzheimer disease brain. *J Neuropathol Exp Neurol* 65:19-25

Armulik A, Genove G, Mae M, Nisancioglu MH, Wallgard E, Niaudet C, He L, Norlin J, Lindblom P, Strittmatter K, Johansson BR, Betsholtz C (2010) Pericytes regulate the blood-brain barrier. *Nature* 468:557-61

Aronowski J, Hall CE (2005) New horizons for primary intracerebral hemorrhage treatment: experience from preclinical studies. *Neurol Res* 27:268-79

Arvilommi AM, Salmi M, Jalkanen S (1997) Organ-selective regulation of vascular adhesion protein-1 expression in man. *Eur J Immunol* 27:1794-800

Ballabh P, Braun A, Nedergaard M (2004) The blood-brain barrier: an overview: structure, regulation, and clinical implications. *Neurobiol Dis* 16:1-13

Barone FC, Feuerstein GZ (1999) Inflammatory mediators and stroke: new opportunities for novel therapeutics. *J Cereb Blood Flow Metab* 19:819-34

Battegay EJ, Rupp J, Iruela-Arispe L, Sage EH, Pech M (1994) PDGF-BB modulates endothelial proliferation and angiogenesis in vitro via PDGF beta-receptors. *J Cell Biol* 125:917-28

Belayev L, Saul I, Curbelo K, Busto R, Belayev A, Zhang Y, Riyamongkol P, Zhao W, Ginsberg MD (2003) Experimental intracerebral hemorrhage in the mouse: histological, behavioral, and hemodynamic characterization of a double-injection model. *Stroke* 34:2221-7

Bergsten E, Uutela M, Li X, Pietras K, Ostman A, Heldin CH, Alitalo K, Eriksson U (2001) PDGF-D is a specific, protease-activated ligand for the PDGF beta-receptor. *Nat Cell Biol* 3:512-6

Betz AL, Iannotti F, Hoff JT (1989) Brain edema: a classification based on blood-brain barrier integrity. *Cerebrovasc Brain Metab Rev* 1:133-54

Blatti SP, Foster DN, Ranganathan G, Moses HL, Getz MJ (1988) Induction of fibronectin gene transcription and mRNA is a primary response to growth-factor stimulation of AKR-2B cells. *Proc Natl Acad Sci U S A* 85:1119-23

Bogdan C, Rollinghoff M, Diefenbach A (2000) Reactive oxygen and reactive nitrogen intermediates in innate and specific immunity. *Curr Opin Immunol* 12:64-76

Bostrom H, Willetts K, Pekny M, Leveen P, Lindahl P, Hedstrand H, Pekna M, Hellstrom M, Gebre-Medhin S, Schalling M, Nilsson M, Kurland S, Tornell J, Heath JK, Betsholtz C (1996) PDGF-A signaling is a critical event in lung alveolar myofibroblast development and alveogenesis. *Cell* 85:863-73

Brott T, Broderick J, Kothari R, Barsan W, Tomsick T, Sauerbeck L, Spilker J, Duldner J, Khoury J (1997) Early hemorrhage growth in patients with intracerebral hemorrhage. *Stroke* 28:1-5

Bullock R, Mendelow AD, Teasdale GM, Graham DI (1984) Intracranial haemorrhage induced at arterial pressure in the rat. Part 1: Description of technique, ICP changes and neuropathological findings. *Neurol Res* 6:184-8

Bullock R, Brock-Utne J, van Dellen J, Blake G (1988) Intracerebral hemorrhage in a primate model: effect on regional cerebral blood flow. *Surg Neurol* 29:101-7

Carrithers MD, Visintin I, Kang SJ, Janeway CA, Jr. (2000) Differential adhesion molecule requirements for immune surveillance and inflammatory recruitment. *Brain* 123 (Pt 6):1092-101

Carroll M, Ohno-Jones S, Tamura S, Buchdunger E, Zimmermann J, Lydon NB, Gilliland DG, Druker BJ (1997) CGP 57148, a tyrosine kinase inhibitor, inhibits the growth of cells expressing BCR-ABL, TEL-ABL, and TEL-PDGFR fusion proteins. *Blood* 90:4947-52

Chandrasekharan UM, Yang L, Walters A, Howe P, DiCorleto PE (2004) Role of CL-100, a dual specificity phosphatase, in thrombin-induced endothelial cell activation. *J Biol Chem* 279:46678-85

Chen W, Jadhav V, Tang J, Zhang JH (2008) HIF-1alpha inhibition ameliorates neonatal brain injury in a rat pup hypoxic-ischemic model. *Neurobiol Dis* 31:433-41

Chen W, Hartman R, Ayer R, Marcantonio S, Kamper J, Tang J, Zhang JH (2009) Matrix metalloproteinases inhibition provides neuroprotection against hypoxia-ischemia in the developing brain. *J Neurochem* 111:726-36

Choudhri TF, Hoh BL, Solomon RA, Connolly ES, Jr., Pinsky DJ (1997) Use of a spectrophotometric hemoglobin assay to objectively quantify intracerebral hemorrhage in mice. *Stroke* 28:2296-302

Clark W, Gunion-Rinker L, Lessov N, Hazel K (1998) Citicoline treatment for experimental intracerebral hemorrhage in mice. *Stroke* 29:2136-40

Cuadrado E, Rosell A, Penalba A, Slevin M, Alvarez-Sabin J, Ortega-Aznar A, Montaner J (2009) Vascular MMP-9/TIMP-2 and neuronal MMP-10 up-regulation in human brain after stroke: a combined laser microdissection and protein array study. *J Proteome Res* 8:3191-7

Deininger MW, O'Brien SG, Ford JM, Druker BJ (2003) Practical management of patients with chronic myeloid leukemia receiving imatinib. *J Clin Oncol* 21:1637-47

Deinsberger W, Vogel J, Kuschinsky W, Auer LM, Boker DK (1996) Experimental intracerebral hemorrhage: description of a double injection model in rats. *Neurol Res* 18:475-7

Dennis MS, Burn JP, Sandercock PA, Bamford JM, Wade DT, Warlow CP (1993) Long-term survival after first-ever stroke: the Oxfordshire Community Stroke Project. *Stroke* 24:796-800

Deschepper CF, Bigornia V, Berens ME, Lapointe MC (1991) Production of thrombin and antithrombin III by brain and astroglial cell cultures. *Brain Res Mol Brain Res* 11:355-8

Dibb NJ, Dilworth SM, Mol CD (2004) Switching on kinases: oncogenic activation of BRAF and the PDGFR family. *Nat Rev Cancer* 4:718-27

Dihanich M, Kaser M, Reinhard E, Cunningham D, Monard D (1991) Prothrombin mRNA is expressed by cells of the nervous system. *Neuron* 6:575-81

Dimitrijevic OB, Stamatovic SM, Keep RF, Andjelkovic AV (2006) Effects of the chemokine CCL2 on blood-brain barrier permeability during ischemia-reperfusion injury. *J Cereb Blood Flow Metab* 26:797-810

Egawa-Tsuzuki T, Ohno M, Tanaka N, Takeuchi Y, Uramoto H, Faigle R, Funa K, Ishii Y, Sasahara M (2004) The PDGF B-chain is involved in the ontogenic susceptibility of the developing rat brain to NMDA toxicity. *Exp Neurol* 186:89-98

Emsley HC, Tyrrell PJ (2002) Inflammation and infection in clinical stroke. *J Cereb Blood Flow Metab* 22:1399-419

Engelhardt B, Ransohoff RM (2005) The ins and outs of T-lymphocyte trafficking to the CNS: anatomical sites and molecular mechanisms. *Trends Immunol* 26:485-95

Fager G (1995) Thrombin and proliferation of vascular smooth muscle cells. *Circ Res* 77:645-50

Fewel ME, Thompson BG, Jr., Hoff JT (2003) Spontaneous intracerebral hemorrhage: a review. *Neurosurg Focus* 15:E1

Fredriksson L, Li H, Eriksson U (2004) The PDGF family: four gene products form five dimeric isoforms. *Cytokine Growth Factor Rev* 15:197-204

Fujii Y (1972) [Studies on induced hypothermia for open heart surgery. II. Adequate flow of hypothermic perfusion in the dog]. *Nippon Geka Hokan* 41:149-59

Fujii Y, Tanaka R, Takeuchi S, Koike T, Minakawa T, Sasaki O (1994) Hematoma enlargement in spontaneous intracerebral hemorrhage. *J Neurosurg* 80:51-7

Garcia JH, Wagner S, Liu KF, Hu XJ (1995) Neurological deficit and extent of neuronal necrosis attributable to middle cerebral artery occlusion in rats. Statistical validation. *Stroke* 26:627-34; discussion 35

Gazendam J, Go KG, van Zanten AK (1979) Composition of isolated edema fluid in cold-induced brain edema. *J Neurosurg* 51:70-7

Gehart H, Kumpf S, Ittner A, Ricci R (2010) MAPK signalling in cellular metabolism: stress or wellness? *EMBO Rep* 11:834-40

Gerlai R, Thibodeaux H, Palmer JT, van Lookeren Campagne M, Van Bruggen N (2000) Transient focal cerebral ischemia induces sensorimotor deficits in mice. *Behav Brain Res* 108:63-71

Gong C, Hoff JT, Keep RF (2000) Acute inflammatory reaction following experimental intracerebral hemorrhage in rat. *Brain Res* 871:57-65

Gordon CR, Merchant RS, Marmarou A, Rice CD, Marsh JT, Young HF (1990) Effect of murine recombinant interleukin-1 on brain oedema in the rat. *Acta Neurochir Suppl (Wien)* 51:268-70

Gustafsson O, Rossitti S, Ericsson A, Raininko R (1999) MR imaging of experimentally induced intracranial hemorrhage in rabbits during the first 6 hours. *Acta Radiol* 40:360-8

Harhaj NS, Barber AJ, Antonetti DA (2002) Platelet-derived growth factor mediates tight junction redistribution and increases permeability in MDCK cells. *J Cell Physiol* 193:349-64

Harrington EA, Bennett MR, Fanidi A, Evan GI (1994) c-Myc-induced apoptosis in fibroblasts is inhibited by specific cytokines. *EMBO J* 13:3286-95

Harris ED, Jr., Krane SM (1974) Collagenases (third of three parts). *N Engl J Med* 291:652-61

He Y, Hua Y, Lee JY, Liu W, Keep RF, Wang MM, Xi G (2010) Brain alpha- and beta-globin expression after intracerebral hemorrhage. *Transl Stroke Res* 1:48-56

Heldin CH (1992) Structural and functional studies on platelet-derived growth factor. *EMBO J* 11:4251-9

Heldin CH, Westermark B (1999) Mechanism of action and in vivo role of platelet-derived growth factor. *Physiol Rev* 79:1283-316

Heldin CH, Eriksson U, Ostman A (2002) New members of the platelet-derived growth factor family of mitogens. *Arch Biochem Biophys* 398:284-90

Hellberg C, Ostman A, Heldin CH (2010) PDGF and vessel maturation. *Recent Results Cancer Res* 180:103-14

Hellstrom M, Kalen M, Lindahl P, Abramsson A, Betsholtz C (1999) Role of PDGF-B and PDGFR-beta in recruitment of vascular smooth muscle cells and pericytes during embryonic blood vessel formation in the mouse. *Development* 126:3047-55

Hernandez-Guillamon M, Garcia-Bonilla L, Sole M, Sosti V, Pares M, Campos M, Ortega-Aznar A, Dominguez C, Rubiera M, Ribo M, Quintana M, Molina CA, Alvarez-Sabin J, Rosell A, Unzeta M, Montaner J (2010) Plasma VAP-1/SSAO activity predicts intracranial hemorrhages and adverse neurological outcome after tissue plasminogen activator treatment in stroke. *Stroke* 41:1528-35

Hernandez-Guillamon M, Sole M, Delgado P, Garcia-Bonilla L, Giralt D, Boada C, Penalba A, Garcia S, Flores A, Ribo M, Alvarez-Sabin J, Ortega-Aznar A, Unzeta M, Montaner J (2011) VAP-1/SSAO Plasma Activity and Brain Expression in Human Hemorrhagic Stroke. *Cerebrovasc Dis* 33:55-63

Hickenbottom SL, Grotta JC, Strong R, Denner LA, Aronowski J (1999) Nuclear factor-kappaB and cell death after experimental intracerebral hemorrhage in rats. *Stroke* 30:2472-7; discussion 7-8

Hickey WF (1991) Migration of hematogenous cells through the blood-brain barrier and the initiation of CNS inflammation. *Brain Pathol* 1:97-105

Hoch RV, Soriano P (2003) Roles of PDGF in animal development. *Development* 130:4769-84

Holmin S, Mathiesen T (2000) Intracerebral administration of interleukin-1beta and induction of inflammation, apoptosis, and vasogenic edema. *J Neurosurg* 92:108-20

Hua Y, Schallert T, Keep RF, Wu J, Hoff JT, Xi G (2002) Behavioral tests after intracerebral hemorrhage in the rat. *Stroke* 33:2478-84

Hua Y, Keep RF, Hoff JT, Xi G (2003) Thrombin preconditioning attenuates brain edema induced by erythrocytes and iron. *J Cereb Blood Flow Metab* 23:1448-54

Hua Y, Wu J, Keep RF, Nakamura T, Hoff JT, Xi G (2006) Tumor necrosis factor-alpha increases in the brain after intracerebral hemorrhage and thrombin stimulation. *Neurosurgery* 58:542-50; discussion -50

Hursting MJ, Alford KL, Becker JC, Brooks RL, Joffrion JL, Knappenberger GD, Kogan PW, Kogan TP, McKinney AA, Schwarz RP, Jr. (1997) Novastan (brand of argatroban): a small-molecule, direct thrombin inhibitor. *Semin Thromb Hemost* 23:503-16

Igarashi K, Murai H, Asaka J (1992) Proteolytic processing of amyloid beta protein precursor (APP) by thrombin. *Biochem Biophys Res Commun* 185:1000-4

Irjala H, Salmi M, Alanen K, Grenman R, Jalkanen S (2001) Vascular adhesion protein 1 mediates binding of immunotherapeutic effector cells to tumor endothelium. *J Immunol* 166:6937-43

Jaakkola K, Nikula T, Holopainen R, Vahasilta T, Matikainen MT, Laukkanen ML, Huupponen R, Halkola L, Nieminen L, Hiltunen J, Parviainen S, Clark MR, Knuuti J, Savunen T, Kaapa P, Voipio-Pulkki LM, Jalkanen S (2000) In vivo detection of vascular adhesion protein-1 in experimental inflammation. *Am J Pathol* 157:463-71

Jalkanen S, Karikoski M, Mercier N, Koskinen K, Henttinen T, Elima K, Salmivirta K, Salmi M (2007) The oxidase activity of vascular adhesion protein-1 (VAP-1) induces endothelial E- and P-selectins and leukocyte binding. *Blood* 110:1864-70

James ML, Warner DS, Laskowitz DT (2008) Preclinical models of intracerebral hemorrhage: a translational perspective. *Neurocrit Care* 9:139-52

Johnsson A, Heldin CH, Westermark B, Wasteson A (1982) Platelet-derived growth factor: identification of constituent polypeptide chains. *Biochem Biophys Res Commun* 104:66-74

Johnston B, Kanwar S, Kubes P (1996) Hydrogen peroxide induces leukocyte rolling: modulation by endogenous antioxidant mechanisms including NO. *Am J Physiol* 271:H614-21

Joukov V, Kaipainen A, Jeltsch M, Pajusola K, Olofsson B, Kumar V, Eriksson U, Alitalo K (1997) Vascular endothelial growth factors VEGF-B and VEGF-C. *J Cell Physiol* 173:211-5

Kane PJ, Modha P, Strachan RD, Cook S, Chambers IR, Clayton CB, Mendelow AD (1992) The effect of immunosuppression on the development of cerebral oedema in an experimental model of intracerebral haemorrhage: whole body and regional irradiation. *J Neurol Neurosurg Psychiatry* 55:781-6

Kanthou C, Benzakour O, Patel G, Deadman J, Kakkar VV, Lupu F (1995) Thrombin receptor activating peptide (TRAP) stimulates mitogenesis, c-fos and PDGF-A gene expression in human vascular smooth muscle cells. *Thromb Haemost* 74:1340-7

Kaplanski G, Marin V, Fabrigoule M, Boulay V, Benoliel AM, Bongrand P, Kaplanski S, Farnarier C (1998) Thrombin-activated human endothelial cells support monocyte adhesion in vitro following expression of intercellular adhesion molecule-1 (ICAM-1; CD54) and vascular cell adhesion molecule-1 (VCAM-1; CD106). *Blood* 92:1259-67

Kaufman HH, Pruessner JL, Bernstein DP, Borit A, Ostrow PT, Cahall DL (1985) A rabbit model of intracerebral hematoma. *Acta Neuropathol* 65:318-21

Kaur J, Woodman RC, Ostrovsky L, Kubes P (2001) Selective recruitment of neutrophils and lymphocytes by thrombin: a role for NF-kappaB. *Am J Physiol Heart Circ Physiol* 281:H784-95

Kavanaugh WM, Harsh GRt, Starksen NF, Rocco CM, Williams LT (1988) Transcriptional regulation of the A and B chain genes of platelet-derived growth factor in microvascular endothelial cells. *J Biol Chem* 263:8470-2

Kazui S, Naritomi H, Yamamoto H, Sawada T, Yamaguchi T (1996) Enlargement of spontaneous intracerebral hemorrhage. Incidence and time course. *Stroke* 27:1783-7

Keep RF, Xiang J, Ennis SR, Andjelkovic A, Hua Y, Xi G, Hoff JT (2008) Blood-brain barrier function in intracerebral hemorrhage. *Acta Neurochir Suppl* 105:73-7

Kim HR, Upadhyay S, Li G, Palmer KC, Deuel TF (1995) Platelet-derived growth factor induces apoptosis in growth-arrested murine fibroblasts. *Proc Natl Acad Sci U S A* 92:9500-4

Kitaoka T, Hua Y, Xi G, Hoff JT, Keep RF (2002) Delayed argatroban treatment reduces edema in a rat model of intracerebral hemorrhage. *Stroke* 33:3012-8

Knauper V, Smith B, Lopez-Otin C, Murphy G (1997) Activation of progelatinase B (proMMP-9) by active collagenase-3 (MMP-13). *Eur J Biochem* 248:369-73

Koeppen AH, Dickson AC, McEvoy JA (1995) The cellular reactions to experimental intracerebral hemorrhage. *J Neurol Sci* 134 Suppl:102-12

Kohler N, Lipton A (1974) Platelets as a source of fibroblast growth-promoting activity. *Exp Cell Res* 87:297-301

Koskinen K, Vainio PJ, Smith DJ, Pihlavisto M, Yla-Herttuala S, Jalkanen S, Salmi M (2004) Granulocyte transmigration through the endothelium is regulated by the oxidase activity of vascular adhesion protein-1 (VAP-1). *Blood* 103:3388-95

Kuker W, Thiex R, Rohde I, Rohde V, Thron A (2000) Experimental acute intracerebral hemorrhage. Value of MR sequences for a safe diagnosis at 1.5 and 0.5 T. *Acta Radiol* 41:544-52

Lalor PF, Edwards S, McNab G, Salmi M, Jalkanen S, Adams DH (2002) Vascular adhesion protein-1 mediates adhesion and transmigration of lymphocytes on human hepatic endothelial cells. *J Immunol* 169:983-92

Lalor PF, Sun PJ, Weston CJ, Martin-Santos A, Wakelam MJ, Adams DH (2007) Activation of vascular adhesion protein-1 on liver endothelium results in an NF-kappaB-dependent increase in lymphocyte adhesion. *Hepatology* 45:465-74

LaRochelle WJ, Jeffers M, McDonald WF, Chillakuru RA, Giese NA, Lokker NA, Sullivan C, Boldog FL, Yang M, Vernet C, Burgess CE, Fernandes E, Deegler LL, Rittman B, Shimkets J, Shimkets RA, Rothberg JM, Lichenstein HS (2001) PDGF-D, a new protease-activated growth factor. *Nat Cell Biol* 3:517-21

Lawson LJ, Perry VH, Gordon S (1992) Turnover of resident microglia in the normal adult mouse brain. *Neuroscience* 48:405-15

Lee EJ, Hung YC, Lee MY (1999) Anemic hypoxia in moderate intracerebral hemorrhage: the alterations of cerebral hemodynamics and brain metabolism. *J Neurol Sci* 164:117-23

Lee KR, Colon GP, Betz AL, Keep RF, Kim S, Hoff JT (1996) Edema from intracerebral hemorrhage: the role of thrombin. *J Neurosurg* 84:91-6

Lee KR, Kawai N, Kim S, Sagher O, Hoff JT (1997) Mechanisms of edema formation after intracerebral hemorrhage: effects of thrombin on cerebral blood flow, blood-brain barrier permeability, and cell survival in a rat model. *J Neurosurg* 86:272-8

Li X, Ponten A, Aase K, Karlsson L, Abramsson A, Uutela M, Backstrom G, Hellstrom M, Bostrom H, Li H, Soriano P, Betsholtz C, Heldin CH, Alitalo K, Ostman A, Eriksson U (2000) PDGF-C is a new protease-activated ligand for the PDGF alpha-receptor. *Nat Cell Biol* 2:302-9

Li X, Eriksson U (2003) Novel PDGF family members: PDGF-C and PDGF-D. *Cytokine Growth Factor Rev* 14:91-8

Lindahl P, Johansson BR, Leveen P, Betsholtz C (1997) Pericyte loss and microaneurysm formation in PDGF-B-deficient mice. *Science* 277:242-5

Liu DZ, Ander BP, Xu H, Shen Y, Kaur P, Deng W, Sharp FR (2010) Blood-brain barrier breakdown and repair by Src after thrombin-induced injury. *Ann Neurol* 67:526-33

Lorant DE, Patel KD, McIntyre TM, McEver RP, Prescott SM, Zimmerman GA (1991) Coexpression of GMP-140 and PAF by endothelium stimulated by histamine or thrombin: a juxtacrine system for adhesion and activation of neutrophils. *J Cell Biol* 115:223-34

Lu A, Tang Y, Ran R, Ardizzone TL, Wagner KR, Sharp FR (2006) Brain genomics of intracerebral hemorrhage. *J Cereb Blood Flow Metab* 26:230-52

Luo J, Wang Y, Chen X, Chen H, Kintner DB, Shull GE, Philipson KD, Sun D (2007) Increased tolerance to ischemic neuronal damage by knockdown of Na+-Ca2+ exchanger isoform 1. *Ann N Y Acad Sci* 1099:292-305

MacLellan CL, Silasi G, Poon CC, Edmundson CL, Buist R, Peeling J, Colbourne F (2008) Intracerebral hemorrhage models in rat: comparing collagenase to blood infusion. *J Cereb Blood Flow Metab* 28:516-25

Marques MA, Tolar M, Harmony JA, Crutcher KA (1996) A thrombin cleavage fragment of apolipoprotein E exhibits isoform-specific neurotoxicity. *Neuroreport* 7:2529-32

Martelius T, Salaspuro V, Salmi M, Krogerus L, Hockerstedt K, Jalkanen S, Lautenschlager I (2004) Blockade of vascular adhesion protein-1 inhibits lymphocyte infiltration in rat liver allograft rejection. *Am J Pathol* 165:1993-2001

Martelius T, Salmi M, Krogerus L, Loginov R, Schoultz M, Karikoski M, Miiluniemi M, Soots A, Hockerstedt K, Jalkanen S, Lautenschlager I (2008) Inhibition of semicarbazide-sensitive amine oxidases decreases lymphocyte infiltration in the early phases of rat liver allograft rejection. *Int J Immunopathol Pharmacol* 21:911-20

Marx M, Perlmutter RA, Madri JA (1994) Modulation of platelet-derived growth factor receptor expression in microvascular endothelial cells during in vitro angiogenesis. *J Clin Invest* 93:131-9

Masada T, Hua Y, Xi G, Yang GY, Hoff JT, Keep RF (2001) Attenuation of intracerebral hemorrhage and thrombin-induced brain edema by overexpression of interleukin-1 receptor antagonist. *J Neurosurg* 95:680-6

Masuda T, Dohrmann GJ, Kwaan HC, Erickson RK, Wollman RL (1988) Fibrinolytic activity in experimental intracerebral hematoma. *J Neurosurg* 68:274-8

Matsuoka H, Hamada R (2002) Role of thrombin in CNS damage associated with intracerebral haemorrhage: opportunity for pharmacological intervention? *CNS Drugs* 16:509-16

Matsushita K, Meng W, Wang X, Asahi M, Asahi K, Moskowitz MA, Lo EH (2000) Evidence for apoptosis after intercerebral hemorrhage in rat striatum. *J Cereb Blood Flow Metab* 20:396-404

Mayer SA, Sacco RL, Shi T, Mohr JP (1994) Neurologic deterioration in noncomatose patients with supratentorial intracerebral hemorrhage. *Neurology* 44:1379-84

Mayer SA (2003) Ultra-early hemostatic therapy for intracerebral hemorrhage. *Stroke* 34:224-9

Mayne M, Fotheringham J, Yan HJ, Power C, Del Bigio MR, Peeling J, Geiger JD (2001a) Adenosine A2A receptor activation reduces proinflammatory events and decreases cell death following intracerebral hemorrhage. *Ann Neurol* 49:727-35

Mayne M, Ni W, Yan HJ, Xue M, Johnston JB, Del Bigio MR, Peeling J, Power C (2001b) Antisense oligodeoxynucleotide inhibition of tumor necrosis factor-alpha expression is neuroprotective after intracerebral hemorrhage. *Stroke* 32:240-8

Megyeri P, Abraham CS, Temesvari P, Kovacs J, Vas T, Speer CP (1992) Recombinant human tumor necrosis factor alpha constricts pial arterioles and increases blood-brain barrier permeability in newborn piglets. *Neurosci Lett* 148:137-40

Mercier N, El Hadri K, Osborne-Pellegrin M, Nehme J, Perret C, Labat C, Regnault V, Lamaziere JM, Challande P, Lacolley P, Feve B (2007) Modifications of arterial phenotype in response to amine oxidase inhibition by semicarbazide. *Hypertension* 50:234-41

Merinen M, Irjala H, Salmi M, Jaakkola I, Hanninen A, Jalkanen S (2005) Vascular adhesion protein-1 is involved in both acute and chronic inflammation in the mouse. *Am J Pathol* 166:793-800

Minami T, Aird WC (2001) Thrombin stimulation of the vascular cell adhesion molecule-1 promoter in endothelial cells is mediated by tandem nuclear factor-kappa B and GATA motifs. *J Biol Chem* 276:47632-41

Montfort I, Perez-Tamayo R (1975) The distribution of collagenase in normal rat tissues. *J Histochem Cytochem* 23:910-20

Morris MM, Dallow KC, Zietman AL, Park J, Althausen A, Heney NM, Shipley WU (1997) Adjuvant and salvage irradiation following radical prostatectomy for prostate cancer. *Int J Radiat Oncol Biol Phys* 38:731-6

Mun-Bryce S, Wilkerson AC, Papuashvili N, Okada YC (2001) Recurring episodes of spreading depression are spontaneously elicited by an intracerebral hemorrhage in the swine. *Brain Res* 888:248-55

Nakamura H, Fujii Y, Ohuchi E, Yamamoto E, Okada Y (1998) Activation of the precursor of human stromelysin 2 and its interactions with other matrix metalloproteinases. *Eur J Biochem* 253:67-75

Nakamura T, Xi G, Hua Y, Schallert T, Hoff JT, Keep RF (2004) Intracerebral hemorrhage in mice: model characterization and application for genetically modified mice. *J Cereb Blood Flow Metab* 24:487-94

Narita M, Usui A, Niikura K, Nozaki H, Khotib J, Nagumo Y, Yajima Y, Suzuki T (2005) Protease-activated receptor-1 and platelet-derived growth factor in spinal cord neurons are implicated in neuropathic pain after nerve injury. *J Neurosci* 25:10000-9

Nath FP, Jenkins A, Mendelow AD, Graham DI, Teasdale GM (1986) Early hemodynamic changes in experimental intracerebral hemorrhage. *J Neurosurg* 65:697-703

Neuwelt EA (2004) Mechanisms of disease: the blood-brain barrier. *Neurosurgery* 54:131-40; discussion 41-2

Nguyen TD, Moody MW, Steinhoff M, Okolo C, Koh DS, Bunnett NW (1999) Trypsin activates pancreatic duct epithelial cell ion channels through proteinase-activated receptor-2. *J Clin Invest* 103:261-9

Nito C, Kamada H, Endo H, Niizuma K, Myer DJ, Chan PH (2008) Role of the p38 mitogen-activated protein kinase/cytosolic phospholipase A2 signaling pathway in blood-brain barrier disruption after focal cerebral ischemia and reperfusion. *J Cereb Blood Flow Metab* 28:1686-96

Noda K, She H, Nakazawa T, Hisatomi T, Nakao S, Almulki L, Zandi S, Miyahara S, Ito Y, Thomas KL, Garland RC, Miller JW, Gragoudas ES, Mashima Y, Hafezi-Moghadam A (2008) Vascular adhesion protein-1 blockade suppresses choroidal neovascularization. *FASEB J* 22:2928-35

O'Brien SG, Guilhot F, Larson RA, Gathmann I, Baccarani M, Cervantes F, Cornelissen JJ, Fischer T, Hochhaus A, Hughes T, Lechner K, Nielsen JL, Rousselot P, Reiffers J, Saglio G, Shepherd J, Simonsson B, Gratwohl A, Goldman JM, Kantarjian H, Taylor K, Verhoef G, Bolton AE, Capdeville R, Druker BJ (2003) Imatinib compared with interferon and low-dose cytarabine for newly diagnosed chronic-phase chronic myeloid leukemia. *N Engl J Med* 348:994-1004

O'Rourke AM, Wang EY, Miller A, Podar EM, Scheyhing K, Huang L, Kessler C, Gao H, Ton-Nu HT, Macdonald MT, Jones DS, Linnik MD (2008) Anti-inflammatory effects of LJP 1586 [Z-3-fluoro-2-(4-methoxybenzyl)allylamine hydrochloride], an amine-based inhibitor of semicarbazide-sensitive amine oxidase activity. *J Pharmacol Exp Ther* 324:867-75

Ostrowski RP, Colohan AR, Zhang JH (2005) Mechanisms of hyperbaric oxygen-induced neuroprotection in a rat model of subarachnoid hemorrhage. *J Cereb Blood Flow Metab* 25:554-71

Peggs K, Mackinnon S (2003) Imatinib mesylate--the new gold standard for treatment of chronic myeloid leukemia. *N Engl J Med* 348:1048-50

Piccio L, Rossi B, Scarpini E, Laudanna C, Giagulli C, Issekutz AC, Vestweber D, Butcher EC, Constantin G (2002) Molecular mechanisms involved in lymphocyte recruitment in inflamed brain microvessels: critical roles for P-selectin glycoprotein ligand-1 and heterotrimeric G(i)-linked receptors. *J Immunol* 168:1940-9

Power C, Henry S, Del Bigio MR, Larsen PH, Corbett D, Imai Y, Yong VW, Peeling J (2003) Intracerebral hemorrhage induces macrophage activation and matrix metalloproteinases. *Ann Neurol* 53:731-42

Qin Y, Rezler EM, Gokhale V, Sun D, Hurley LH (2007) Characterization of the G-quadruplexes in the duplex nuclease hypersensitive element of the PDGF-A promoter and modulation of PDGF-A promoter activity by TMPyP4. *Nucleic Acids Res* 35:7698-713

Qureshi AI, Wilson DA, Hanley DF, Traystman RJ (1999a) No evidence for an ischemic penumbra in massive experimental intracerebral hemorrhage. *Neurology* 52:266-72

Qureshi AI, Wilson DA, Traystman RJ (1999b) Treatment of elevated intracranial pressure in experimental intracerebral hemorrhage: comparison between mannitol and hypertonic saline. *Neurosurgery* 44:1055-63; discussion 63-4

Qureshi AI, Ling GS, Khan J, Suri MF, Miskolczi L, Guterman LR, Hopkins LN (2001) Quantitative analysis of injured, necrotic, and apoptotic cells in a new experimental model of intracerebral hemorrhage. *Crit Care Med* 29:152-7

Qureshi AI, Suri MF, Ostrow PT, Kim SH, Ali Z, Shatla AA, Guterman LR, Hopkins LN (2003) Apoptosis as a form of cell death in intracerebral hemorrhage. *Neurosurgery* 52:1041-7; discussion 7-8

Rahman A, Anwar KN, True AL, Malik AB (1999) Thrombin-induced p65 homodimer binding to downstream NF-kappa B site of the promoter mediates endothelial ICAM-1 expression and neutrophil adhesion. *J Immunol* 162:5466-76

Raines SM, Richards OC, Schneider LR, Schueler KL, Rabaglia ME, Oler AT, Stapleton DS, Genove G, Dawson JA, Betsholtz C, Attie AD (2011) Loss of PDGF-B activity increases hepatic vascular permeability and enhances insulin sensitivity. *Am J Physiol Endocrinol Metab* 301:E517-26

Ribo M, Grotta JC (2006) Latest advances in intracerebral hemorrhage. *Curr Neurol Neurosci Rep* 6:17-22

Rieckmann P, Engelhardt B (2003) Building up the blood-brain barrier. *Nat Med* 9:828-9

Risau W, Drexler H, Mironov V, Smits A, Siegbahn A, Funa K, Heldin CH (1992) Platelet-derived growth factor is angiogenic in vivo. *Growth Factors* 7:261-6

Rohde V, Rohde I, Thiex R, Ince A, Jung A, Duckers G, Groschel K, Rottger C, Kuker W, Muller HD, Gilsbach JM (2002) Fibrinolysis therapy achieved with tissue plasminogen activator and aspiration of the liquefied clot after experimental intracerebral hemorrhage: rapid reduction in hematoma volume but intensification of delayed edema formation. *J Neurosurg* 97:954-62

Romashkova JA, Makarov SS (1999) NF-kappaB is a target of AKT in anti-apoptotic PDGF signalling. *Nature* 401:86-90

Ropper AH, Zervas NT (1982) Cerebral blood flow after experimental basal ganglia hemorrhage. *Ann Neurol* 11:266-71

Ropper AH (1986) Lateral displacement of the brain and level of consciousness in patients with an acute hemispheral mass. *N Engl J Med* 314:953-8

Rosell A, Alvarez-Sabin J, Arenillas JF, Rovira A, Delgado P, Fernandez-Cadenas I, Penalba A, Molina CA, Montaner J (2005) A matrix metalloproteinase protein array reveals a strong relation between MMP-9 and MMP-13 with diffusion-weighted image lesion increase in human stroke. *Stroke* 36:1415-20

Rosenberg GA, Mun-Bryce S, Wesley M, Kornfeld M (1990) Collagenase-induced intracerebral hemorrhage in rats. *Stroke* 21:801-7

Rosenberg GA, Kornfeld M, Estrada E, Kelley RO, Liotta LA, Stetler-Stevenson WG (1992) TIMP-2 reduces proteolytic opening of blood-brain barrier by type IV collagenase. *Brain Res* 576:203-7

Rosenberg GA, Estrada E, Kelley RO, Kornfeld M (1993) Bacterial collagenase disrupts extracellular matrix and opens blood-brain barrier in rat. *Neurosci Lett* 160:117-9

Rosenberg GA, Navratil M (1997) Metalloproteinase inhibition blocks edema in intracerebral hemorrhage in the rat. *Neurology* 48:921-6

Ross R, Glomset J, Kariya B, Harker L (1974) A platelet-dependent serum factor that stimulates the proliferation of arterial smooth muscle cells in vitro. *Proc Natl Acad Sci U S A* 71:1207-10

Rynkowski MA, Kim GH, Komotar RJ, Otten ML, Ducruet AF, Zacharia BE, Kellner CP, Hahn DK, Merkow MB, Garrett MC, Starke RM, Cho BM, Sosunov SA, Connolly ES (2008) A mouse model of intracerebral hemorrhage using autologous blood infusion. *Nat Protoc* 3:122-8

Salmi M, Jalkanen S (1992) A 90-kilodalton endothelial cell molecule mediating lymphocyte binding in humans. *Science* 257:1407-9

Salmi M, Kalimo K, Jalkanen S (1993) Induction and function of vascular adhesion protein-1 at sites of inflammation. *J Exp Med* 178:2255-60

Salmi M, Jalkanen S (2001) VAP-1: an adhesin and an enzyme. *Trends Immunol* 22:211-6

Salmi M, Yegutkin GG, Lehvonen R, Koskinen K, Salminen T, Jalkanen S (2001) A cell surface amine oxidase directly controls lymphocyte migration. *Immunity* 14:265-76

Salmi M, Jalkanen S (2005) Cell-surface enzymes in control of leukocyte trafficking. *Nat Rev Immunol* 5:760-71

Sarker KP, Yamahata H, Nakata M, Arisato T, Nakajima T, Kitajima I, Maruyama I (1999) Recombinant thrombomodulin inhibits thrombin-induced vascular endothelial growth factor production in neuronal cells. *Haemostasis* 29:343-52

Seiffert E, Dreier JP, Ivens S, Bechmann I, Tomkins O, Heinemann U, Friedman A (2004) Lasting blood-brain barrier disruption induces epileptic focus in the rat somatosensory cortex. *J Neurosci* 24:7829-36

Shankar R, de la Motte CA, DiCorleto PE (1992) Thrombin stimulates PDGF production and monocyte adhesion through distinct intracellular pathways in human endothelial cells. *Am J Physiol* 262:C199-206

Shen J, Ishii Y, Xu G, Dang TC, Hamashima T, Matsushima T, Yamamoto S, Hattori Y, Takatsuru Y, Nabekura J, Sasahara M (2011) PDGFR-beta as a positive regulator of tissue repair in a mouse model of focal cerebral ischemia. *J Cereb Blood Flow Metab*

Shimizu S, Gabazza EC, Hayashi T, Ido M, Adachi Y, Suzuki K (2000) Thrombin stimulates the expression of PDGF in lung epithelial cells. *Am J Physiol Lung Cell Mol Physiol* 279:L503-10

Sinar EJ, Mendelow AD, Graham DI, Teasdale GM (1987) Experimental intracerebral hemorrhage: effects of a temporary mass lesion. *J Neurosurg* 66:568-76

Smith DJ, Salmi M, Bono P, Hellman J, Leu T, Jalkanen S (1998) Cloning of vascular adhesion protein 1 reveals a novel multifunctional adhesion molecule. *J Exp Med* 188:17-27

Stenina OI, Shaneyfelt KM, DiCorleto PE (2001) Thrombin induces the release of the Y-box protein dbpB from mRNA: a mechanism of transcriptional activation. *Proc Natl Acad Sci U S A* 98:7277-82

Stolen CM, Marttila-Ichihara F, Koskinen K, Yegutkin GG, Turja R, Bono P, Skurnik M, Hanninen A, Jalkanen S, Salmi M (2005) Absence of the endothelial oxidase AOC3 leads to abnormal leukocyte traffic in vivo. *Immunity* 22:105-15

Stratman AN, Schwindt AE, Malotte KM, Davis GE (2010) Endothelial-derived PDGF-BB and HB-EGF coordinately regulate pericyte recruitment during vasculogenic tube assembly and stabilization. *Blood* 116:4720-30

Strbian D, Durukan A, Tatlisumak T (2008) Rodent models of hemorrhagic stroke. *Curr Pharm Des* 14:352-8

Striggow F, Riek M, Breder J, Henrich-Noack P, Reymann KG, Reiser G (2000) The protease thrombin is an endogenous mediator of hippocampal neuroprotection against ischemia at low concentrations but causes degeneration at high concentrations. *Proc Natl Acad Sci U S A* 97:2264-9

Su EJ, Fredriksson L, Geyer M, Folestad E, Cale J, Andrae J, Gao Y, Pietras K, Mann K, Yepes M, Strickland DK, Betsholtz C, Eriksson U, Lawrence DA (2008) Activation of PDGF-CC by tissue plasminogen activator impairs blood-brain barrier integrity during ischemic stroke. *Nat Med* 14:731-7

Sugama Y, Tiruppathi C, offakidevi K, Andersen TT, Fenton JW, 2nd, Malik AB (1992) Thrombin-induced expression of endothelial P-selectin and intercellular adhesion molecule-1: a mechanism for stabilizing neutrophil adhesion. *J Cell Biol* 119:935-44

Sugi T, Fujishima M, Omae T (1975) Lactate and pyruvate concentrations, and acid-base balance of cerebrospinal fluid in experimentally induced intracerebral and subarachnoid hemorrhage in dogs. *Stroke* 6:715-9

Takasugi S, Ueda S, Matsumoto K (1985) Chronological changes in spontaneous intracerebral hematoma--an experimental and clinical study. *Stroke* 16:651-8

Tang J, Liu J, Zhou C, Alexander JS, Nanda A, Granger DN, Zhang JH (2004) Mmp-9 deficiency enhances collagenase-induced intracerebral hemorrhage and brain injury in mutant mice. *J Cereb Blood Flow Metab* 24:1133-45

Tang J, Liu J, Zhou C, Ostanin D, Grisham MB, Neil Granger D, Zhang JH (2005) Role of NADPH oxidase in the brain injury of intracerebral hemorrhage. *J Neurochem* 94:1342-50

Tang Z, Arjunan P, Lee C, Li Y, Kumar A, Hou X, Wang B, Wardega P, Zhang F, Dong L, Zhang Y, Zhang SZ, Ding H, Fariss RN, Becker KG, Lennartsson J, Nagai N, Cao Y, Li X (2010) Survival effect of PDGF-CC rescues neurons from apoptosis in both brain and retina by regulating GSK3beta phosphorylation. *J Exp Med* 207:867-80

Tejima E, Zhao BQ, Tsuji K, Rosell A, van Leyen K, Gonzalez RG, Montaner J, Wang X, Lo EH (2007) Astrocytic induction of matrix metalloproteinase-9 and edema in brain hemorrhage. *J Cereb Blood Flow Metab* 27:460-8

Thiex R, Mayfrank L, Rohde V, Gilsbach JM, Tsirka SA (2004) The role of endogenous versus exogenous tPA on edema formation in murine ICH. *Exp Neurol* 189:25-32

Titova E, Ostrowski RP, Kevil CG, Tong W, Rojas H, Sowers LC, Zhang JH, Tang J (2008) Reduced brain injury in CD18-deficient mice after experimental intracerebral hemorrhage. *J Neurosci Res* 86:3240-5

Tohka S, Laukkanen M, Jalkanen S, Salmi M (2001) Vascular adhesion protein 1 (VAP-1) functions as a molecular brake during granulocyte rolling and mediates recruitment in vivo. *FASEB J* 15:373-82

Vantler M, Caglayan E, Zimmermann WH, Baumer AT, Rosenkranz S (2005) Systematic evaluation of anti-apoptotic growth factor signaling in vascular smooth muscle cells. Only phosphatidylinositol 3'-kinase is important. *J Biol Chem* 280:14168-76

Vantler M, Karikkineth BC, Naito H, Tiburcy M, Didie M, Nose M, Rosenkranz S, Zimmermann WH (2010) PDGF-BB protects cardiomyocytes from apoptosis and improves contractile function of engineered heart tissue. *J Mol Cell Cardiol* 48:1316-23

Wagner KR, Xi G, Hua Y, Kleinholz M, de Courten-Myers GM, Myers RE, Broderick JP, Brott TG (1996) Lobar intracerebral hemorrhage model in pigs: rapid edema development in perihematomal white matter. *Stroke* 27:490-7

Wagner KR, Beiler S, Beiler C, Kirkman J, Casey K, Robinson T, Larnard D, de Courten-Myers GM, Linke MJ, Zuccarello M (2006) Delayed profound local brain hypothermia markedly reduces interleukin-1beta gene expression and vasogenic edema development in a porcine model of intracerebral hemorrhage. *Acta Neurochir Suppl* 96:177-82

Wang J, Rogove AD, Tsirka AE, Tsirka SE (2003) Protective role of tuftsin fragment 1-3 in an animal model of intracerebral hemorrhage. *Ann Neurol* 54:655-64

Wang J, Tsirka SE (2005a) Neuroprotection by inhibition of matrix metalloproteinases in a mouse model of intracerebral haemorrhage. *Brain* 128:1622-33

Wang J, Tsirka SE (2005b) Tuftsin fragment 1-3 is beneficial when delivered after the induction of intracerebral hemorrhage. *Stroke* 36:613-8

Wang J, Tsirka SE (2005c) Contribution of extracellular proteolysis and microglia to intracerebral hemorrhage. *Neurocrit Care* 3:77-85

Wang J, Dore S (2007) Inflammation after intracerebral hemorrhage. *J Cereb Blood Flow Metab* 27:894-908

Wang J, Fields J, Dore S (2008) The development of an improved preclinical mouse model of intracerebral hemorrhage using double infusion of autologous whole blood. *Brain Res* 1222:214-21

Wang W, Merrill MJ, Borchardt RT (1996) Vascular endothelial growth factor affects permeability of brain microvessel endothelial cells in vitro. *Am J Physiol* 271:C1973-80

Wekerle H, Linington C, Lassmann H, Meyermann R (1986) Cellular immune reactivity within the CNS. *Trends in Neurosciences* 9:271-7

Wu B, Ma Q, Khatibi N, Chen W, Sozen T, Cheng O, Tang J (2010) Ac-YVAD-CMK Decreases Blood-Brain Barrier Degradation by Inhibiting Caspase-1 Activation of Interleukin-1beta in Intracerebral Hemorrhage Mouse Model. *Transl Stroke Res* 1:57-64

Xi G, Wagner KR, Keep RF, Hua Y, de Courten-Myers GM, Broderick JP, Brott TG, Hoff JT (1998) Role of blood clot formation on early edema development after experimental intracerebral hemorrhage. *Stroke* 29:2580-6

Xi G, Keep RF, Hua Y, Xiang J, Hoff JT (1999) Attenuation of thrombin-induced brain edema by cerebral thrombin preconditioning. *Stroke* 30:1247-55

Xi G, Hua Y, Keep RF, Younger JG, Hoff JT (2001) Systemic complement depletion diminishes perihematomal brain edema in rats. *Stroke* 32:162-7

Xi G, Keep RF, Hoff JT (2002) Pathophysiology of brain edema formation. *Neurosurg Clin N Am* 13:371-83

Xi G, Keep RF, Hoff JT (2006) Mechanisms of brain injury after intracerebral haemorrhage. *Lancet Neurol* 5:53-63

Xu HL, Salter-Cid L, Linnik MD, Wang EY, Paisansathan C, Pelligrino DA (2006) Vascular adhesion protein-1 plays an important role in postischemic inflammation and neuropathology in diabetic, estrogen-treated ovariectomized female rats subjected to transient forebrain ischemia. *J Pharmacol Exp Ther* 317:19-29

Xue M, Del Bigio MR (2000a) Intracerebral injection of autologous whole blood in rats: time course of inflammation and cell death. *Neurosci Lett* 283:230-2

Xue M, Del Bigio MR (2000b) Intracortical hemorrhage injury in rats : relationship between blood fractions and brain cell death. *Stroke* 31:1721-7

Xue M, Fan Y, Liu S, Zygun DA, Demchuk A, Yong VW (2009) Contributions of multiple proteases to neurotoxicity in a mouse model of intracerebral haemorrhage. *Brain* 132:26-36

Yang GY, Betz AL, Chenevert TL, Brunberg JA, Hoff JT (1994) Experimental intracerebral hemorrhage: relationship between brain edema, blood flow, and blood-brain barrier permeability in rats. *J Neurosurg* 81:93-102

Yao H, Duan M, Buch S (2010) Cocaine-mediated induction of platelet-derived growth factor: implication for increased vascular permeability. *Blood*

Yilmaz G, Granger DN (2008) Cell adhesion molecules and ischemic stroke. *Neurol Res* 30:783-93

Yoong KF, McNab G, Hubscher SG, Adams DH (1998) Vascular adhesion protein-1 and ICAM-1 support the adhesion of tumor-infiltrating lymphocytes to tumor endothelium in human hepatocellular carcinoma. *J Immunol* 160:3978-88

Yu PH, Zuo DM (1997) Aminoguanidine inhibits semicarbazide-sensitive amine oxidase activity: implications for advanced glycation and diabetic complications. *Diabetologia* 40:1243-50

Zausinger S, Hungerhuber E, Baethmann A, Reulen H, Schmid-Elsaesser R (2000) Neurological impairment in rats after transient middle cerebral artery occlusion: a comparative study under various treatment paradigms. *Brain Res* 863:94-105

Zhang J, Cao R, Zhang Y, Jia T, Cao Y, Wahlberg E (2009) Differential roles of PDGFR-alpha and PDGFR-beta in angiogenesis and vessel stability. *FASEB J* 23:153-63

Zhao X, Zhang Y, Strong R, Grotta JC, Aronowski J (2006) 15d-Prostaglandin J2 activates peroxisome proliferator-activated receptor-gamma, promotes expression of catalase, and reduces inflammation, behavioral dysfunction, and neuronal loss after intracerebral hemorrhage in rats. *J Cereb Blood Flow Metab* 26:811-20

Zheng L, Ishii Y, Tokunaga A, Hamashima T, Shen J, Zhao QL, Ishizawa S, Fujimori T, Nabeshima Y, Mori H, Kondo T, Sasahara M (2010) Neuroprotective effects of PDGF against oxidative stress and the signaling pathway involved. *J Neurosci Res* 88:1273-84

Zvalova D, Cordier J, Mesnil M, Junier MP, Chneiweiss H (2004) p38/SAPK2 controls gap junction closure in astrocytes. *Glia* 46:323-33